Energy metabolic configuration of human adipose tissue-derived cells and its changes due to *in vitro* culture with osteogenic and adipogenic differentiation

Kumulative Dissertation
zur Erlangung des akademischen Grades
doctor rerum naturalium (Dr. rer. nat.)
der Mathematisch-Naturwissenschaftlichen Fakultät
der Universität Rostock

vorgelegt von

Juliane Meyer, geb. am 31.07.1986 in Rostock

https://doi.org/10.18453/rosdok_id00002600

Datum der Einreichung: 30.07.2019

Datum der Verteidigung 29.12.2019

1. Gutachter:
   PD Dr. Kirsten Peters
   Universitätsmedizin Rostock, Arbeitsbereich Zellbiologie

2. Gutachter:
   Prof. Dr. Fritz-Olaf Lehmann
   Universität Rostock, Arbeitsbereich Tierphysiologie

Index

Abbreviations

acetyl-CoA	acetyl coenzyme A
adMSC/ASC*	adipose tissue-derived mesenchymal stem/stromal cells
ADP	adenosine diphosphate
ALP	bone-specific alkaline phosphatase
ATP	adenosine triphosphate
BMI	body mass index
bmMSC	bone marrow-derived mesenchymal stem cells
CD	cluster of differentiation
CK	creatine kinase
DNA	deoxyribonucleic acid
ECM	extra cellular matrix
$FADH_2$	flavin adenine dinucleotide hydroquinone
FBPase	fructose-1,6-bis-phosphatase
G6PDH	glucose 6-phosphate dehydrogenase
GAPDH	glyceraldehyde-3-phosphate dehydrogenase
GSR	glutathione disulfide reductase
HOADH	ß-hydroxyacyl-CoA dehydrogenase
LDH	lactate dehydrogenase
MSC	mesenchymal stem/stromal cells
NAD^+	nicotinamide adenine dinucleotide
NADH	nicotinamide adenine dinucleotide anion
NAD-IDH	NAD^+-dependent isocitrate dehydrogenase
$NADP^+$	nicotinamide adenine dinucleotide phosphate
NADPH	nicotinamide adenine dinucleotide phosphate anion
NADP-IDH	$NADP^+$-dependent isocitrate dehydrogenase
Ox Phos	oxidative phosphorylation
PFK	phosphofructokinase
PPP	pentose phosphate pathway
RNA	ribonucleic acid
ROS	reactive oxygen species
SVF	stromal vascular fraction
TCC	tricarbolic acid cycle
UCP1	uncoupling protein 1

*Due to deviating demands by reviewers, the term “adipose tissue-derived mesenchymal stem/stromal cells” was abbreviated with adMSC in study 1 and 3 and with ASC in study 2. For consistency only the abbreviation adMSC was used in the dissertation.

List of tables and figures

1 Zusammenfassung

Vor knapp 20 Jahren wurde Fettgewebe als Reservoir adulter mesenchymaler Stammzellen identifiziert. Während die therapeutische Anwendung der Zellen in der Praxis Realität ist, ist die Grundlagenerforschung noch lange nicht abgeschlossen.

Erstes Ziel der vorliegenden Arbeit war es, zu charakterisieren, wie viele adulte Stammzellen in humanem Fettgewebe enthalten sind, das mit Wasserstrahl-assistierter Liposuktion gewonnen wurde. An Hand der erzielten Daten konnte quantitativ nachgewiesen werden, dass das so gewonnene Gewebe eine valide Quelle für die Gewinnung adulter mesenchymaler Stammzellen mit hoher Viabilität und mesenchymalem Differenzierungspotential ist.

Jeder einzelne Zelltyp im humanen Fettgewebe, erfüllt Aufgaben, die der Erhaltung der physiologischen Homöostase im Gewebe dienen und verfügt über einen Stoffwechsel, der je nach Funktion und Bedarf verändert werden kann. Ist der zelluläre Stoffwechsel gestört, kann das Defekte in der Verrichtung der zelltypspezifischen Aufgaben hervorrufen. Um solche Defekte im zellulären Stoffwechsel zu erkennen oder einzuordnen, muss zunächst der Metabolismus nativer Zellen beschrieben werden. Es war daher das nächste Ziel der Studie den energie-metabolischen Phänotyp zweier distinkter nativer Zellpopulationen des humanen Fettgewebes zu charakterisieren. Untersucht wurden adulte Adipozyten und die $CD34^+$-Zellpopulation der stromalen vaskulären Fraktion desselben Gewebes. In ersten Charakterisierungen konnte zunächst gezeigt werden, dass die $CD34^+$ Zellpopulation der stromalen vaskulären Fraktion mit mesenchymalen Progenitorzellen angereichert ist. Aktuelle Literatur liefert Hinweise darauf, dass Progenitorzellen ein höheres Potential für Proliferation und Differenzierung zeigen, als adulte Adipozyten. Bei beiden Zellpopulationen wurden dann die maximalen Enzymaktivitäten (=Enzymkapazitäten) verschiedener Markerenzyme wesentlicher Wege des Energiestoffwechsels quantifiziert und verglichen. Bei Markerenzymen handelt es sich um Enzyme, die irreversible oder Geschwindigkeits-limitierende Reaktionen verschiedener Stoffwechselwege katalysieren. Sie dienen so als Indikatoren für die Gesamtaktivität des jeweiligen Stoffwechselweges. Die untersuchten Adipozyten zeigten höhere Kapazitäten der Markerenzyme des Tricarbonsäurezyklus und der ß-Oxidation verglichen mit den $CD34^+$ Zellen der stromalen vaskulären Fraktion. Dies deutet auf eine höhere mitochondriale Stoffwechselaktivität hin. Die $CD34^+$ Zellen der

stromalen vaskulären Fraktion zeigten verglichen mit den Adipozyten höhere Kapazitäten der Markerenzyme von Glykolyse und Pentosephosphatweg, was Hinweise auf eine höhere Aktivität des zytosolischen Kohlenhydratstoffwechsels gibt. Es ist zu vermuten, dass Adipozyten so einen kontrollierten Lipidumsatz gewährleisten, während die $CD34^+$ Zellen der stromalen vaskulären Fraktion ihre Versorgung mit Pentosen und Reduktionsäquivalenten für die Replikation von DNA und anderen Makromolekülen für die Proliferation absichern. Die gewonnenen Daten zeigen, dass die zwei untersuchten Zellpopulationen des humanen Fettgewebes sich in der grundlegenden Strukturierung ihres Energiestoffwechsels unterscheiden. Dies könnte eine Anpassung an ihre jeweiligen physiologischen Funktionen und Gegebenheiten *in vivo* sein.

Zwei distinkte, native Zellpopulationen des menschlichen Fettgewebes mit unterschiedlichem Potential zu differenzieren und zu proliferieren, zeigen eine unterschiedliche Strukturierung ihres Stoffwechsels. Beim Übergang von Zellen aus einem nativen in ein *in vitro* Umfeld, wie es in Zellkulturmodellen der Fall ist, kommt es zu phänotypischen Veränderungen der Zellen. Werden die Zellen mit zusätzlichen Substanzen zur Differenzierung angeregt, finden weitere, ausgeprägtere Veränderungen in Phänotyp und Verhalten der Zellen statt. Die Beobachtung solcher Veränderungen in etablierten Modellen der osteogenen und adipogenen Differenzierung isolierter mesenchymaler Stammzellen des Fettgewebes führten zu der Frage, ob es auch in der Strukturierung des Energiestoffwechsels zu Änderungen kommt. Um dies zu untersuchen wurden die Zellen ohne und mit osteogener und adipogener Differenzierungsstimulation kultiviert. Proliferations- und Differenzierungsstatus der Zellen wurden quantifiziert und die Aktivitäten wesentlicher Wege des Energiestoffwechsels der Zellen wurden anhand von Aktivitätsbestimmungen bzw. RNA-Quantifizierungen von Markerenzymen erfasst. So konnten wir in nicht-differenzierenden und osteogen differenzierenden Zellen Proliferation nachweisen. Diese ging einher mit erhöhten Aktivitäten der Markerenzyme von Glykolyse und Pentosephosphatweg. Adipogen differenzierende Zellen, die nicht proliferierten, zeigten verminderte glykolytische Aktivität aber zur gleichen Zeit ebenso einen Anstieg ihrer mitochondrialen Enzymaktivitäten. Das gemeinsame Auftreten von metabolischer Umstrukturierung und Proliferationsverhalten der Zellen zeigten sich in ähnlicher Weise, wie es zuvor in den nativen Zellpopulationen des Fettgewebes beobachtet worden war. Die Veränderungen der Strukturierung des zellulären Energiestoffwechsels

können Anpassungen an den erhöhten Energiebedarf während der Proliferation repräsentieren sowie an spezifische zelluläre Funktionen, die sich während der osteogenen und adipogenen Differenzierung entwickeln.

Mit der vorliegenden Arbeit konnten wir zur grundsätzlichen Charakterisierung des Energiestoffwechsels unterschiedlicher Zelltypen des menschlichen Fettgewebes im nativen Zustand sowie unter *in vitro* Bedingungen beitragen. Diese Arbeiten dienen als Grundlage weitergehender Untersuchungen des zellulären Energiestoffwechsel in klinischen sowie in Laborfragestellungen.

2 Summary

Just under 20 years ago adipose tissue has been identified as a source of adult mesenchymal stem cells. While these regenerative cells are already being clinically applied, basic research and the fundamental characterization of the cells is ongoing.

The first aim of the presented work was to quantify and characterize the content of adult mesenchymal stem cells within adipose tissue harvested with water-jet assistance. From our collected data we can conclude that adipose tissue harvested with water-jet assistance is a valid source for the isolation of adult mesenchymal stem cells with high viability and mesenchymal differentiation potential.

Each of the cell types in adipose tissue, fulfills different tasks ensuring the physiological homeostasis within the tissue and possesses a metabolism that can be adapted to meet demands for diverging functions and needs. Defects of that cellular metabolism can lead to malfunctions of the cells that may prevent the execution of their essential tasks. In order to identify such defects, the cellular metabolism of native cells must be thoroughly described. It was thus the second aim of this study to characterize the energy metabolic phenotype of two distinct cell populations of the adipose tissue. We thus examined native adult adipocytes and $CD34^+$ cells of the stromal vascular fraction, separated from the same tissue. In first characterization steps we could show that $CD34^+$ cells of the stromal vascular fraction are a population enriched in adipose tissue-derived mesenchymal progenitors. Current literature indicates, that these kinds of progenitor cell types display a higher potential for proliferation and differentiation than adult adipocytes. For both cell populations, the maximum enzyme activities (=enzyme capacities) of marker enzymes of major energy metabolic pathways were quantified and compared. Marker enzymes are enzymes that catalyze irreversible or rate-limiting steps of different metabolic pathways. They thus serve as indicators for the overall activity of their respective pathways. Compared to the $CD34^+$ cells of the stromal vascular fraction the examined adipocytes showed higher capacities of the marker enzymes of the tricarbolic acid cycle and the ß-oxidation. This indicates significantly higher metabolic activity of the mitochondria. The $CD34^+$ cells of the stromal vascular fraction showed higher capacities of the marker enzymes of glycolysis and the pentose phosphate pathway, which suggests a higher activity of the cytosolic carbohydrate metabolism. This way the adipocytes may facilitate a controlled lipid turnover, while the

$CD34^+$ cells of the stromal vascular fraction may ensure the provision of pentose phosphates and reduction equivalents for the replication of DNA and other macromolecules during potential proliferation. The data indicate that these two cell fractions of the human adipose tissue differ in their metabolic configuration. This might represent adaptations to their physiological tasks and demands *in vivo*.

We had observed the substantial differences in the energy metabolic configuration of two distinct cell populations of adipose tissue and their divergent potential to differentiate and proliferate. The transition of adipose-derived progenitors from their *in vivo* to an *in vitro* environment leads to significant phenotypic changes. An additional stimulation of the cells to differentiate leads to even more pronounced changes in the cell's phenotype and behavior. These changes observed in established cell culture models of osteogenic and adipogenic differentiation lead to the question, if cultivation of adipose tissue-derived mesenchymal stem cells with osteogenic and adipogenic differentiation stimuli would also cause adaptations in the cell's energy metabolic structure. For that we cultured adMSC with and without differentiation stimulation. The proliferation and differentiation status of the cells was quantified, and major energy metabolic pathways were analyzed with respect to their activity and gene expression. We could show that cells in non-differentiating and osteogenic cultivation conditions displayed active proliferation and showed increasing activities of the marker enzymes of glycolysis and the pentose phosphate pathway. Adipogenically differentiating cells, that did not proliferate, showed a reduced glycolytic capacity and increased mitochondrial marker enzyme activities at the same time. Thus, we could observe a similar connection between the energy metabolic configuration and the proliferation potential as we did before in the two native cell populations of the adipose tissue. These changes in energy metabolism might represent an adaptation of adMSC to the high energy demand during proliferation and to the specific cellular functions during osteogenic or adipogenic differentiation respectively.

With the present work we were able to contribute to the characterization of the energy metabolism of distinct cell types of the human adipose tissue in the native state and after *in vitro* culturing. We were thus able to add to the groundwork needed for further examinations of the cellular metabolism of human adipose tissue in the clinical as well as the laboratory setting.

3 Introduction

3.1 Adipose tissue

The adipose tissue of the human body is a multi-depot organ consisting of subcutaneous and visceral depots. For a long time, adipose tissue has been regarded as an organ of mere energy storage. Today its role as an endocrine organ that participates in the regulation of the metabolism, blood pressure, vascular homeostasis, bone metabolism and the immune system has generally been recognized (reviewed in (Trayhurn, 2005; Ferris and Crowther, 2011)). Adipose tissue is composed of a variety of cell types. Two major groups can be classified: adipocytes and stromal vascular cells, the latter being a heterogeneous cell population consisting of all cell types of the adipose tissue except the mature adipocytes. In the recent past the potential of adipose tissue in regenerative medicine has been discovered and studied. While the tissue itself is being used in clinical applications (reviewed in (Hsu *et al.*, 2012)), it has furthermore been identified as a source of multipotent adult stem cells (Zuk *et al.*, 2001; Zuk, 2010).

3.1.1 Adipocytes

Adipocytes can be classified as white, brite/beige and brown adipocytes. They differ regarding specific energy metabolic characteristics. White adipocytes store and release energy by turning over lipids (Strawford *et al.*, 2004; Spalding *et al.*, 2008), whereas brite/beige and brown adipocytes rather release energy in the form of heat through the uncoupling of oxidative phosphorylation from adenosine triphosphate (ATP) production (Cannon and Nedergaard, 2004; Hyvönen and Spalding, 2014). The main portion of adipose tissue is comprised of white adipocytes (Cypess *et al.*, 2009). White adipocytes are unilocular, meaning they possess one big lipid vacuole for the accumulation of fatty acids. Their size may vary from 25 to 200 µm (Trujillo and Scherer, 2006). The size and number of white adipocytes in the tissue depend on the energy balance and are highly variable. Quantifications of the adipocyte content of adipose tissue range from 15 % to 80 % (Van Harmelen *et al.*, 2003; Eto *et al.*, 2009). A surplus of energy intake initially leads to a growth of the cells, called hypertrophy. When adipocytes have grown to their maximum size, they increase in number. This is called hyperplasia (Hausman *et al.*, 2001). Amongst other factors white adipocytes can release the hormone leptin that regulates the body mass by influencing the individual food

intake (reviewed in (Ailhaud, 2006)). Brown adipocytes have been found in several depots of the human body but not in all adult humans brown adipose tissue can be identified and the brown adipocyte content appears to decrease depending on the individual's age and body mass index (BMI) (Cypess *et al.*, 2009; Saito *et al.*, 2009; Zingaretti *et al.*, 2009; Sacks and Symonds, 2013). In contrast to white adipocytes, brown adipocytes accumulate fatty acids in smaller, multilocular vacuoles and contain more mitochondria. The most distinct feature setting brown adipocytes apart from any other cell type is the expression of the uncoupling protein 1 (UCP1). UCP1 uncouples the proton gradient produced by oxidative phosphorylation from the ATP-production (reviewed in (Rosen and Spiegelman, 2006)).

3.1.2 Stromal vascular fraction

All cells of the so-called stromal vascular fraction (SVF) can be conjointly collected during the process of enzymatic dissociation and centrifugation of the adipose tissue. Cell types of the SVF that could be identified so far include nucleated cells like blood and blood derived cells, endothelial cells, smooth muscle cells, macrophages, pericytes, fibroblasts, hematopoietic progenitor cells and mesenchymal stem/stromal cells as well as non-nucleated cells, erythrocytes (Furness and McNagny, 2006; Zimmerlin *et al.*, 2010; Tallone *et al.*, 2011; Sidney *et al.*, 2014). The composition of the SVF underlies a substantial patient to patient variability. It depends on the vascularization of the tissue and methodical aspects like the technique used for adipose tissue harvest, SVF extraction procedure and the applied analyses methods ((Patrick, 2000; Bourin *et al.*, 2013)). Most characterizations of the cell type composition of the SVF are done via surface marker expression analysis in flow cytometry. To this day most research groups use different panels of surface markers. Furthermore, the time points, when the cells are subjected to analyses, differ. Some groups use freshly isolated cells, others examine cells that have been in an *in vitro* cell culture environment for several passages. Thus, at this point no conclusive statement can be made on the quantity distribution of the different cell types in the SVF. In animal studies the SVF has shown the ability to promote the assembly of vascular networks (Koh *et al.*, 2011; Nunes *et al.*, 2013).

3.1.2.1 Adipose tissue-derived stem/stromal cells

Adipose tissue-derived mesenchymal stem/stromal cells (adMSC) are the type of mesenchymal stem/stromal cell (MSC) that is resident in adipose tissue.

Friedenstein and colleagues were the first to mention MSC as marrow stromal stem cells (Friedenstein, Piatetzky-Shapiro and Petrakova, 1966). They defined the cells to be adherent to tissue culture plastic, clonogenic, nonphagocytic and with a fibroblastic phenotype. Since then many efforts have been made to find and define their exact *in vivo* localization and function. One reasonable model that has been suggested is a perivascular association of MSC where they stabilize the vasculature and contribute to the homeostasis of the surrounding tissue and the immune system. This model also makes sense regarding the fact, that MSC have not only been found in bone marrow (Friedenstein, Piatetzky-Shapiro and Petrakova, 1966) but in essentially all organs (da Silva Meirelles, 2006). They have been isolated from adipose tissue, periosteum, tendon, periodontal ligament, muscle, synovial membrane, spleen, kidney, lung, aorta, vena cava, brain, thymus, skin and lungs ((da Silva Meirelles, 2006) and reviewed in (da Silva Meirelles, Caplan and Nardi, 2008)).

Based on the available data the Mesenchymal and Tissue Stem Cell Committee of the International Society for Cellular Therapy (ISCT) has drafted minimal criteria to define human MSC (Dominici *et al.*, 2006). The cells must be plastic adherent under standard culture conditions, and they must be able to differentiate into osteoblasts, adipocytes and chondroblasts *in vitro* when stimulated accordingly. Third they must be positive for cluster of differentiation 105 (CD105), CD73, and CD90 and negative for CD45, CD34, CD14 or CD11b, CD79a or CD19, and HLA-DR. The CD nomenclature is widely adopted by the scientific community and is officially approved by the International Union of Immunological Societies and approved by the World Health Organization (Engel *et al.*, 2015). The identification of a CD antigen or a group of CD antigens on a cell surface is used for the characterization of cell types, as CD molecules may be specific for one cell or cell lineage (Actor, 2014). The authors acknowledge the need to amend and correct the proposed definitions with the progressing data base on MSC.

The *in vitro* differentiation potential of MSC is versatile. Besides the mesenchymal lineages like osteoblasts, adipocytes, myocytes and chondrocytes, the cells were found to

differentiate into endothelial cells, hepatocytes, smooth muscle cells, neurogenic cells and epithelial cells (Planat-Benard *et al.*, 2004; Rodriguez *et al.*, 2006; Sotiropoulou *et al.*, 2006; Banas *et al.*, 2007; Păunescu *et al.*, 2007; de la Garza-Rodea *et al.*, 2012). As these are all phenomena observed in *in vitro* environments, the trans-differentiation potential of MSC *in vivo* remains in question.

The minimal criteria identifying MSC postulated by the Mesenchymal and Tissue Stem Cell Committee of the ISCT in 2006 have been adjusted and refined for the definition of adMSC by the International Federation for Adipose Therapeutics and Science (IFATS) together with the ISCT in 2013 (Bourin *et al.*, 2013). According to their definition adMSC that are plastic adherent are positive for the surface markers CD90, CD73, CD105, and CD44 and negative for CD45 and CD31 and also possess adipogenic, osteogenic and chondrogenic differentiation potential. One of the most important aspects, that has been added to the criteria is that before submission into tissue culture plastic the cells are also positive for CD34. CD34 was first identified in stromal progenitor cells in adult bone marrow from humans (Simmons and Torok-Storb, 1991). The Stro-1 antibody, frequently used for the isolation of MSC, was subsequently generated using CD34-positive MSC (Simmons and Torok-storb, 1991). CD34 was then found to be expressed also by activated hematopoietic stem cells cycling in the blood stream. Hematopoietic stem cells in a quiescent state reside in the bone marrow and have been found to be CD34 negative (Lin *et al.*, 2013). The panel of CD34-expressing cells was later extended to muscle satellite cells, interstitial cells, epithelial, and endothelial precursors (reviewed in (Sidney *et al.*, 2014)). CD34 is currently thought to be expressed by all perivascular cells *in situ* (Crisan *et al.*, 2012). According to existing literature, approximately 60–85 % of the $CD34^+$ cells of the stromal vascular fraction ($CD34^+$ SVF-cells) are adMSC (Lin *et al.*, 2008; Eto *et al.*, 2009; Zimmerlin *et al.*, 2013; Feisst *et al.*, 2014; Klar *et al.*, 2016). It has been proposed that CD34 promotes proliferation and migration and blocks differentiation *in vivo* (Krause *et al.*, 1996; Nielsen and Mcnagny, 2008). This might be substantiated by the general observation, that CD34-expression decreases with increasing culture time, when the cells in fact do proliferate, migrate and differentiate (Mitchell *et al.*, 2006; Kaiser *et al.*, 2007) .

Compared to bone marrow adipose tissue can be harvested in large quantities in minimally invasive procedures. These procedures are also associated with fewer

discomfort and donor site morbidity for patients (Man and Meyer, 2007). immunomodulatory capacity has been demonstrated in bmMSC and adMSC (Melief *et al.*, 2013). *In vivo* the immunosuppressive function of MSC is thought to be essential for a balanced immune response and the prevention of autoimmunity (reviewed in (da Silva Meirelles, Caplan and Nardi, 2008)).

3.2 Adipose tissue and derived cells in the clinic

Adipose tissue as well as isolated cellular components are clinically applied for regenerative therapy approaches. Adipose tissue has been used to treat for example carpometa-carpal joint osteoarthritis, wound healing deficits and radiation damage (Rigotti *et al.*, 2007; Stasch *et al.*, 2015; Herold *et al.*, 2017). The SVF separated from adipose tissue has also been applied in the clinical setting for a wide variety of indications. They have been applied to treat ischemic cardiomyopathy, urinary incontinence, osteoarthritis, chronic ulcers, enterocutaneous fistula, systemic sclerosis (Marino *et al.*, 2013; Gotoh *et al.*, 2014; Perin *et al.*, 2014; Guillaume-Jugnot *et al.*, 2015; Michalek *et al.*, 2015; Mizushima *et al.*, 2015). Also adMSC have been isolated and cultured prior to their clinical application. In the course of some studies the influence of adMSC on multiple sclerosis, graft versus host disease and osteoarthritis (Fang *et al.*, 2007; D. *et al.*, 2010; Pers *et al.*, 2016) was examined with promising results. In case studies, human adMSC were also successfully used to treat critical-size calvaria and maxilla defects (Lendeckel *et al.*, 2004; Mesimäki *et al.*, 2009).

3.3 Energy metabolic analyses of cells and tissues

3.3.1 Rational of determining the energy metabolic phenotype by enzyme activity measurements

Changes in metabolism can be caused by and also be dependent on cell fates such as proliferation, differentiation or apoptosis (reviewed in (Ochocki and Simon, 2013; Shyh-Chang and Daley, 2015)). The demands on energy supply of different cell types vary dependent on their function and environment (reviewed in (Lonergan, Bavister and Brenner, 2007; Vander Heiden, Cantley and Thompson, 2009)). Short-term changes in energy demand that require adaptation within seconds (e.g. in the active muscle), can be realized by modifications of regulatory enzymes that will lead to increases or decreases

of activity. These modifications can be of non-covalent (allosteric regulation) or of covalent nature (e. g. phosphorylation). Changes of enzyme concentrations are rather an indication of long term adaptations of energy metabolism to specific environments or cell functions (Nelson and Cox, 2011). Enzyme activities measured *in vitro* under standard optimal conditions are designated as international units per mg DNA (1 U=1 µmol substrate transformed per min at 37 °C). Thus, *in vitro* measured maximum activities represent a capacity of metabolic turnover and not the turnover *in vivo* in a specific metabolic state. However, the maximum activities of enzymes which catalyze irreversible or flux-limiting reactions of different metabolic pathways serve as indicators of the participation of these pathways in energy metabolism, as previous studies have shown a good correlation of the capacities of energy metabolic pathway marker enzymes with their contribution to the energy metabolism (Newsholme and Start, 1977). This is the case for enzymes that catalyze reactions far away from the equilibrium (called non-equilibrium reactions), that will show enzyme activities close to the actual activities *in vivo*. In contrast, enzymes working near the thermodynamic equilibrium of the reaction (called near-equilibrium reactions), will likely show lower activities *in vivo* than measured *in vitro* (Pette, 1970).

3.3.2 Analyzed enzymes of the cellular energy metabolism

Metabolism accomplishes four essential functions for cells. It breaks down complex nutrients into simpler molecules and generates energy (i.e. catabolism). It builds up macromolecules from simpler molecules which consumes energy (i.e. anabolism). It provides energy in the form of ATP in order to facilitate cellular functions, for example the transportation of molecules into and out of the cell. Finally, many metabolites from various pathways also play a role in cellular signaling and gene transcription (Chandel, 2015). The presented studies focus on catabolic processes leading to the provision of energy as well as anabolic processes utilizing cellular energy in the form of ATP.

Glycolysis is the initial step in the metabolic breakdown of glucose. During glycolysis one molecule of glucose is broken down in to two molecules of pyruvate. Two molecules of ATP and nicotinamide adenine dinucleotide anion (NADH) are produced respectively. This takes place in the cytosol and does not require oxygen. The **phosphofructokinase** (**PFK**; EC 2.7.1.11) catalyzes the second of the three irreversible

reactions of glycolysis (Chandel, 2015), the conversion of fructose-6-phosphate and ATP to fructose-1,6-bisphosphate and adenosine diphosphate (ADP). It is thus one of the essential, rate limiting steps of glycolysis. The maximum PFK activity measured *in vitro* can be recognized as the capacity of glycolysis *in vivo.* The sixth step of glycolysis, the reversible oxidative phosphorylation of glyceraldehyde-3-phosphate to 1,3-bisphosphoglycerate, in the presence of inorganic phosphate and nicotinamide adenine dinucleotide (NAD^+), is catalyzed by the **glyceraldehyde-3-phosphate dehydrogenase** (**GAPDH**; EC 1.2.1.12) (Veech, Raijman and Krebs, 1970).

The pyruvate molecules resulting from glycolysis can be used by the cells in different ways. If the oxygen supply of the cell is sufficient, the pyruvate is transported into the mitochondria where it is decarboxylated to acetyl coenzyme A (acetyl-CoA) and as such enters the tricarbolic acid cycle (TCC). The TCC has been identified to be amphibolic. Depending on the current supply of energy within the cell, intermediates of the TCC can be metabolized in a circulatory fashion producing the reduction equivalents NADH and flavin adenine dinucleotide hydroquinone ($FADH_2$), which donate electrons to the electron transport chain, resulting in the formation of the proton gradient that is needed for ATP production. This would be the catabolic function of the TCC. If the cell is in need of building blocks for biosynthesis, the anabolic function of the TCC is primarily active. The intermediate α-ketoglutarate, for example, is produced by the irreversible (and thus rate limiting) oxidative decarboxylation of isocitrate, catalyzed by the **NAD^+-dependent isocitrate dehydrogenase** (**NAD-IDH**; EC 1.1.1.41) or the reversible oxidative decarboxylation of isocitrate, catalyzed by the **$NADP^+$-dependent isocitrate dehydrogenase** (**NADP-IDH**; EC 1.1.1.42) (Henderson, 1965). It can be converted to glutamate, that can generate glutamine, a precursor for the synthesis of purine nucleotides (Chandel, 2015), building blocks of deoxyribonucleic acid (DNA).

In cells lacking physiologic oxygen supply for oxidative phosphorylation (Nelson and Cox, 2011), or in highly proliferative cells, a mechanism is activated in which **lactate dehydrogenase** (**LDH**; EC 1.1.1.27) reduces pyruvate into lactate under the conversion of NADH into NAD^+ (Warburg, Wind and Negelein, 1927; Lunt and Vander Heiden, 2011). This way the production of lactate is coupled to the regeneration of NAD^+ that can re-enter glycolysis, that may thus be kept active without the need for oxidative phosphorylation. If the need of the cells for energy and building blocks is saturated,

pyruvate can be converted into glucose via gluconeogenesis. In order to avoid a futile cycle, gluconeogenesis and glycolysis are tightly regulated pathways, that are reciprocally controlled. If one process is active, the other is not entirely shut down but strongly inhibited(Chandel, 2015). The pyruvate for gluconeogenesis will thus not be derived from glycolysis but from precursors like lactate, glycerin or some amino acids. Glycolysis and gluconeogenesis share the enzymes that control the reversible reaction steps. The three irreversible reactions of glycolysis are bypassed by alternative enzymes so gluconeogenesis can proceed (Nelson and Cox, 2011). While fructose-6-phosphate is converted to fructose-1,6-bisphosphate by PFK during glycolysis, the dephosphorylation of fructose-1,6-bisphosphate to fructose 6-phosphate is catalyzed by **fructose-1,6-bisphosphatase** (**FBPase**, EC 3.1.3.11) during gluconeogenesis. FBPase represents one of the rate limiting steps of gluconeogenesis.

The FBPase is also of major importance for the function of the pentose phosphate pathway (PPP). The PPP can be subdivided into an oxidative and a nonoxidative phase. In the nonoxidative phase, depending on the demand of the cell, carbohydrates with a different amount of carbon atoms can be converted into one another by transketolases and transaldolases. These can then be used as precursors for different anabolic pathways. Ribose-5-phosphate for example is needed for the synthesis of nucleotides (Chandel, 2015). During the oxidative phase of the PPP ribose-5-phosphate is oxidized, resulting in the formation of carbon dioxide, hydrogen ions and NADPH. The first step of the oxidative phase of the PPP, the oxidation of glucose-6-phosphate to 6-phosphoglucono-δ-lactone, is catalyzed by the **glucose 6-phosphate dehydrogenase** (**G6PDH**; EC 1.1.1.49). The produced NADPH is on one hand required for the biosynthesis of fatty acids and isoprenoids; on the other hand, it is needed for the maintenance of the antioxidative activity of glutathione. Glutathione is a scavenger of reactive oxygen species (ROS) that are formed during oxidative phosphorylation in the mitochondria. During the neutralization of ROS, glutathione is oxidized and forms a dimer with another oxidized glutathione. For the restoration of its antioxidative properties the glutathione disulfide is reduced and converted back into two monomers by the **glutathione disulfide reductase** (**GSR**; EC 1.8.1.7). For this reaction the GSR uses the NADPH supplied by the G6PDH reaction. By measuring the GSR activity, the level of oxidative stress and thus the level of oxidative phosphorylation for ATP production in the mitochondria can be assessed indirectly.

If the glucose supply is low, fatty acids are the primary source of cellular energy. The catabolic breakdown of fatty acids is called β-oxidation. This pathway is located in the mitochondrial matrix, generates NADH and $FADH_2$ and thus facilitates ATP production. The **ß-hydroxyacyl-CoA dehydrogenase** (**HOADH**; EC 1.1.1.35) catalyzes the third of four steps that are continuously repeated during the degradation of the fatty acid chain molecules (Wakil *et al.*, 1954). In this step, β-hydroxyacyl-CoA is oxidized to β-ketoacyl-CoA while NAD^+ is reduced to NADH. Following this step acetyl-CoA is released from the fatty acid molecule. Acetyl-CoA can then be transferred into the TCC.

Finally, an enzyme known to be found in cells with temporarily high or fluctuating energy turnover like striated muscle or nervous tissue (Berlet, Bonsmann and Birringer, 1976; Wallimann and Hemmer, 1994b) was examined. The **creatine kinase** (**CK**; EC 2.7.3.2) catalyzes the near-equilibrium reaction of the conversion of creatine into phosphocreatine under the consumption of ATP (Lohmann, 1934). As this reaction is reversible, ATP can also be generated from phosphocreatine and ADP by the CK. The enzyme was first identified in the cytosol, but the finding of a mitochondrial isozyme led to the idea of a functional coupling of CK with oxidative phosphorylation, the so called phosphocreatine shuttle (Bessman, 1972; Saks *et al.*, 1985; Wallimann and Hemmer, 1994b). In the mitochondria the synthesis of phosphocreatine is catalyzed by the mitochondrial CK with nascent ATP. It diffuses to the myofibrils. As during a contraction myosin-ATPases generate ADP, the muscular creatine kinase catalyzes the regeneration of ATP from phosphocreatine and ADP to allow the contraction to continue. Creatine is thus released from the myofibrils and diffuses back to the mitochondria where it is re-phosphorylated to creatine phosphate. The immediate return of ADP in the mitochon-dria, stimulates oxygen uptake (Bessman, 1972; Bessman and Carpenter, 1985).

3.4 Energy metabolism of adipose tissue and derived cell types

3.4.1 Energy metabolism of adipose tissue

First specimens of energy metabolic studies were homogenates of whole adipose tissue from living as well as deceased patients (Schmidt and Schmidt, 1960; Shonk *et al.*, 1964; Schwandt *et al.*, 1970). Due to the aforementioned variations in cellular composition of the adipose tissue these examinations of adipose tissue metabolism

cannot give a differentiated picture regarding the metabolic configuration of specific cell populations. Those limitations have been recognized and discussed. As such, varying blood contents of the specimens as well as *post mortem* enzyme activation and inactivation may cause major deviations in the spectrum of identified enzymes and measured enzyme activities (Schmidt and Schmidt, 1960).

Early examinations have found low glycolytic enzyme activities compared to other tissues like skeletal muscle. The determined activities of glycolysis were comparable to measured activities of gluconeogenesis (Shonk *et al.*, 1964; Schwandt *et al.*, 1970). Moreover, it was uncovered, that the energy metabolic configuration strongly diverges between different mammalian species. As such activities measured in rat adipose tissue for example cannot automatically be conferred to another mammalian species. First examinations of the glucose metabolism of rat adipocytes and cells of the stromal vascular fraction separated from the same tissue were carried out in 1964 (Rodbell, 1964). It was suggested that the glucose metabolism of the whole adipose tissue was quantitatively made up by the measured adipocyte glucose metabolism. Stromal vascular cells did not take part in triglyceride synthesis.

Recent studies compared the metabolism of adipocytes and stromal vascular cells from human tissue. Protein expression analysis implies that glycolysis and gluconeogenesis are upregulated in adipocytes compared to SVF-cells separated from the same tissue (Kheterpal *et al.*, 2011). Ribonucleic acid (RNA)-expression analysis showed an upregulation of lipolysis related genes and GAPDH mRNA in adipocytes compared to SVF-cells (Fain *et al.*, 2008).

The presence and high activity of CK in white as well as brown adipocytes has been verified (Berlet, Bonsmann and Birringer, 1976; Wallimann and Hemmer, 1994a). In white adipocytes creatine could accept its phosphate group from cytoplasmic ATP generated during glycolytic substrate phosphorylation. It could also be synthesized in the mitochondria from nascent ATP produced during oxidative phosphorylation, as it was earlier described for the phosphocreatine shuttle (Bessman and Carpenter, 1985).

3.4.2 Energy metabolism of adipose tissue-derived stem/stromal cells *in vitro*

Based on the paucity of scientific knowledge on the energy metabolism of adMSC, conclusions can mainly be drawn from studies examining MSC. Studies concerning the

energy metabolism of MSC, typically describe bmMSC. In these studies, the metabolism is mainly characterized using the quantification of the uptake of nutrients and release of metabolites. Rather than using oxidative phosphorylation, bmMSC primarily metabolize glucose via aerobic glycolysis (Schop *et al.*, 2009). Pattappa et. al. thus suspected the MSC to show the Warburg effect (Pattappa *et al.*, 2011). The Warburg effect is defined as the utilization of glycolysis followed by lactate production as the major energy source despite sufficient oxygen being present for the cells to carry out oxidative phosphorylation (Warburg, 1956). This metabolic configuration had previously been shown mostly for cancer cells (Pelicano *et al.*, 2006).

Osteogenically stimulated bmMSC as well as bmMSC without stimulation were found to produce ATP via a mixture of glycolysis as well as oxidative phosphorylation (Pattappa *et al.*, 2011). By gene expression analysis, it was uncovered that the osteogenic differentiation of bmMSC leads to an increase of mitochondrial DNA copies. At the same time the intracellular amount of ATP and the activity of anti-oxidative enzymes increase, suggesting an increase of oxidative metabolism due to osteogenic differentiation (Chen *et al.*, 2008). There are divergent findings on the development of oxygen uptake during osteogenic differentiation (Chen *et al.*, 2008; Pattappa *et al.*, 2011). While Chen et al. had documented an increasing rate of cellular oxygen consumption upon osteogenic stimulation of bmMSC, Pattapa et al. had observed similar rates of cellular oxygen consumption in bmMSC cultured without stimuli and following osteogenic stimulation.

Adipogenic differentiation of bmMSC is described to be regulated by mitochondrial respiration (Zhang *et al.*, 2013). In bmMSC undergoing early adipogenic differentiation antioxidative defense components become more oxidized, remaining in this state throughout the process. This suggests a regulation of differentiation by the redox state of the cell and thus assigns an essential role to antioxidative components like glutathione (Imhoff and Hansen, 2011). Adipogenic differentiation of adMSC is accompanied by an increase in the amount of mitochondrial as well as glycolytic and fatty acid metabolism associated proteins (DeLany *et al.*, 2005).

3.5 **Working hypothesis and objectives**

The development of new possibilities for the therapeutic application of extracted adipose tissue have made the choice of the liposuction technique a vital issue. In this context not only aspects of patient comfort and donor site morbidity are of importance. Also, basic properties of the aspirated tissue like the cellular composition and viability need to be characterized. Water-jet assisted liposuction has proven to provide a favorable aesthetic outcome combined with lowered risk of cardiovascular side effects compared with conventional liposuction procedures (Man and Meyer, 2007; Stutz and Krahl, 2009; Stabile *et al.*, 2014). Thus, in the first study we examined adipose tissue aspirated with water-jet assistance for the presence of adMSC possessing the characteristic properties defined for this cell type by the ISCT.

Each of the cell types in adipose tissue, contributes to the physiological homeostasis of the tissue and possesses a metabolism that can be adapted to meet demands for diverging functions and needs. It is known, that different cell populations residing within adipose tissue show distinct behavior regarding proliferation and differentiation (Vander Heiden, Cantley and Thompson, 2009; Lunt and Vander Heiden, 2011). The intent of the second study was thus to compare maximum catalytic activities of major energy metabolic pathways of isolated mature adipocytes and $CD34^+$ SVF-cells.

After showing that differing proliferative potential of distinct cell populations from adipose tissue is accompanied by differing energy metabolic configurations, we hypothesized that the *in vitro* culture and differentiation of adMSC that is accompanied by changes in their proliferative behavior causes a diverging energy metabolic phenotype. Therefore, we analyzed major metabolic pathway activities in undifferentiated and differentiating adMSC in parallel with the cell numbers and degree of differentiation.

With these new data we would be able to contribute to the characterization of the energy metabolic phenotype of distinct cell populations of the human adipose tissue in the native state and after *in vitro* culturing with osteogenic and adipogenic differentiation.

4 Summary and discussion of the publications

4.1 Summary and discussion Study I - *Isolation and differentiation potential of human mesenchymal stem cells from adipose tissue harvested by water jet-assisted liposuction*

As water jet-assisted lipoplasty is a favorable aspiration method regarding aesthetic outcome and patient comfort (Man and Meyer, 2007), it was necessary to assess the tissues suitability as a source of adMSC. Therefore, we examined the amount of isolatable SVF cells and the content of adMSC in the SVF. After isolation the proliferation and mesenchymal differentiation capacities of the cells were examined. This work was published in the Aesthetic Surgery Journal under the title "Isolation and differentiation potential of human mesenchymal stem cells from adipose tissue harvested by water jet-assisted liposuction".

By flow cytometric characterization we could show that from 1 ml of tissue on average 6.1 x 10^5 viable nucleated cells of the stromal vascular fraction may be isolated (Fig. 1). Different SVF cell numbers have been found after using different tissue harvesting methods. A study not selecting for a specific liposuction technique found an average of 3×10^5 isolatable SVF-cells per ml tissue (Mitchell *et al.*, 2006). Another study found 6×10^5 SVF-cells per ml tissue after ultrasound-assisted liposuction and 7×10^5 SVF-cells per mL tissue after adipose tissue resection (Oedayrajsingh-Varma *et al.*, 2006).

Determined by magnetic bead selection we determined an average of 43 % of the viable plastic adherent SVF-cells to be CD34 positive. Examinations of other groups resulted in averages of 22.5 % (James *et al.*, 2012) and 15 % to 40 % cells per ml tissue (Yoshimura *et al.*, 2006). One portion of the CD34-positive cells is of hematopoietic origin while the other is adMSC. This was confirmed by Bourin *et al*. by detecting a CD34-positive, yet CD45-negative population of cells within the SVF of adipose tissue. Hematopoietic precursors would be positive for both surface markers (Bourin *et al.*, 2013). The mesenchymal and hematopoietic populations could also be separated by selecting them for tissue culture polystyrene adherence because adMSC are plastic adherent (Rada, Reis and Gomes, 2011) whereas hematopoietic stem cells are not

(Glimm and Eaves, 1999; Handgretinger *et al.*, 2002). While the adMSC content is often quantified solely by flow cytometric analysis of the SVF, in our study the absolute adMSC content was ultimately determined after 24 hours of plastic adherence. About 18 % of the viable SVF became adherent to tissue culture plastic. After 24 hours nearly 8 % of the initially isolated SVF could be identified as plastic-adherent and CD34-positive and thus representing a homogenous population of adMSC. Other groups have found 6.3 %±1.8 % to be functional adMSC residing in the SVF of resected adipose tissue, 1.9 %±1.3 % functional adMSC in the SVF of tissue obtained by tumescent liposuction, and 0.4 %±0.1 % functional adMSC in the SVF of tissue obtained by ultrasound-assisted liposuction (Oedayrajsingh-Varma *et al.*, 2006).

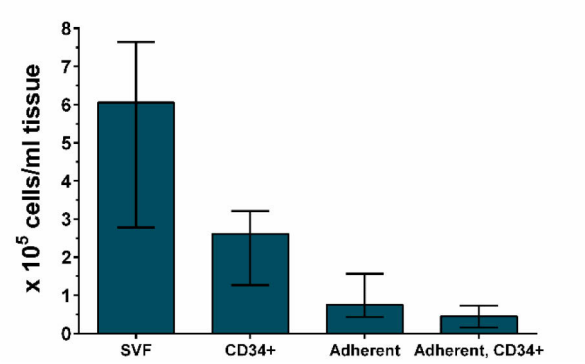

Fig. 1: Quantification of cell amount after each isolation step. 6.1x10^5 cells/g tissue in the SVF; 2.6x10^5 CD34$^+$ cells/g tissue in the SVF; 0.8x10^5 cells/g tissue adherent after 24 h; 0.45x10^5 cells/g tissue adherent after 24 hand CD34$^+$; data displayed as medians of 7 donors; measurements as technical duplicates; adapted from (Meyer *et al.*, 2015)

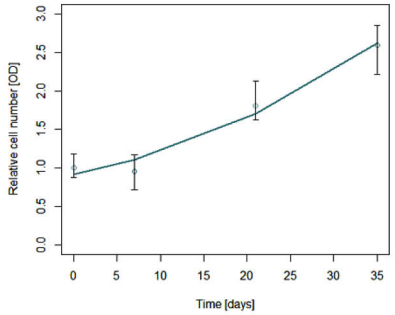

Fig. 2: Quantification of proliferation of adMSC under steady state standard cultivation. Cells show continuous proliferation over 35 d of cultivation. Data displayed as medians of 8 donors; measurements as technical triplicates; adapted from (Meyer *et al.*, 2015)

With a range from 2.3 % to 17.9 %, broad deviations of adMSC content in the SVF are evident for our data. Such ranges have been obtained by others before. Philips et al. for example found the range of adMSC content in the SVF to range from 4 % to 37 % (Philips *et al.*, 2013). The overall differences between the study outcomes result from differences between the aspiration methods and differences between the methods used for the analysis of adMSC content in adipose tissue.

Measurements under steady state standard culturing conditions at 0, 7, 21 and 35 days, confirmed increasing cell numbers over time and thus the ability of the cells to proliferate (Fig. 2). The mesenchymal differentiation potential of the isolated adMSC was determined by cytochemical staining of specific markers of differentiation after culture with adipogenic and osteogenic stimulation. After 14 days of adipogenic stimulation, a

significant 3-fold increase of the formation of lipid-filled vacuoles in adMSC was detectable, whereas no vacuoles were found in adMSC under control conditions (Fig. 3). This proves the adipogenic differentiation potential of the adMSC from WAL tissue.

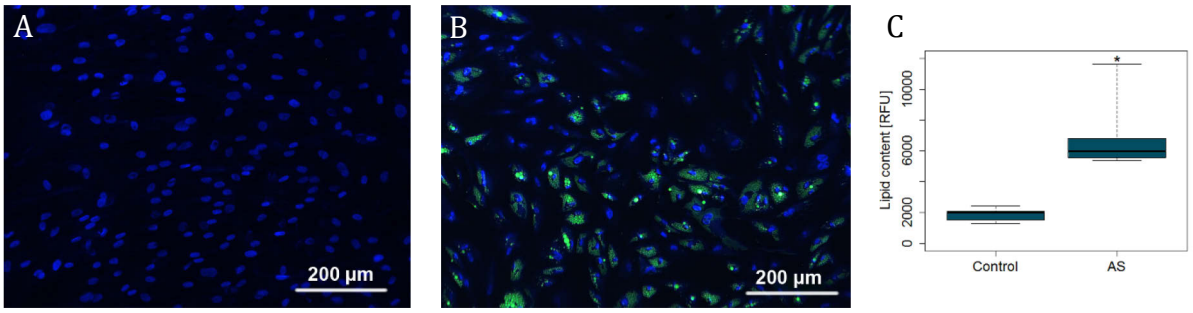

Fig. 3: Adipogenic differentiation of adMSC. Staining of lipid vacuoles (green) and nuclei (blue) in unstimulated control cultures (A) and adipogenically stimulated adMSC (AS) after 14 days (B). Quantification of lipid content (C, quantification of fluorescence intensity; data displayed as medians of 5 donors; measurements as technical triplicates; *=significantly different; Mann-Whitney U Test, $p < 0.05$). Adapted from (Meyer *et al.*, 2015)

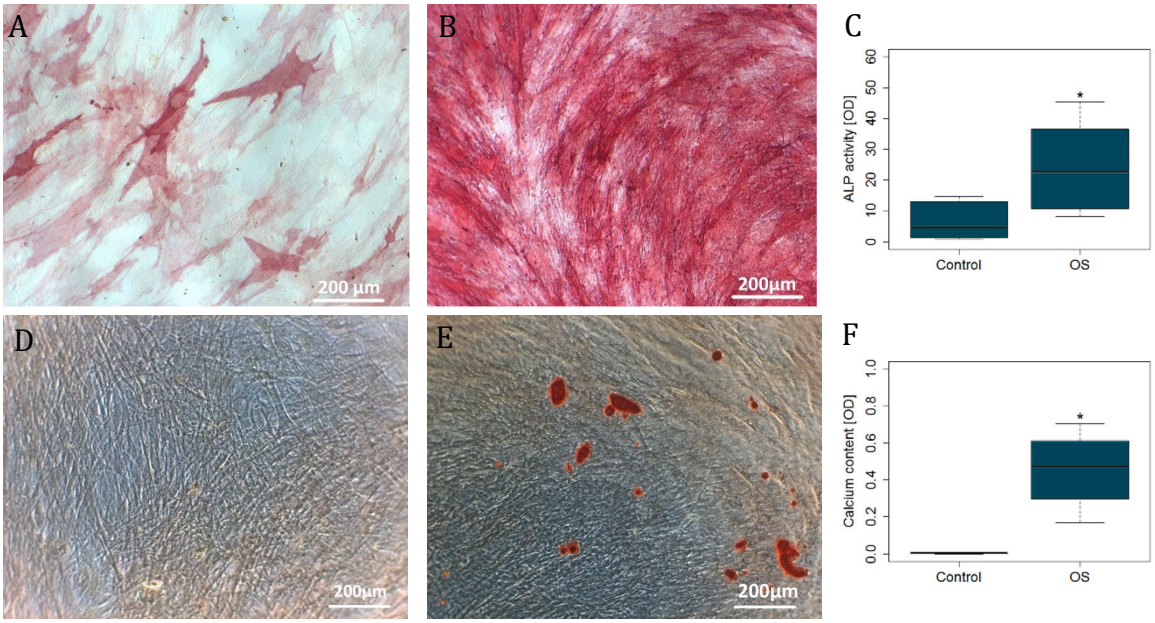

Fig. 4: Osteogenic differentiation of adMSC. ALP-staining (red) in control cultures (A) and in osteogenically stimulated cultures (OS) after cultivation for 21 days (B). Quantification of ALP activity (C; data displayed as medians of 6 donors; *=significantly different; measurements as technical triplicates; Mann-Whitney U Test, $p < 0.05$). Staining of ECM calcium deposition in control cultures (D) and osteogenically induced cultures after cultivation for 35 days (E). Quantification of ECM calcium content (F, cresolphthalein staining; data displayed as medians of 4 donors; measurements as technical triplicates; *=significantly different; Mann-Whitney U Test, $p < 0.05$). Compared with non-stimulated control cultures, osteogenically stimulated cultures showed a 4-fold increase in ALP activity after 21 days and a 100-fold higher calcium deposition in the ECM after 35 days. Adapted from (Meyer *et al.*, 2015)

The osteogenic differentiation potential was examined by the quantification of the activity of the enzyme bone-specific alkaline phosphatase (ALP) and the amount of calcium phosphate deposited to the extracellular matrix (ECM). After 21 days in culture osteogenically stimulated cells showed a 4-fold higher ALP-activity then the cells in

control cultures without specific stimulation. ECM calcium phosphate deposition by adMSC stimulated osteogenically for 35 days was almost 100-times higher than in the control cultures, which showed almost no calcium phosphate deposition (Fig. 5). We were thus able to verify the mesenchymal differentiation potential of adMSC from WAL tissue.

4.2 Summary and discussion Study II - *Human adipocytes and CD34$^+$ cells from the stromal vascular fraction of the same adipose tissue differ in their energy metabolic enzyme configuration*

Dependent on the developmental stage of the individual and the depot location, adipose tissue varies in cellular composition and metabolic phenotype. As the knowledge about the energy metabolism of specific cell types of human adipose tissue is limited, we compared marker enzyme activities of major energy metabolic pathways of human adipocytes with those of the CD34$^+$ SVF-cell population with enriched adMSC content (Lin *et al.*, 2008; Eto *et al.*, 2009; Zimmerlin *et al.*, 2013; Feisst *et al.*, 2014; Klar *et al.*, 2016). This work was published in Experimental Cell Research under the title "Human adipocytes and CD34$^+$ cells from the stromal vascular fraction of the same adipose tissue differ in their energy metabolic enzyme configuration".

For the separation of the two cell populations, human adipose tissue was subjected to enzymatic dissociation, generating a single-cell suspension. Via washing, filtration and centrifugation the lipid phase containing only adipocytes was separated from the aqueous phase that contained the SVF-cells. Through this procedure adipocytes, recognizable due to their monolocular vacuole and SVF-cells, characterized by diversity in morphology, were collected. A significant subpopulation of the SVF shows a surface expression of the transmembrane phosphoglycoprotein CD34 (Mitchell *et al.*, 2006; Zimmerlin *et al.*, 2010; Tallone *et al.*, 2011; Bourin *et al.*, 2013). Flow cytometry showed that 36.9 % of the total isolated SVF-cells were CD34$^+$. Concurrent positivity for CD34 as well as for CD45 was detected for only 0.9 % of the SVF-cells. Thus, within the CD34$^+$ SVF, 97.6 % of the cells were CD45-negative (CD45$^-$). By means of a magnetic bead selection, the CD34$^+$ cells were accumulated and separated (Fig. 5). The CD34$^+$ SVF-cell population contains endothelial cells, endothelial progenitors, hematopoietic progenitors, adMSC and adipocyte progenitors (Furness and McNagny, 2006; Sidney *et al.*,

2014). Other groups have found 13.3 % to 15.4 % of the adipose tissue SVF to be CD45$^-$/CD34$^+$ and CD31$^+$. SVF-cells with this composition of surface markers are mature endothelial cells or endothelial progenitors (Eto *et al.*, 2009; Zimmerlin *et al.*, 2013). We found only 0.9 % of the nucleated SVF-cells to be hematopoietic precursors, that are CD34$^+$/CD45$^+$ (Tavian *et al.*, 1996). In other studies, 2–4 % of SVF-cells were detected to be CD34$^+$/CD45$^+$ (Astori *et al.*, 2007; Rose *et al.*, 2015). Altogether 60–85 % of the SVF-cells collected with the described method of CD34-bead selection can be considered adMSC (Lin *et al.*, 2008; Zimmerlin *et al.*, 2013; Feisst *et al.*, 2014; Klar *et al.*, 2016).

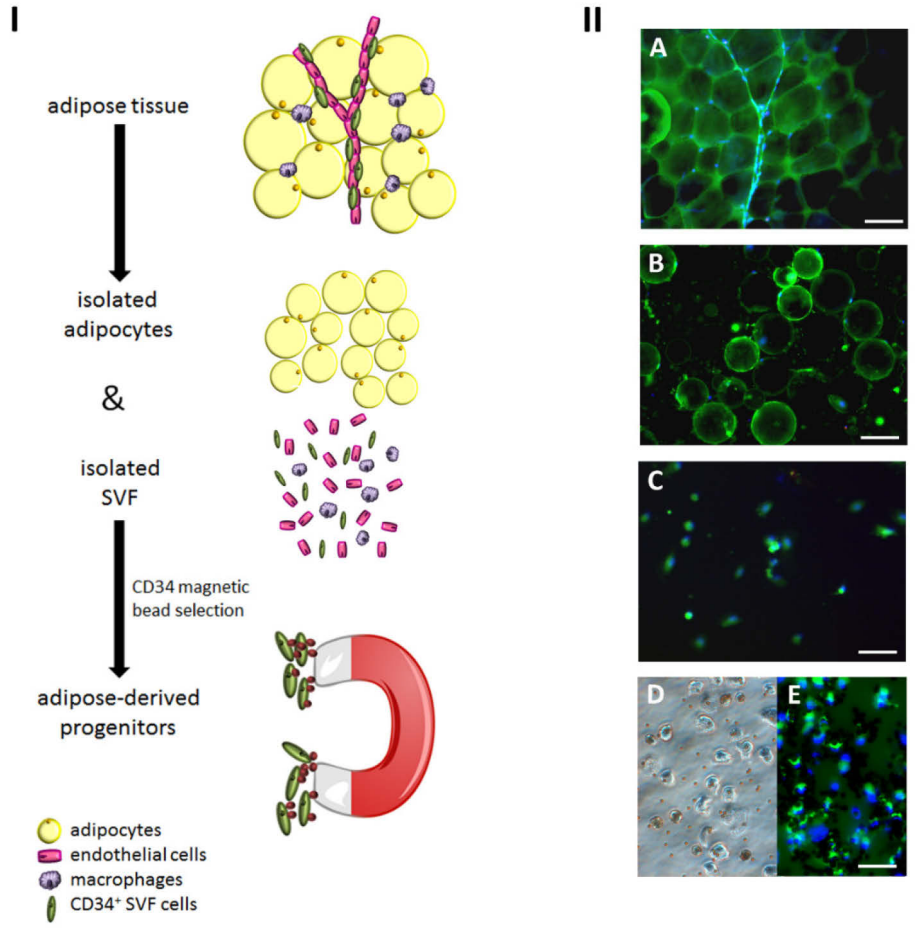

Fig. 5 I: Schematic depiction of the adipose tissue processing and II: Microscopic depiction of the tissue and cell fractions during processing. A) aspirated adipose tissue, (B) adipocytes from the lipid phase of the tissue preparation, (C) SVF after separation, (D) phase contrast micrograph of CD34+ SVF-cells with magnetic beads, (E) vital/nuclear stain of the CD34+ SVF-cells from the SVF with magnetic beads (green: vital stain, blue: nuclei, scale bar=100 µm in A and B; 50 µm in C, D and E). Adapted from (Meyer *et al.*, 2019)

Mature adipocytes are considered to not proliferate but continuously turnover their stored lipids (Hausman *et al.*, 2001; Strawford *et al.*, 2004; Spalding *et al.*, 2008). As the majority of the CD34$^+$ SVF-cells possess a precursor status, they have the potential to proliferate and differentiate (Ogawa, 1993; Hausman *et al.*, 2001; Zuk *et al.*, 2002; Yoder,

2012). Adipocytes and CD34+ SVF-cells thus face distinct physiological requirements that might cause differences in their metabolic configuration.

Activity of the glycolysis-related enzymes PFK (0.21 U/mg DNA in adipocytes; 0.95 U/mg DNA in CD34+ SVF-cells), GAPDH (10.8 U/mg DNA in adipocytes; 6.37 U/mg DNA in CD34+ SVF-cells) and LDH (25.3 U/mg DNA in adipocytes; 11.1 U/mg DNA in CD34+ SVF-cells) could be detected in both cell populations, and thus indicate the capacity for glycolysis (Scrutton and Utter, 1968; Schwandt *et al.*, 1970) (Fig 6A, B & C). Herein the glycolytic enzymes GAPDH and LDH displayed the highest activities in both cell populations and were significantly higher than the measured PFK activities. Shonk et al. detected PFK, GAPDH and LDH activities in human whole adipose tissue homogenates in similar proportions (Shonk *et al.*, 1964). As the PFK catalysis the flux-determining, non-equilibrium reaction of glycolysis making it the rate limiting step, it can be concluded, that there is higher capacity for glycolysis in CD34+ SVF-cells than in adipocytes. Kheterpal et al. found conflicting results regarding the capacity of glycolysis when they detected a higher GAPDH protein amount in adipocytes compared with the whole SVF and lower protein amounts of triosephosphate isomerase at the same time (Kheterpal *et al.*, 2011). Anaplerosis of the glycolytic pathway from glycerol could be an explanation for this inverse behavior. The substrate of GAPDH, i.e. 3-phosphoglyceraldehyde, would then originate from glycerol, synthesized by the activities of the enzymes glycerol kinase, glycerol-3-phosphate dehydrogenase and triose phosphate isomerase (Nelson and Cox, 2011) instead of fructose-1,6-bisphosphate. All three enzymes have been identified in white adipose tissue or adipocytes respectively (Chakrabarty, Chaudhuri and Jeffay, 1983; Swierczynski *et al.*, 2003; Kheterpal *et al.*, 2011; Sledzinski *et al.*, 2013). Glycolysis is increased in cells that proliferate actively (Vander Heiden, Cantley and Thompson, 2009). In contrast to adipocytes CD34+ SVF-cells possess proliferative potential (Strawford *et al.*, 2004). Contrary to cultured adMSC that proliferate actively, cultured adMSC that do not proliferate have been shown to decrease their glycolytic capacity. Under the same *in vitro* conditions the activity of the marker enzyme of gluconeogenesis, FBPase, was below the detection limit (Meyer *et al.*, 2018). In this study the activity of the FBPase was low but detectable (0.04 U/mg DNA in adipocytes; 0.01 U/mg DNA in CD34+ SVF-cells) (Fig. 6E). This deviation could demonstrate an adaptation to the *in vitro* conditions with a surplus of glucose available, compared to the *in vivo* situation (Cunha *et al.*, 2016).

Thus, it may be concluded that *in vivo* adipocytes and CD34⁺ SVF-cells from adipose tissue keep up a metabolic flexibility to be able to facilitate gluconeogenesis if necessary.

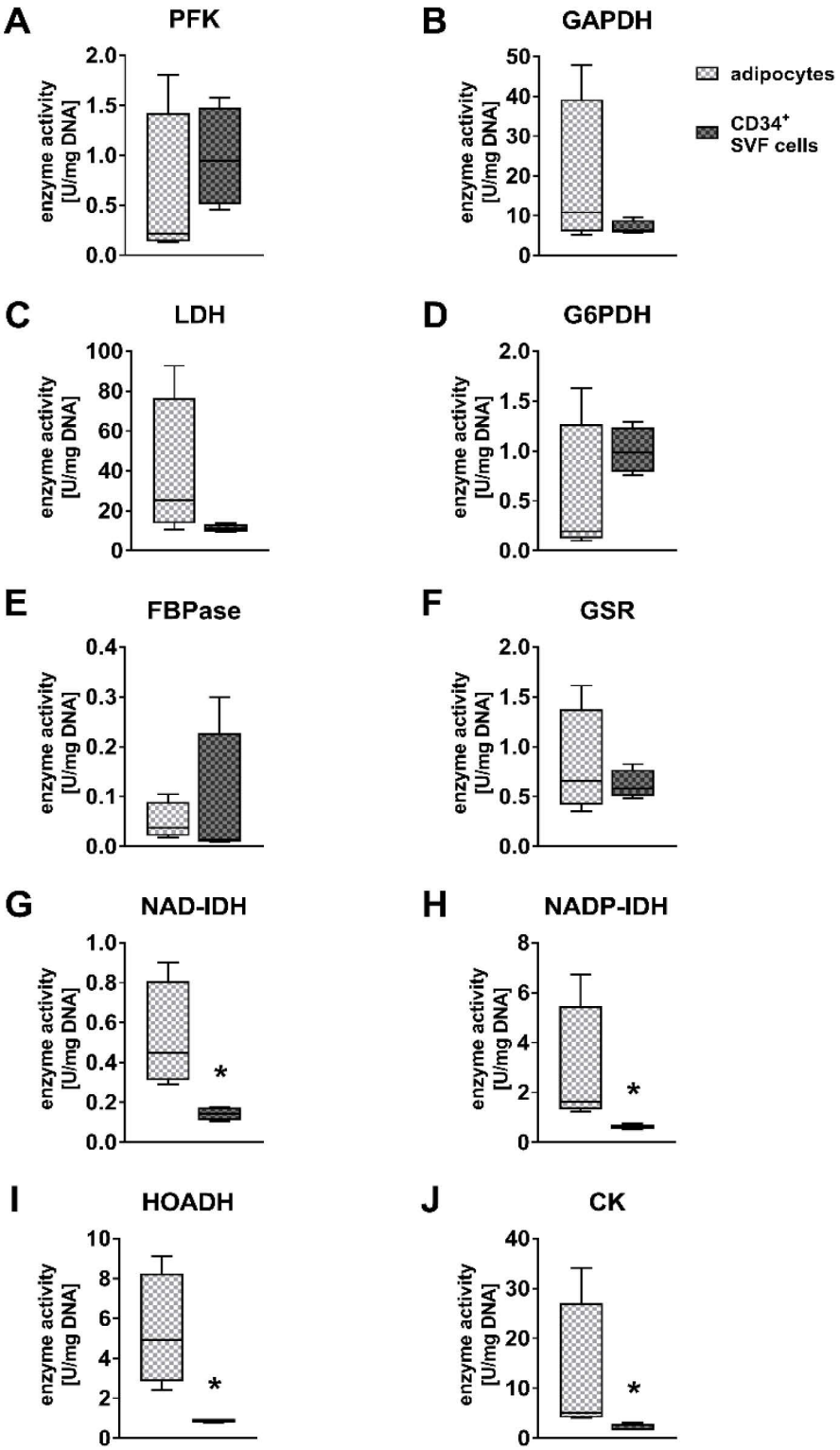

Fig. 6: Marker enzyme activities in adipocytes and the CD34+ SVF-cells. (A) PFK; (B) GAPDH; (C) LDH; (D) G6PDH; (E) FBPase; (F) GSR; (G) NAD-IDH; (H) NADP-IDH; (I) HOADH and (J) CK; activities were normalized to the overall DNA content of the cells (data displayed as medians of 4 donors; measurements as technical duplicates; *=significantly different; Mann-Whitney U Test, $p < 0.05$). Adapted from (Meyer *et al.*, 2019)

Intermediates of glycolysis can be branched off to the PPP (Chandel, 2015). Rate-limiting enzyme of the PPP is the G6PDH. Similar activities were determined for the G6PDH (0.19 U/mg DNA in adipocytes; 0.98 U/mg DNA in CD34$^+$ SVF-cells) as for PFK, suggesting a similar capacity for the PPP and glycolysis (Fig. 6D). Highly active proliferation *in vitro* has been associated with high G6PDH activity (Tian *et al.*, 1998). These *in vitro* observations are confirmed by the data of this study where both cell types have been examined without prior subjection to *in vitro* conditions. Adipocytes that do not proliferate (Si, Yoon and Lee, 2007) display lower G6PDH activity. CD34$^+$ SVF-cells that possess the potential to proliferate (Zuk *et al.*, 2001) displayed higher G6PDH activity.

All measured enzymes, that are involved in mitochondrial metabolism, showed significantly higher activities in adipocytes than in CD34$^+$ SVF-cells. The activities of NAD-IDH (0.44 U/mg DNA in adipocytes; 0.14 U/mg DNA in CD34$^+$ SVF-cells), NADP-IDH (1.63 U/mg DNA in adipocytes; 0.63 U/mg DNA in CD34$^+$ SVF-cells) and HOADH (4.93 U/mg DNA in adipocytes; 0.92 U/mg DNA in CD34$^+$ SVF-cells) indicate a distinguished role of mitochondrial and lipid metabolism in differentiated human adipocytes (Fig. 6G, H & I). This is substantiated by findings, that while mitochondrial proteins represent only 4.8 % of the total human proteome in adipocytes (Guda, Fahy and Subramaniam, 2004), 22 % of the overall protein amount were identified as of mitochondrial origin (Xie *et al.*, 2010). The difference in activity between adipocytes and CD34$^+$ SVF-cells for the HOADH, have been documented in other studies in a similar fashion. Fain et al. documented enriched mRNAs encoding enzymes involved in lipid turnover in adipocytes compared to SVF-cells of human omental adipose tissue (Fain *et al.*, 2008). When comparing *in vitro* adMSC with and without adipogenic stimulation, the capacities of HOADH displayed the same difference (Meyer *et al.*, 2018).

The NADP-IDH supplies NADPH for the antioxidative defense catalyzed by the GSR in mitochondria (Koh *et al.*, 2004). No difference between the two examined cell populations was measured in GSR activity (0.65 U/mg DNA in adipocytes; 0.58 U/mg DNA in CD34$^+$ SVF-cells) (Fig. 6F). Thus, the higher NADP-IDH activity measured in adipocytes compared to CD34$^+$ SVF-cells may be derived from the cytosolic isoform that delivers reduction equivalents for lipid synthesis (Koh *et al.*, 2004). Nevertheless, this issue needs further investigation, as the antioxidative defense system is complex.

Adipocytes displayed a CK activity that was almost three times higher compared to $CD34^+$ SVF-cells (5.11 U/mg DNA in adipocytes; 1.82 U/mg DNA in $CD34^+$ SVF-cells) (Fig. 6J). In white adipocytes CK activity might be facilitated as a phosphocreatine shuttle in order to overcome spatial restrictions of energy transport (Dzeja and Terzic, 2003). As the main volume of adipocytes is occupied by a monolocular lipid vacuole surrounded by only a thin layer of cytoplasm, a strictly diffusional transport from ATP-producing to ATP-consuming reactions might not suffice to supply all energy required (Wallimann *et al.*, 1992). A similar pattern was documented when comparing CK activities in *in vitro*-cultured adMSC with and without adipogenic stimulation (Meyer *et al.*, 2018).

4.3 Summary and discussion Study III - *Energy metabolic capacities of human adipose-derived mesenchymal stromal cells in vitro and their adaptations in osteogenic and adipogenic differentiation*

For some clinical applications of adMSC an expansion and/or differentiation of the cells might be necessary. We have observed the substantial differences in the energy metabolic configuration of native adipocytes and $CD34^+$ SVF-cells in connection with their diverging differentiation and proliferation potential. We thus hypothesized that the transition of adipose-derived progenitors from their *in vivo* to an *in vitro* environment would cause adaptations in the cell's energy metabolism. To assess this hypothesis, we analyzed activities of major metabolic pathways in non-differentiating and differentiating adMSC. This work was published in Experimental Cell Research under the title "Energy metabolic capacities of human adipose-derived mesenchymal stromal cells *in vitro* and their adaptations in osteogenic and adipogenic differentiation".

After isolation and expansion adMSC were subjected to culturing conditions without differentiation stimuli as well as culturing conditions with osteogenic and adipogenic differentiation stimuli. After 7 and 21 d in non-stimulated adMSC cultures a 1.3-fold increase in cell number had occurred from day 7 to day 21. After 7 d of osteogenic stimulation the amount of cells was 1.4-fold higher than in non-stimulated adMSC. After 21 d in osteogenic culture the amount of cells had increased 3.7-fold compared to non-stimulated adMSC. In contrast, the cell numbers of adipogenically stimulated adMSC did not change significantly over the cultivation period of 21 d. At this

point of time the amount of cells in adipogenic cultures was 2.0-fold lower than in the non-stimulated ones. The viability of the cells was monitored via fluorescence microscopy and a mitochondrial metabolic activity assay. So, while the non-stimulated cultures displayed moderate proliferative activity, high proliferative activity was induced with osteogenic differentiation. This and the constant cell amount in the adipogenically differentiating adMSC, that indicates a lack of proliferative activity, have previously been shown for the used stimuli (Salamon *et al.*, 2013).

The measurement of the ALP activity was used to characterize the osteogenic differentiation. Osteogenic stimulation over 21 days led to a distinct positivity for ALP activity with a 5-fold increase compared to non-stimulated cultures. The ALP activity of adipogenically stimulated adMSC was 6-fold lower than the ALP activity in osteogenically stimulated adMSC. Adipogenic differentiation was examined by the quantification of the formation of lipid-filled vacuoles. In non-stimulated adMSC no lipid accumulation was detectable, whereas adipogenically stimulated adMSC showed numerous lipid-filled vacuoles yielding 5-6-fold higher values compared to those in non-stimulated and osteogenic cultures. The detected levels of ALP activity clearly show that the osteogenic stimulation of adMSC led to osteogenic differentiation. The osteogenic differentiation initialized by the stimulants used in this study, has previously been shown to be accompanied by increased expression of the osteoblastogenic marker ZBTB16 (zinc finger and BTB domain containing 16) (Salamon *et al.*, 2014) and increased expression of osteocalcin and osteopontin (Lee *et al.*, 2003; Astori *et al.*, 2007). The detected lipid vacuole formation in the adipogenic cultures verified the adipogenic differentiation of the stimulated adMSC. The differentiation protocol applied in this study has previously been shown to also induce expression of leptin, glucose transporter GLUT4, PPARγ2 (peroxisome-proliferating activated receptor γ), LPL (lipoprotein lipase), and aP2 (adipocyte protein 2) (Zuk *et al.*, 2001, 2002; Astori *et al.*, 2007; Liu *et al.*, 2007), that are established markers of adipogenic differentiation.

After 7 and 21 d in culture with and without differentiation stimuli, important energy metabolic pathways were examined by measuring the maximum activities of marker enzymes. The PFK is the regulatory enzyme of glycolysis. In non-differentiating cultures, PFK activity increased during cultivation (0.25 U/mg DNA and 0.5 U/mg DNA after 7 and 21 d) (Fig. 7A). The GAPDH, also an enzyme of glycolysis, showed the highest

activities of all enzymes tested (e.g. 48 U/mg DNA after 7 d) (Fig. 7B). The GAPDH activity was increased 1.6-fold after 21 d (75 U/mg DNA). The LDH, that facilitates the reversible conversion of pyruvate to lactate, was 2.3-fold higher in activity after 21 d in culture compared to its activity after 7 d (16 U/mg DNA and 7 U/mg DNA respectively) (Fig 7C). The G6PDH, marker enzyme of the PPP, showed constant capacities in non-differentiating cells (3.1 U/mg DNA after 7 d and 3.5 U/mg DNA after 21 d) (Fig. 7D). The maximum activities of the marker enzymes NAD-IDH and NADP-IDH were measured in order to evaluate the relevance of the TCC. At all points of time under all cultivation conditions the NAD-IDH activity was below the detectable level. In non-differentiating cultures the NADH-IDH showed a capacity of 1.2 U/mg DNA after 7 d, which did not change significantly during cultivation (1.0 U/mg DNA after 21 d) (Fig. 7E). The HOADH, mitochondrial marker enzyme of fatty acid oxidation, showed low maximum activities (0.5 U/mg DNA and 0.6 U/mg DNA after 7 and 21 d) (Fig 7F). The GSR has a function in the antioxidative defense system where it facilitates the reduction of glutathione disulfide to glutathione. Maximum activities in the non-differentiating cultures were 0.9 U/mg DNA after 7 d and 1.7 U/mg DNA after 21 d (Fig. 7G). CK, that is involved in buffering and recovery of ATP displayed capacities of 2.1 U/mg DNA after 7 d and 2.2 U/mg DNA after 21 d in non-differentiating adMSC cultures (Fig 7H).

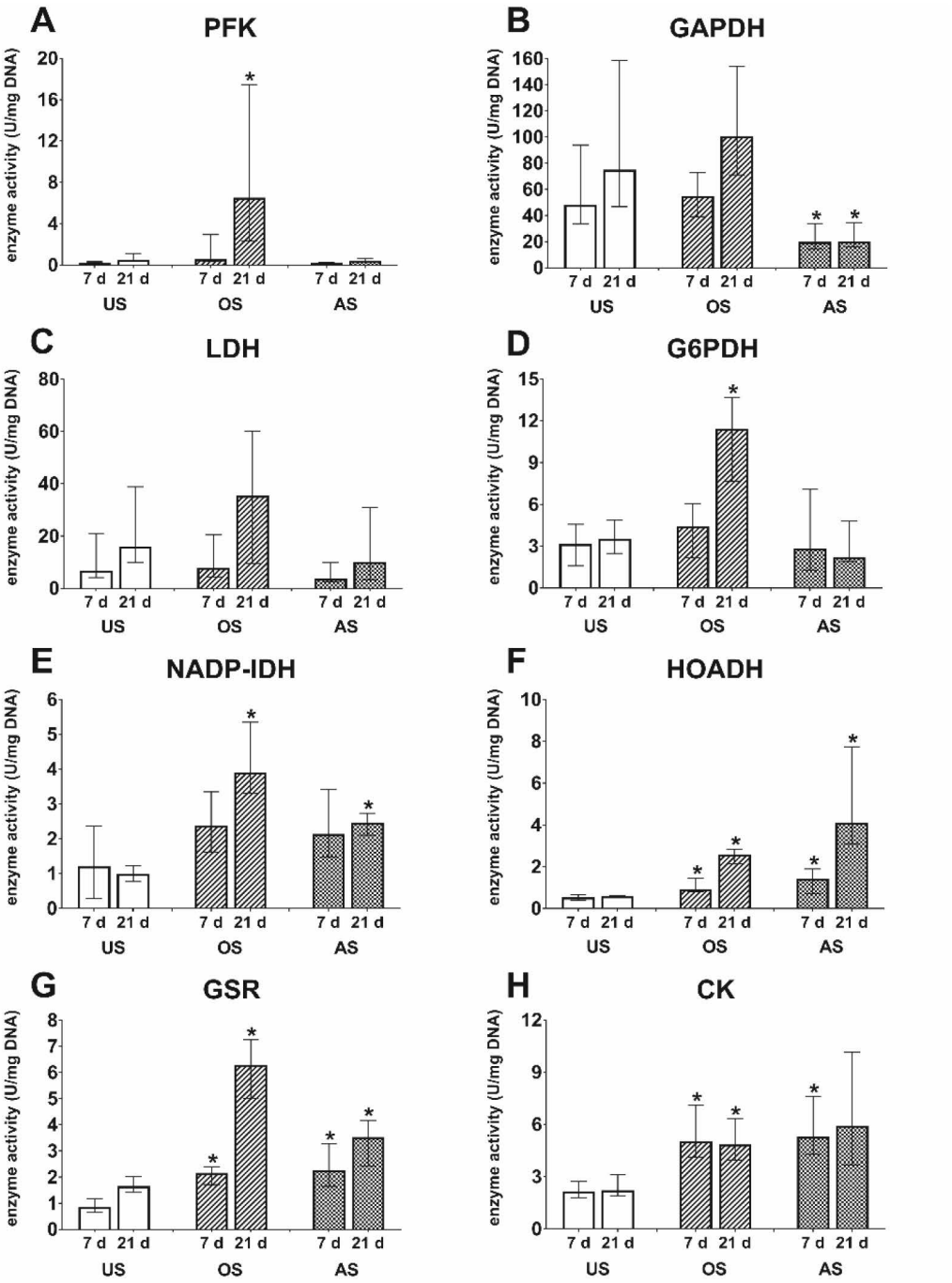

Fig. 7: Marker enzyme activities in adMSC *in vitro*. non-differentiating (US), osteogenically (OS) or adipogenically (AS) differentiating after 7 and 21 d, (A) PFK, (B) GAPDH, (C) LDH, (D) G6PDH, (E) NADP-IDH, (F) HOADH, (G) GSR, (H) CK; Activities normalized to the overall DNA content of the cells (data displayed as medians of 8 donors; measurements as technical duplicates; *significantly different from US cultures at the respective time point; *=significantly different; Mann-Whitney U Test, $p < 0.05$). Adapted from (Meyer *et al.*, 2018)

The total increase of maximum PFK activity in osteogenically differentiating adMSC was 13-fold from 0.5 U/mg DNA after 7 d to 6.5 U/mg DNA after 21 d. The increases in maximum GAPDH and LDH activities were much lower. The increase of GAPDH was 1.8-fold (55 U/mg DNA and 101 U/mg DNA after 7 and 21 d) the increase LDH activity was 4-fold (8 U/mg DNA and 35 U/mg DNA after 7 and 21 d). In

osteogenically differentiating cultures the ratio GAPDH/PFK was 15 after 21 d. This is 15-fold lower than in the non-differentiating cultures. G6PDH activity increased 2.6-fold during osteogenic differentiation (4.4 U/mg DNA after 7 d and 11.4 U/mg DNA after 21 d). NADH-IDH activity also increased over the period of osteogenic culture (2.4 U/mg DNA after 7 d and 3.9 U/mg DNA after 21 d). It was thus significantly higher after 21 d than in the non-differentiating cultures. The HOADH activity after 7 d was slightly higher than in non-differentiating cells (0.9 U/mg DNA). It increased 2.9-fold to 2.6 U/mg DNA after 21 d. The GSR capacity was more than twice as high after 7 d compared to the non-differentiating cultures (2.2 U/mg DNA) and increased over the osteogenic culturing period (6.3 U/mg DNA after 21 d). As in the non-differentiating cultures, the CK capacities did not show significant changes over the culturing period in the osteogenically differentiating cultures but were overall higher (4.1 U/mg DNA and 3.9 U/mg DNA after 7 and 21 d).

The maximum activities of PFK, GAPDH and LDH measured in adipogenically differentiating cultures were overall lower than in the non-differentiating cultures. There was a 2-fold increase of the maximum PFK activity over the culturing period (0.2 U/mg DNA after 7 d and 0.4 U/mg DNA after 21 d). At the same time GAPDH activity remained the same (20 U/ mg DNA after 7 and 21 d). During adipogenic differentiation a 2.7-fold increase of the LDH activities (3.7 U/mg DNA after 7 d and 10 U/mg DNA after 21 d) was observed. The ratio GAPDH/PFK decreased from 135 after 7 d to 61 after 21 d. As for the GAPDH, the G6PDH activity was below the activities in non-differentiating cultures as well and did not vary significantly over the adipogenic cultivation period (2.8 U/mg DNA after 7 d and 2.2 U/mg DNA after 21 d). In contrast, the NADH-IDH activities were significantly higher after 7 and 21 d than those in the non-differentiation cultures (2.1 U/mg DNA and 2.5 U/mg DNA respectively). The HOADH activities detected in adipogenically differentiating adMSC were the highest overall (1.4 U HOADH/mg DNA after 7 d and 4 U/mg DNA after 21 d). The GSR showed a similar capacity compared to osteogenically differentiating cells after 7 d (2.3 U/mg DNA). The increase over the culturing period was less pronounced (3.5 U/mg DNA). Like the HOADH, the CK displayed higher capacities in the adipogenically differentiating cultures than in the non-differentiating and osteogenically differentiating cultures (5.3 U/mg DNA and 5.9 U/mg DNA after 7 and 21 d).

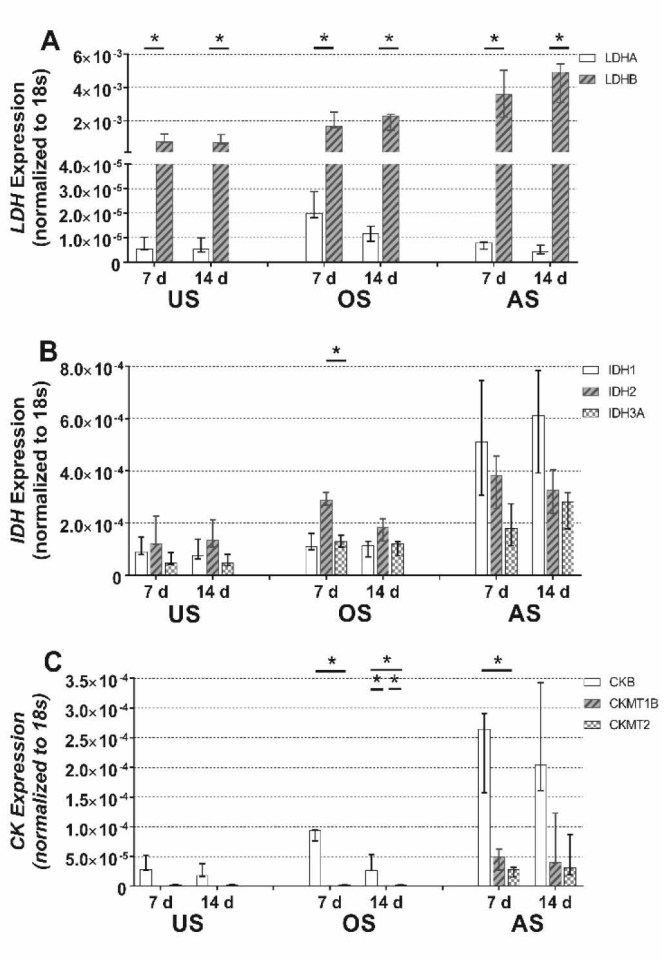

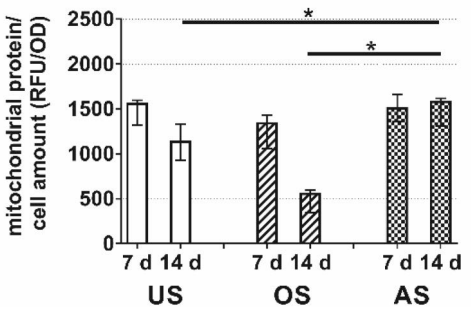

↑ **Fig. 8: Relative mitochondrial mass of adMSC *in vitro*.** mitochondrial protein normalized to cell number after 7 & 14 d in control (US) and in osteogenic (OS) or adipogenic differentiation (AS). (data displayed as medians of 5 donors; measurements as technical duplicates; *=significantly different; Mann-Whitney U Test, $p < 0.05$). Adapted from (Meyer *et al.*, 2018)

← **Fig. 9. Isoenzyme gene expression levels of adMSC *in vitro*** in control (US) and osteogenic (OS) or adipogenic (AS) culture after 7 and 14 d. (A) LDH isoforms LDHA and LDHB, (B) IDH isoforms IDH1, IDH2 and IDH3A, (C) CK isoforms CKB, CKMT1B and CKMT2, normalized to 18s RNA-expression (data displayed as medians of 3 donors; measurements as technical duplicates; all culture conditions were compared within one time point; *=significantly different; Mann-Whitney U Test, $p < 0.05$). Adapted from (Meyer *et al.*, 2018)

The capacities measured for PFK, GAPDH and LDH suggest a high capacity of carbohydrate catabolism, i.e. glycolysis, in non-differentiating and osteogenically differentiating adMSC. This is accompanied by the high proliferative activity that was found in those cell cultures. Cell division as well as differentiation require the *de novo* synthesis of macromolecules like proteins and DNA (Ralph J DeBerardinis *et al.*, 2008; Musumeci *et al.*, 2014). A preference for carbohydrate metabolism yielding lactate under aerobic conditions has been observed in various proliferating cell cultures (Peters *et al.*, 2009; Vander Heiden, Cantley and Thompson, 2009). This phenomenon has been defined as the Warburg effect (Warburg, 1956). The carbon flux through biosynthetic pathways might be increased by facilitation of this less efficient pathway (Vander Heiden, Cantley and Thompson, 2009). Despite the indications of some of the present data, an explicit deduction on the manifestation of the Warburg effect in *in vitro* proliferating adMSC cannot be made solely based on our present data. The presence of LDH activity and its increase within the cultivation period might also imply the ability of adMSC to utilize lactate as an aerobic substrate. This is supported by the striking dominance of the RNA expression of the B subunit of LDH (heart type) (Fig. 9A) which

shows a preference for the conversion of lactate to the 3-carbon compound pyruvate (Dawson, Goodfriend and Kaplan, 1964). A capacity for carbohydrate anabolism cannot be anticipated from the results attained in this study, as no activities of the marker enzyme of gluconeogenesis, FBPase, were at a detectable level at any time point under any of the culturing conditions. The use of lactate for gluconeogenesis is thus unlikely. Previous studies have yielded controversial results regarding the metabolism of MSC during osteogenic differentiation. Pattappa et al. and Chen et al. demonstrated a suppression of glycolysis in osteogenically differentiating bmMSC, suggesting a proportionate increase in oxidative phosphorylation (Chen *et al.*, 2008; Pattappa *et al.*, 2011). Shum et al. reported steady levels glycolysis upon osteogenic differentiation of bmMSC. At the same time oxidative phosphorylation increased (Shum *et al.*, 2016). Our results show a simultaneous increase of carbohydrate metabolism, oxidative phosphorylation and β-oxidation upon osteogenic differentiation accompanied by osteogenic differentiation. These divergent findings may result from different analytical methods as well as the fact that, in the other studies, mostly bmMSC were examined (Quarto *et al.*, 2010). Also cell metabolism is likely influenced by variations in cell culturing, e.g. as displayed in the differences of medium composition with partially supraphysiological levels of glucose, glutamine and pyruvate (Brand and Nicholls, 2011). No proliferative activity was detected in adipogenically differentiated adMSC. Thus, the steady GAPDH activities and the slight increase of PFK activity over the culturing period may be caused by the initiation of lipid synthesis. During anabolic lipid synthesis, dihydroxyacetone phosphate is diverted from glycolysis prior to the action of GAPDH (Lunt and Vander Heiden, 2011). As deducible from studies with rat white adipose tissue and the 2.7-fold increase of LDH within 2 weeks recorded in the present study, the main role of LDH may be the conversion of excess available lactose into pyruvate in order to limit tissue self-utilization as a substrate (Arriarán *et al.*, 2015). This is again supported by the dominance of the expression of the LDH B subunit (Fig. 9A).

The G6PDH and thus the PPP competes with glycolysis for glucose metabolism. The relatively high G6PDH activities in non-differentiating and differentiating adMSC indicate the importance of the PPP for anabolism (Tian *et al.*, 1998; Peters *et al.*, 2009). When compared, the measured G6PDH activities were higher than the control enzyme of glycolysis PFK, under each culturing condition. A high ratio of G6PDH/PFK might be typical for proliferating and/or differentiating cells, as these are characterized by

relatively high anabolic activity (Peters *et al.*, 2009). Besides the provision of pentoses for the biosynthesis of macromolecules like nucleic acids (Chandel, 2015), the G6PDH also delivers the reduction equivalent $NAPDH+H^+$ which is essential for biosynthesis (particularly lipogenesis) and antioxidative defense (Horecker, 1976).

Lipid synthesis entails a high consumption of $NAPDH+H^+$ in the cytoplasm by the NADP-IDH encoded by IDH1. Correspondingly, the expression level of IDH1 prevails in adipogenically induced adMSC (Fig. 9C) where lipids are evidently accumulated in vacuoles. This is substantiated by the fact, that the regulation of the PPP capacity is strongly dependent on the regulation of lipid synthesis (Kather, Rivera and Brand, 1972). A part of the measured NADP-IDH might also be located in the mitochondria because IDH is required for the TCC and an activity of mitochondrial NAD-dependent IDH activity could not be detected (Nelson and Cox, 2011). The expression of IDH2 RNA in adMSC, that increases during osteogenesis and adipogenesis substantiates the presence of mitochondrial NADP-IDH. Also, IDH3A RNA, the mitochondrial catalytic NAD-IDH subunit, is expressed in adMSC under all culturing conditions. The NAD-IDH contains two different regulatory subunits which allow allosteric regulation of the activity, particularly by cell energy charge (e.g. ADP/ATP) (Hartong *et al.*, 2008). Translation to an active NAD-IDH can still be suppressed through alternatively spliced gene products of the regulatory subunits. Thus, the expression of the catalytic α-subunit of IDH3A does not represent the total expression of NAD-IDH. This might be the reason for the apparent discrepancy between the measured NAD-IDH activity and the IDH3A expression level (Fig. 9B). While in proliferating cells the NADP-IDH is the prevailing IDH isoform (Peters *et al.*, 2009) NAD-IDH is particularly present in tissues with a high respiratory ATP turnover, like aerobic muscles. In proliferating cells most of the carbon that enters the TCC will be directed towards biosynthetic pathways rather than ATP production (Ralph J. DeBerardinis *et al.*, 2008). Thus, citrate could be diverted away from the TCC before it is converted to α-ketoglutarate by the NAD-IDH, e.g. for fatty acid synthesis. In contrast to the irreversible reaction of NAD^+-dependent conversion of isocitrate to oxoglutarate, the $NADP^+$-dependent reaction is reversible. Therefore, the NADP-IDH might be favored in biosynthetically active cells. Using the anaplerotic pathway of glutaminolysis, glutamine can compensate for a lack of glucose not only for ATP-production but also for the supply of anabolic precursors (Board, Humm and Newsholme, 1990; Smolková and Jezek, 2012).

As our *in vitro* measurements of HOADH activity and quantification of mitochondria show (Fig. 7F and Fig. 8), the capacity for ß-oxidation increases distinctly under adipogenic as well as osteogenic differentiation. Our results, are substantiated by different studies that reported a constant mitochondrial mass during osteogenic differentiation (Chen *et al.*, 2008; Shum *et al.*, 2016) and a distinct increase in mitochondrial mass during adipogenic differentiation (Wilson-Fritch *et al.*, 2003; Zhang *et al.*, 2013). It is still a matter of controversy if the fatty acid synthesis and ß-oxidation do occur simultaneously within one cell. While studies with white adipose tissue have shown that lipolysis is inhibited during anabolic phases (Chandel, 2015; Rutkowski, Stern and Scherer, 2015), the conversion of white to brown adipocytes entails an upregulation of both fatty acid anabolic and catabolic pathways (Barquissau *et al.*, 2016). It remains to be elucidated if *in vitro* adipogenic stimulation leads to a homogenous cell population where fatty acid synthesis and ß-oxidation actually do occur simultaneously within one cell, or if it leads to a heterogenous cell population where some cells facilitate fatty acid synthesis while others facilitate ß-oxidation.

A low production of ROS and thus low activity of oxidative phosphorylation is indicated by low GSR activities in non-differentiating, proliferating cells. In proliferating thymocytes a low oxidative phosphorylation activity has also been shown (Brand and Hermfisse, 1997). The enhanced anabolic activities during *in vitro* osteogenic and adipogenic differentiation might increase the demand for a regeneration of the detoxification system of reactive oxygen species (Chakravarthi, Jessop and Bulleid, 2006). This could be reflected by the significant increase of GSR activity in osteogenically and the slight increase in adipogenically differentiating adMSC. Furthermore, an increased oxygen consumption has been correlated with the adipogenic differentiation of bmMSC and adipose progenitors, while antioxidative defense enzymes were upregulated at the same time (Heimburg *et al.*, 2005; Zhang *et al.*, 2013). These together with our data suggest an association of the mitochondrial oxidative activity, enhanced anabolism and regulation of antioxidative defense. This will need further validation in order to find conclusions on actual correlative and causal connections.

CK regenerates ATP for seconds in cells with temporarily high or fluctuating energy demands (Wallimann and Hemmer, 1994b). Under all culturing conditions adMSC displayed CK activities. The gene expression data imply that mitochondrial CKs

were expressed particularly in adipogenically stimulated cells, suggesting that adipogenic stimulation shifted the energy metabolism towards a more oxidative metabolism than osteogenic stimulation did. Also, a functional phosphocreatine-CK shuttle has been found in human skin, that was characterized as having high metabolic rates and energy turnover. In these cells the shuttle was mainly made up of the brain type CK and the ubiquitous mitochondrial CK (Wallimann and Hemmer, 1994b; Schlattner *et al.*, 2002). With progressing adipogenic differentiation the expression levels of CKB, CKMT1B and CKMT2 increase (Fig. 9C). Thus, adipogenically differentiating adMSC show a metabolic phenotype that is characteristic for rapid ATP turnover even though they are not actively proliferating.

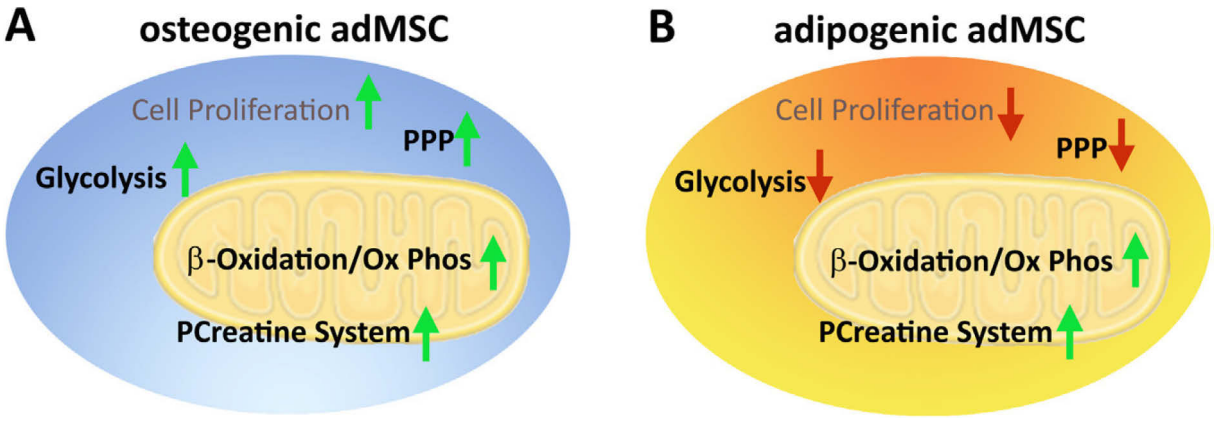

Fig. 10: Schematic depiction of the metabolic changes in adMSC *in vitro* during (A) osteogenic and (B) adipogenic differentiation in relation to non-differentiating adMSC (increased↑, decreased↓; Ox Phos: oxidative phosphorylation, PCreatine: phosphocreatine). Adapted from (Meyer *et al.*, 2018)

According to the present data osteogenically differentiating adMSC attained a strongly proliferative phenotype that entailed an increase in the capacity of all examined energy metabolic pathways. Adipogenic differentiation of adMSC, characterized by a lack of proliferation, shift their energy metabolic capacity towards lipid metabolism (Fig. 10).

5 Conclusion & future prospects

Adipose tissue is a simply available source of adult stem cells with regenerative therapeutic potential. It was demonstrated that adipose tissue harvested with water jet-assistance yields cells in numbers and viability competitive with other aspiration methods. The adMSC isolated from WAL tissue display plastic adherence and mesenchymal differentiation potential, making it a valid source for adMSC isolation.

Two distinct cell populations from adipose tissue, adipocytes and $CD34^+$ SVF-cells were examined for their energy metabolic configuration. The enzymes related to mitochondrial and lipid metabolism showed a higher representation in adipocytes, whereas the activity of the rate-limiting enzyme of glycolysis was higher in the $CD34^+$ SVF-cells. These distinctions exist in parallel with the potential of $CD34^+$ SVF-cells to proliferate and differentiate, whereas adipocytes do not.

The transition of adMSC from their *in vivo* to an *in vitro* environment with osteogenic and adipogenic differentiation stimulation led to changes in the cell's proliferative behavior together with adaptations of their respective energy metabolism. Osteogenically differentiating adMSC attained a strongly proliferative phenotype that entailed an increase in the capacity of all examined energy metabolic pathways. Adipogenic differentiation of adMSC, characterized by a lack of proliferation, is accompanied by decreasing capacities of PPP and carbohydrate metabolism. At the same time, growing capacities for oxidative phosphorylation and β-oxidation are indicated by the increasing mitochondrial enzyme activities. Thus, adipogenically differentiating adMSC display a shift of their energy metabolic capacity towards lipid metabolism. We thus observed a similar relationship between the energy metabolic configuration and the proliferation potential as we did before in the two native cell populations of the adipose tissue.

Considering the limitations regarding the comparability and interpretation of results in comparison to available literature, due to differences in the applied methodologies, further examinations will be needed to decipher the metabolic configurations of the different cell types of adipose tissue. As a next step the analysis of the uptake and release of radio-labeled metabolites could elucidate the metabolic structure of the cells on an additional level. Furthermore, it is essential to determine if the observed relationships between cell behavior and energy-metabolic phenotype are

actual correlations and causal relations. In order to achieve this, knock down experiments of the expression of single enzymes or groups of enzymes could be considered in order to observe changes in the differentiation and proliferation potential of the cells. Knock out experiments should be refrained from as a complete depletion of the examined enzymes might likely render the cells nonviable. Moving forward to achieve insights on the more clinical aspects of the cells it will be of interest to relate specific donor patient parameters like body mass index, age and/or tissue depot localization to the amount and viability of the contained adipocytes and CD34+ SVF-cells. Also, the differentiation potential and metabolic phenotype of adMSC in relation to the mentioned donor patient parameters can be of clinical interest.

With the present work we were able to contribute to the characterization of the energy metabolism of distinct cell types of the human adipose tissue in the native state and after *in vitro* culturing. We were thus able to add to the groundwork needed for further examinations of the cellular metabolism of human adipose tissue in the clinical as well as the laboratory setting as can be seen in ongoing investigations the emission of volatile organic compounds between non-differentiating and adipogenically differentiating adMSC (Klemenz *et al.*, 2019).

6 References

Actor, J. K. (2014) 'Chapter 1 - A Functional Overview of the Immune System and Immune Components', in *Introductory Immunology*. Academic Press, pp. 1–15.

Ailhaud, G. (2006) 'Adipose tissue as a secretory organ: from adipogenesis to the metabolic syndrome', *Comptes Rendus - Biologies*, 329(8), pp. 570–577.

Arriarán, S. *et al.* (2015) 'Evidences of Basal lactate production in the main white adipose tissue sites of rats. effects of sex and a cafeteria diet', *PLoS ONE*, 10(3), pp. 1–19.

Astori, G. *et al.* (2007) '"In vitro" and multicolor phenotypic characterization of cell subpopulations identified in fresh human adipose tissue stromal vascular fraction and in the derived mesenchymal stem cells.', *Journal of translational medicine*, 5, p. 55.

Banas, A. *et al.* (2007) 'Adipose tissue-derived mesenchymal stem cells as a source of human hepatocytes.', *Hepatology*, 46(1), pp. 219–228.

Barquissau, V. *et al.* (2016) 'White-to-brite conversion in human adipocytes promotes metabolic reprogramming towards fatty acid anabolic and catabolic pathways', *Molecular Metabolism*. Elsevier GmbH, 5(5), pp. 352–365.

Berlet, H. H., Bonsmann, I. and Birringer, H. (1976) 'Occurrence of free creatine, phosphocreatine and creatine phosphokinase in adipose tissue', *Biochimica et Biophysica Acta - General Subjects*, 437, pp. 166–174.

Bessman, S. P. (1972) 'Hexokinase acceptor theory of insuline action. New evidence.', *Israel journal of medical sciences*, 8(3), pp. 344–352.

Bessman, S. P. and Carpenter, C. L. (1985) 'The Creatine-Creatine Phosphate Energy Shuttle', *Annual Review of Biochemistry*, 54(1), pp. 831–862.

Board, M., Humm, S. and Newsholme, E. A. (1990) 'Maximum activities of key enzymes of glycolysis, glutaminolysis, pentose phosphate pathway and tricarboxylic acid cycle in normal, neoplastic and suppressed cells.', *The Biochemical journal*, 265(2), pp. 503–509.

Bourin, P. *et al.* (2013) 'Stromal cells from the adipose tissue-derived stromal vascular fraction and culture expanded adipose tissue-derived stromal/stem cells: a joint statement of the International Federation for Adipose Therapeutics and Science (IFATS) and the International So', *Cytotherapy*. Elsevier Inc, 15(6), pp. 641–8.

Brand, K. A. and Hermfisse, U. (1997) 'Aerobic glycolysis by proliferating cells: a protective strategy against reactive oxygen species', *The FASEB Journal*, 5, pp. 388–395.

Brand, M. D. and Nicholls, D. G. (2011) 'Assessing mitochondrial dysfunction in cells', *Biochemical Journal*, 435, pp. 297–312.

Cannon, B. and Nedergaard, J. (2004) 'Brown adipose tissue : function and physiological significance', *Physiological reviews*, 84, pp. 277–359.

Chakrabarty, K., Chaudhuri, B. and Jeffay, H. (1983) 'Glycerokinase activity in human brown adipose tissue', *J Lipid Res*, 24(4), pp. 381–390. Available at: http://www.ncbi.nlm.nih.gov/pubmed/6304216%5Cnhttp://www.jlr.org/content/24/4/381.full.pdf.

Chakravarthi, S., Jessop, C. E. and Bulleid, N. J. (2006) 'The role of glutathione in

disulphide bond formation and endoplasmic-reticulum-generated oxidative stress', *EMBO Reports*, 7(3), pp. 271–275.

Chandel, N. S. (2015) *Navigating Metabolism*. 1st edn. Edited by R. Sever et al. Cold Spring Harbor: Inglis, John.

Chen, C.-T. *et al.* (2008) 'Coordinated Changes of Mitochondrial Biogenesis and Antioxidant Enzymes During Osteogenic Differentiation of Human Mesenchymal Stem Cells', *Stem Cells*, 26(4), pp. 960–968.

Crisan, M. *et al.* (2012) 'Perivascular cells for regenerative medicine', *Journal of Cellular and Molecular Medicine*, 16(12), pp. 2851–2860.

Cunha, R. A. M. *et al.* (2016) 'Changes in blood glucose among trained normoglycemic adults during a mini-trampoline exercise session .', *The Journal of Sports Medicine and Physical Fitness*, 56(12), pp. 1547–53.

Cypess, A. M. *et al.* (2009) 'Identification and importance of brown adipose tissue in adult humans.', *The New England journal of medicine*, 360(15), pp. 1509–1517.

D., K. *et al.* (2010) 'Safety and immunological effects of mesenchymal stem cell transplantation in patients with multiple sclerosis and amyotrophic lateral sclerosis', *Archives of Neurology*, 67(10), pp. 1187–1194. Available at: http://archneur.ama-assn.org/cgi/reprint/67/10/1187%5Cnhttp://ovidsp.ovid.com/ovidweb.cgi?T=JS&PAGE=reference&D=emed12&NEWS=N&AN=359770079.

Dawson, D. M., Goodfriend, T. L. and Kaplan, N. O. (1964) 'Lactic dehydrogenases : Functions of the two types', *Science*, 143, pp. 929–933.

DeBerardinis, Ralph J *et al.* (2008) 'The biology of cancer: metabolic reprogramming fuels cell growth and proliferation.', *Cell metabolism*, 7(1), pp. 11–20.

DeBerardinis, Ralph J. *et al.* (2008) 'The Biology of Cancer: Metabolic Reprogramming Fuels Cell Growth and Proliferation', *Cell Metabolism*, 7(1), pp. 11–20.

DeLany, J. P. *et al.* (2005) 'Proteomic analysis of primary cultures of human adipose-derived stem cells: modulation by adipogenesis', *Mol Cell Proteomics*, 4(6), pp. 731–740.

Dominici, M. *et al.* (2006) 'Minimal criteria for defining multipotent mesenchymal stromal cells. The International Society for Cellular Therapy position statement', *Cytotherapy*, 8(4), pp. 315–317.

Dzeja, P. P. and Terzic, A. (2003) 'Phosphotransfer networks and cellular energetics.', *The Journal of experimental biology*, 206(Pt 12), pp. 2039–2047.

Engel, P. *et al.* (2015) 'CD Nomenclature 2015: Human Leukocyte Differentiation Antigen Workshops as a Driving Force in Immunology', *The Journal of Immunology*, 195(10), pp. 4555–4563.

Eto, H. *et al.* (2009) 'Characterization of structure and cellular components of aspirated and excised adipose tissue', *Plastic and Reconstructive Surgery*, 124(4), pp. 1087–1097.

Fain, J. N. *et al.* (2008) 'Comparison of messenger RNA distribution for 60 proteins in fat cells vs the nonfat cells of human omental adipose tissue', *Metabolism: Clinical and Experimental*, 57(7), pp. 1005–1015.

Fang, B. *et al.* (2007) 'Favorable Response to Human Adipose Tissue-Derived Mesenchymal Stem Cells in Steroid-Refractory Acute Graft-Versus-Host Disease', *Transplantation Proceedings*, 39(10), pp. 3358–3362.

Feisst, V. *et al.* (2014) 'Characterization of Mesenchymal Progenitor Cell Populations Directly Derived from Human Dermis', *Stem Cells and Development*, 23(6), pp. 631–642.

Ferris, W. F. and Crowther, N. J. (2011) 'Once fat was fat and that was that: our changing perspectives on adipose tissue', *Cardiovascular journal of Africa*, 22(3), pp. 147–154.

Friedenstein, A. J., Piatetzky-Shapiro, I. I. and Petrakova, K. V. (1966) 'Osteogenesis in transplants of bone marrow cells.', *Journal of embryology and experimental morphology*, 16(3), pp. 381–90. Available at: http://www.ncbi.nlm.nih.gov/pubmed/5336210.

Furness, S. G. B. and McNagny, K. (2006) 'Beyond mere markers: Functions for CD34 family of sialomucins in hematopoiesis', *Immunologic Research*, 34(1), pp. 13–32.

Glimm, H. and Eaves, C. J. (1999) 'Direct evidence for multiple self-renewal divisions of human in vivo repopulating hematopoietic cells in short-term culture.', *Blood*, 94(7), pp. 2161–8.

Gotoh, M. *et al.* (2014) 'Regenerative treatment of male stress urinary incontinence by periurethral injection of autologous adipose-derived regenerative cells: 1-year outcomes in 11 patients', *International Journal of Urology*, 21(3), pp. 294–300.

Guda, C., Fahy, E. and Subramaniam, S. (2004) 'MITOPRED: A genome-scale method for prediction of nucleus-encoded mitchondrial proteins', *Bioinformatics*, 20(11), pp. 1785–1794.

Guillaume-Jugnot, P. *et al.* (2015) 'Autologous adipose-derived stromal vascular fraction in patients with systemic sclerosis: 12-month follow-up.', *Rheumatology (Oxford, England)*, (September 2015), pp. 301–306.

Handgretinger, R. *et al.* (2002) 'Biology and Plasticity of CD133+ Hematpoietic Stem Cells', *Annals of the New York Academy of Sciences*, 996, pp. 141–151.

Van Harmelen, V. *et al.* (2003) 'Effect of BMI and age on adipose tissue cellularity and differentiation capacity in women', *International Journal of Obesity*, 27(8), pp. 889–895.

Hartong, D. T. *et al.* (2008) 'Novel insights into the contributions of isocitrate dehydrogenase to the Krebs cycle from patients with retinitis pigmentosa', *Nature genetics*, 40(10), pp. 1230–1234.

Hausman, D. B. *et al.* (2001) 'The biology of white adipocyte proliferation', *Obesity Reviews*, 2(4), pp. 239–254.

Vander Heiden, M. G., Cantley, L. C. and Thompson, C. B. (2009) 'Understanding the Warburg Effect: The metabolic requirements of cell proliferation', *Science*, 324(5930), pp. 1029–1033.

Heimburg, D. Von *et al.* (2005) 'Oxygen consumption in undifferentiated versus differentiated adipogenic mesenchymal precursor cells', *Respiratory Physiology and Neurobiology*, 146(2–3), pp. 107–116.

Henderson, N. S. (1965) 'Isozymes of isocitrate dehydrogenase: Subunit structure and intracellular location', *Journal of Experimental Zoology*, 158(3), pp. 263–273.

Herold, C. *et al.* (2017) 'Autologous Fat Transfer for Thumb Carpometacarpal Joint Osteoarthritis', *Plastic and Reconstructive Surgery*, 140(2), pp. 327–335.

Horecker, B. L. (1976) 'The biochemistry of sugars', *Int. Z. für Vitam. - und Ernähr. Beih. 15*, pp. 1–21.

Hsu, V. M. *et al.* (2012) 'Fat grafting's past, present, and future: why adipose tissue is emerging as a critical link to the advancement of regenerative medicine.', *Aesthetic surgery journal / the American Society for Aesthetic Plastic surgery*, 32(7), pp. 892–9.

Hyvönen, M. T. and Spalding, K. L. (2014) 'Maintenance of white adipose tissue in man', *International Journal of Biochemistry and Cell Biology*, 56, pp. 123–132.

Imhoff, B. R. and Hansen, J. M. (2011) 'Differential redox potential profiles during adipogenesis and osteogenesis', *Cellular and Molecular Biology Letters*, 16(1), pp. 149–161.

James, A. W. *et al.* (2012) 'Perivascular stem cells: a prospectively purified mesenchymal stem cell population for bone tissue engineering.', *Stem cells translational medicine*, 1(6), pp. 510–9.

Kaiser, S. *et al.* (2007) 'BM cells giving rise to MSC in culture have a heterogeneous CD34 and CD45 phenotype', *Cytotherapy*. Elsevier, 9(5), pp. 439–450.

Kather, H., Rivera, M. and Brand, K. (1972) 'Interrelationship and control of glucose metabolism and lipogenesis in isolated fat-cells - control of pentose phosphate-cycle activity by cellular requirement for reduced nicotinamide adenine dinucleotide phosphate', *Biochemical Journal*, 128(5), pp. 1097–1102.

Kheterpal, I. *et al.* (2011) 'Proteome of human subcutaneous adipose tissue stromal vascular fraction cells vs. mature adipocytes based on DIGE', *Journal of Proteome Research*, 10(4), pp. 1519–1527.

Klar, A. S. *et al.* (2016) 'Characterization of vasculogenic potential of human adipose-derived endothelial cells in a three-dimensional vascularized skin substitute', *Pediatric Surgery International*, 32(1), pp. 17–27.

Klemenz, A.-C. *et al.* (2019) 'Differences in the Emission of Volatile Organic Compounds (VOCs) between Non-Differentiating and Adipogenically Differentiating Mesenchymal Stromal/Stem Cells from Human Adipose Tissue', *Cells*, 8(7), p. 697.

Koh, H. J. *et al.* (2004) 'Cytosolic NADP+-dependent isocitrate dehydrogenase plays a key role in lipid metabolism', *Journal of Biological Chemistry*, 279(38), pp. 39968–39974.

Koh, Y. J. *et al.* (2011) 'Stromal vascular fraction from adipose tissue forms profound vascular network through the dynamic reassembly of blood endothelial cells', *Arteriosclerosis, Thrombosis, and Vascular Biology*, 31(5), pp. 1141–1150.

Krause, B. D. S. *et al.* (1996) 'CD34: Structure, biology and clinical utility', *Blood*, 87(1), pp. 1–13.

de la Garza-Rodea, A. S. *et al.* (2012) 'Myogenic properties of human mesenchymal stem cells derived from three different sources', *Cell Transplantation*,

21(1), pp. 153–173.

Lee, J. A. *et al.* (2003) 'Biological alchemy: Engineering bone and fat from fat-derived stem cells', *Annals of Plastic Surgery*, 50(6), pp. 610–617.

Lendeckel, S. *et al.* (2004) 'Autologous stem cells (adipose) and fibrin glue used to treat widespread traumatic calvarial defects: case report.', *Journal of cranio-maxillo-facial surgery : official publication of the European Association for Cranio-Maxillo-Facial Surgery*, 32(6), pp. 370–3.

Lin, C. *et al.* (2013) 'Is CD34 Truly a Negative Marker for Mesenchymal Stem Cells? Ching-Shwun', *Cytotherapy*, 14(10).

Lin, G. *et al.* (2008) 'Defining Stem and Progenitor Cells within Adipose Tissue', *Stem Cells and Development*, 17(6), pp. 1053–1063.

Liu, T. M. *et al.* (2007) 'Identification of common pathways mediating differentiation of bone marrow- and adipose tissue-derived human mesenchymal stem cells into three mesenchymal lineages.', *Stem cells (Dayton, Ohio)*, 25(3), pp. 750–60.

Lohmann, K. (1934) 'Ueber den Chemismus der Muskelkontraktion .', *Naturwissenschaften*, 22(22–24), pp. 409–411.

Lonergan, T., Bavister, B. and Brenner, C. (2007) 'Mitochondria in stem cells', *Mitochondrion*, 7(5), pp. 289–296.

Lunt, S. Y. and Vander Heiden, M. G. (2011) 'Aerobic Glycolysis: Meeting the Metabolic Requirements of Cell Proliferation', *Annual Review of Cell and Developmental Biology*, 27(1), pp. 441–464.

Man, D. and Meyer, H. (2007) 'Water jet-assisted lipoplasty.', *Aesthetic surgery journal / the American Society for Aesthetic Plastic surgery*, 27(3), pp. 342–6.

Marino, G. *et al.* (2013) 'Therapy with autologous adipose-derived regenerative cells for the care of chronic ulcer of lower limbs in patients with peripheral arterial disease', *Journal of Surgical Research*, pp. 36–44.

Melief, S. M. *et al.* (2013) 'Adipose Tissue-Derived Multipotent Stromal Cells Have a Higher Immunomodulatory Capacity Than Their Bone Marrow-Derived Counterparts', *Stem cells*, 2(6), pp. 455–463.

Mesimäki, K. *et al.* (2009) 'Novel maxillary reconstruction with ectopic bone formation by GMP adipose stem cells.', *International journal of oral and maxillofacial surgery*, 38(3), pp. 201–9.

Meyer, J. *et al.* (2015) 'Isolation and differentiation potential of human mesenchymal stem cells from adipose tissue harvested by water jet-assisted liposuction', *Aesthetic Surgery Journal*, 35(8), pp. 1–10.

Meyer, J. *et al.* (2018) 'Energy metabolic capacities of human adipose-derived mesenchymal stromal cells in vitro and their adaptations in osteogenic and adipogenic differentiation', *Experimental Cell Research*. Elsevier Inc., 370(2), pp. 632–642.

Meyer, J. *et al.* (2019) 'Human adipocytes and CD34+ cells from the stromal vascular fraction of the same adipose tissue differ in their energy metabolic enzyme configuration', *Experimental Cell Research*. Elsevier Inc., 380(1), pp. 47–54.

Michalek, J. *et al.* (2015) 'Autologous adipose tissue-derived stromal vascular

fraction cells application in patients with osteoarthritis', *Cell transplantation*, pp. 1–36.

Mitchell, J. B. *et al.* (2006) 'Immunophenotype of Human Adipose-Derived Cells: Temporal Changes in Stromal-Associated and Stem Cell-Associated Markers', *Stem Cells*, 24(2), pp. 376–385.

Mizushima, T. *et al.* (2015) 'A clinical trial of autologous adipose-derived regenerative cell transplantation for a postoperative enterocutaneous fistula', *Surgery Today*. Springer Japan.

Musumeci, G. *et al.* (2014) 'Biosynthesis of collagen I, II, RUNX2 and lubricin at different time points of chondrogenic differentiation in a 3D in vitro model of human mesenchymal stem cells derived from adipose tissue', *Acta Histochemica*, pp. 1407–1417.

Nelson, D. L. and Cox, M. M. (2011) *Principles of Biochemistry*. 5th edn. New York: Tenney, Sara.

Newsholme, E. A. and Start, C. (1977) *Regulation des Stoffwechsels. Homöostase im menschlichen und tierischen Organismus*. 1. Weinheim: Verlag Chemie.

Nielsen, J. S. and Mcnagny, K. M. (2008) 'Novel functions of the CD34 family', *Journal of Cell Science*, 121(22), pp. 3683–3692.

Nunes, S. S. *et al.* (2013) 'Generation of a functional liver tissue mimic using adipose stromal vascular fraction cell-derived vasculatures', *Scientific Reports*, 3, pp. 1–7.

Ochocki, J. D. and Simon, M. C. (2013) 'Nutrient-sensing pathways and metabolic regulation in stem cells', *Journal of Cell Biology*, 203(1), pp. 23–33.

Oedayrajsingh-Varma, M. J. *et al.* (2006) 'Adipose tissue-derived mesenchymal stem cell yield and growth characteristics are affected by the tissue-harvesting procedure', *Cytotherapy*, 8(2), pp. 166–177.

Ogawa, M. (1993) 'Differentiation and proliferation of hematopoietic stem cells', *Blood*, 81(11), pp. 2844–2853.

Patrick, C. W. (2000) 'Adipose tissue engineering : the future of breast and soft tissue reconstruction following tumor resection', *Seminars in Surgical Oncology*, 19(713), pp. 302–311.

Pattappa, G. *et al.* (2011) 'The metabolism of human mesenchymal stem cells during proliferation and differentiation', *Journal of Cellular Physiology*, 226(10), pp. 2562–2570.

Păunescu, V. *et al.* (2007) 'In vitro differentiation of human mesenchymal stem cells to epithelial lineage', *Journal of Cellular and Molecular Medicine*, 11(3), pp. 502–508.

Pelicano, H. *et al.* (2006) 'Mitochondrial respiration defects in cancer cells cause activation of Akt survival pathway through a redox-mediated mechanism', *Journal of Cell Biology*, 175(6), pp. 913–923.

Perin, E. C. *et al.* (2014) 'Adipose-derived regenerative cells in patients with ischemic cardiomyopathy: The PRECISE Trial', *American Heart Journal*. Mosby, Inc., 168(1), pp. 88-95.e2.

Pers, Y. *et al.* (2016) 'Adipose mesenchymal stromal cell-based therapy for severe osteoarthritis of the knee : A phase I dose escalation trial .', *Stem cells in translational*

medicine, 5(7), pp. 847–856.

Peters, K. *et al.* (2009) 'Changes in human endothelial cell energy metabolic capacities during in vitro cultivation. The role of "aerobic glycolysis" and proliferation', *Cell Physiol Biochem*, 24(5–6), pp. 483–492.

Pette, D. (1970) *Zellphysiologie des Stoffwechsels*. 12th edn. Konstanz: Konstanzer Universitätsverlag.

Philips, B. J. *et al.* (2013) 'Prevalence of endogenous CD34+ adipose stem cells predicts human fat graft retention in a xenograft model.', *Plastic and reconstructive surgery*, 132(4), pp. 845–58.

Planat-Benard, V. *et al.* (2004) 'Plasticity of human adipose lineage cells toward endothelial cells: physiological and therapeutic perspectives', *Circulation*, 109(5), pp. 656–663.

Quarto, N. *et al.* (2010) 'Origin Matters : Differences in Embryonic Tissue', *Journal of bone and mineral research*, 25(7), pp. 1680–1694.

Rada, T., Reis, R. L. and Gomes, M. E. (2011) 'Distinct Stem Cells Subpopulations Isolated from Human Adipose Tissue Exhibit Different Chondrogenic and Osteogenic Differentiation Potential', *Stem Cell Reviews and Reports*, 7(1), pp. 64–76.

Rigotti, G. *et al.* (2007) 'Clinical treatment of radiotherapy tissue damage by lipoaspirate transplant: A healing process mediated by adipose-derived adult stem cells', *Plastic and Reconstructive Surgery*, 119(5), pp. 1409–1422.

Rodbell, M. (1964) 'Metabolism of isolated fat cells: I. Effects of hormones on glucose metabolism and lipolysis', *Journal of Biological Chemistry*, 239(2), pp. 375–380.

Rodriguez, L. V *et al.* (2006) 'Clonogenic multipotent stem cells in human adipose tissue differentiate into functional smooth muscle cells', *PNAS*, 103(32), pp. 12167–12172.

Rose, L. C. *et al.* (2015) 'Fluorine-19 labeling of stromal vascular fraction cells for clinical imaging applications', *Stem cells translational medicine*, 4, pp. 1472–1481.

Rosen, E. D. and Spiegelman, B. M. (2006) 'Adipocytes as regulators of energy balance and glucose homeostasis', *Nature*, 444(7121), pp. 847–853.

Rutkowski, J. M., Stern, J. H. and Scherer, P. E. (2015) 'The cell biology of fat expansion', *Journal of Cell Biology*, 208(5), pp. 501–512.

Sacks, H. and Symonds, M. E. (2013) 'Anatomical locations of human brown adipose tissue: Functional relevance and implications in obesity and type 2 diabetes', *Diabetes*, 62(6), pp. 1783–1790.

Saito, M. *et al.* (2009) 'High incidence of metabolically active brown adipose tissue in healthy adult humans: effects of cold exposure and adiposity.', *Diabetes*, 58(7), pp. 1526–1531.

Saks, V. A. *et al.* (1985) 'Creatine kinase of rat heart mitochondria. The demonstration of functional coupling to oxidative phosphorylation in an inner membrane-matrix preparation', *Journal of Biological Chemistry*, 260(12), pp. 7757–7764.

Salamon, A. *et al.* (2013) 'Articular cartilage-derived cells hold a strong osteogenic differentiation potential in comparison to mesenchymal stem cells in vitro',

Experimental Cell Research. Elsevier, 319(18), pp. 2856–2865.

Salamon, A. *et al.* (2014) 'Long-term tumor necrosis factor treatment induces NFκB activation and proliferation, but not osteoblastic differentiation of adipose tissue-derived mesenchymal stem cells in vitro', *The International Journal of Biochemistry & Cell Biology*. Elsevier Ltd, 54, pp. 149–162.

Schlattner, U. *et al.* (2002) 'Creatine kinase and creatine transporter in normal, wounded, and diseased skin', *Journal of Investigative Dermatology*, 118(3), pp. 416–423.

Schmidt, F. W. and Schmidt, E. (1960) 'Enzym-Muster menschlicher Gewebe', *Klinische Wochenschrift*, 38(19), pp. 957–961.

Schop, D. *et al.* (2009) 'Growth, Metabolism and Growth Inhibitors of Mesenchymal Stem Cells', *Tissue engineering. Part A*, 15(8), pp. 1877–1886.

Schwandt, P. *et al.* (1970) 'Aktivitätsbestimmung von Schlüsselenzymen im menschlichen Fettgewebe', *Klinische Wochenschrift*, 48(4), pp. 224–227.

Scrutton, M. C. and Utter, M. F. (1968) 'The regulation of glycolysis and gluconeogenesis in animal tissues', *Annual Revision of Biochemistry*, 37, pp. 249–302.

Shonk, C. E. *et al.* (1964) 'Enzyme patterns in human tissues. II. Glycolytic enzyme patterns in nonmalignant human tissues', *Cancer research*, 24(4), pp. 709–721.

Shum, L. C. *et al.* (2016) 'Energy Metabolism in Mesenchymal Stem Cells During Osteogenic Differentiation', *Stem Cells and Development*, 25(2), pp. 114–122.

Shyh-Chang, N. and Daley, G. Q. (2015) 'Metabolic switches linked to pluripotency and embryonic stem cell differentiation', *Cell Metabolism*. Elsevier Inc., 21(3), pp. 349–350.

Si, Y., Yoon, J. and Lee, K. (2007) 'Flux profile and modularity analysis of time-dependent metabolic changes of de novo adipocyte formation', *American Journal of Physiology-Endocrinology and Metabolism*, 292(6), pp. E1637–E1646.

Sidney, L. E. *et al.* (2014) 'Concise review: Evidence for CD34 as a common marker for diverse progenitors', *Stem Cells*, 32(6), pp. 1380–1389.

da Silva Meirelles, L. (2006) 'Mesenchymal stem cells reside in virtually all post-natal organs and tissues', *Journal of Cell Science*, 119(11), pp. 2204–2213.

da Silva Meirelles, L., Caplan, A. I. and Nardi, N. B. (2008) 'In Search of the In Vivo Identity of Mesenchymal Stem Cells', *Stem Cells*, 26(9), pp. 2287–2299.

Simmons, P. J. and Torok-storb, B. (1991) 'Identification of Stromal Cell Precursors in Human Bone Marrow by a Novel Monoclonal Antibody, STRO-1', *Blood*, 78(1), pp. 55–62.

Simmons, P. J. and Torok-Storb, B. (1991) 'CD34 expression by stromal precursors in normal human adult bone marrow.', *Blood*, 78(11), pp. 2848–2853.

Sledzinski, T. *et al.* (2013) 'Association between cytosolic glycerol 3-phosphate dehydrogenase gene expression in human subcutaneous adipose tissue and BMI', *Cellular Physiology and Biochemistry*, 32(2), pp. 300–309.

Smolková, K. and Jezek, P. (2012) 'The role of mitochondrial NADPH-dependent isocitrate dehydrogenase in cancer cells', *International Journal of Cell Biology*, 2012, pp.

1–12.

Sotiropoulou, P. a *et al.* (2006) 'Characterization of the optimal culture conditions for clinical scale production of human mesenchymal stem cells.', *Stem cells*, 24(2), pp. 462–71.

Spalding, K. L. *et al.* (2008) 'Dynamics of fat cell turnover in humans', *Nature*, 453(7196), pp. 783–787.

Stabile, M. *et al.* (2014) 'Jet-assisted fat transfer to the female breast: preliminary experiences', *European Journal of Plastic Surgery*, 37(5), pp. 267–272.

Stasch, T. *et al.* (2015) 'Débridement and Autologous Lipotransfer for Chronic Ulceration of the Diabetic Foot and Lower Limb Improves Wound Healing', *Plastic and Reconstructive Surgery*, 136(6), pp. 1357–1366.

Strawford, A. *et al.* (2004) 'Adipose tissue triglyceride turnover, de novo lipogenesis, and cell proliferation in humans measured with 2H2O', *AJP: Endocrinology and Metabolism*, 286(4), pp. E577–E588.

Stutz, J. J. and Krahl, D. (2009) 'Water jet-assisted liposuction for patients with Lipoedema: Histologic and immunohistologic analysis of the aspirates of 30 lipoedema patients', *Aesthetic Plastic Surgery*, 33(2), pp. 153–162.

Swierczynski, J. *et al.* (2003) 'Enhanced glycerol 3-phosphate dehydrogenase activity in adipose tissue of obese humans', *Molecular and Cellular Biochemistry*, 254(1–2), pp. 55–59.

Tallone, T. *et al.* (2011) 'Adult Human Adipose Tissue Contains Several Types of Multipotent Cells', *Journal of Cardivascular and Translational Research*, 4(2), pp. 200–210.

Tavian, M. *et al.* (1996) 'Aorta-Associated CD34+ Hematopoietic Cells in the Early Human Embryo', *Blood*, 87(1), pp. 67–72.

Tian, W. *et al.* (1998) 'Importance of glucose-6-phosphate dehydrogenase activity for cell growth', *The Journal of Biological Chemistry*, 273(17), pp. 10609–10617.

Trayhurn, P. (2005) 'Endocrine and signalling role of adipose tissue: New perspectives on fat', *Acta Physiologica Scandinavica*, 184(4), pp. 285–293.

Trujillo, M. E. and Scherer, P. E. (2006) 'Adipose tissue-derived factors: Impact on health and disease', *Endocrine Reviews*, 27(7), pp. 762–778.

Veech, R. L., Raijman, L. and Krebs, H. A. (1970) 'Equilibrium relations between the cytoplasmic adenine nucleotide system and nicotinamide–adenine nucleotide system in rat liver', *Biochemical Journal*, 117(3), pp. 499–503.

Wakil, S. J. *et al.* (1954) 'Studies on the fatty acid oxidizing system of animal tissues', *Journal of Biological Chemistry*, 207(2), pp. 631–638.

Wallimann, T. *et al.* (1992) 'Intracellular compartmentation, structure and function of creatine kinase isoenzymes in tissues with high and fluctuating energy demands: the "phosphocreatine circuit" for cellular energy homeostasis', *Biochemical Journal*, 281(1), pp. 21–40.

Wallimann, T. and Hemmer, W. (1994a) '111-2 Creatine kinase in non-muscle tissues and cells', *Molecular and cellular biochemistry*, 133(134), pp. 193–220.

Wallimann, T. and Hemmer, W. (1994b) 'Creatine kinase in non-muscle tissues and cells', *Molecular and Cellular Biochemistry*, 133–134(1), pp. 193–220.

Warburg, O. (1956) 'On the origin of cancer cells', *Science*, 123(3191), pp. 309–314.

Warburg, O., Wind, F. and Negelein, E. (1927) 'The metabolism of tumors in the body', *The Journal of General Physiology*, 8, pp. 519–530.

Wilson-Fritch, L. *et al.* (2003) 'Mitochondrial Biogenesis and Remodeling during Adipogenesis and in Response to the Insulin Sensitizer Rosiglitazone', *Molecular and Cellular Biology*, 23(3), pp. 1085–1094.

Xie, X. *et al.* (2010) 'Characterization of the human adipocyte proteome and reproducibility of protein abundance by one-dimensional gel electrophoresis and HPLC-ESI-MS/MS', *J Proteome Res*, 9(9), pp. 4521–34.

Yoder, M. C. (2012) 'Human endothelial progenitor cells', *Cold Spring Harbor Perspectives in Medicine*, 2(7), pp. 1–14.

Yoshimura, K. *et al.* (2006) 'Characterization of Freshly Isolated and Cultured Cells Derived From the Fatty and Fluid Portions of Liposuction Aspirates', *Journal of cellular physiology*, 208(1), pp. 64–76.

Zhang, Y. *et al.* (2013) 'Mitochondrial Respiration Regulates Adipogenic Differentiation of Human Mesenchymal Stem Cells', *PLoS ONE*, 8(10), pp. 1–12.

Zimmerlin, L. *et al.* (2010) 'Stromal vascular progenitors in adult human adipose tissue', *Cytometry. Part A : the journal of the International Society for Analytical Cytology*, 77(1), pp. 22–30.

Zimmerlin, L. *et al.* (2013) 'Mesenchymal markers on human adipose stem/progenitor cells Ludovic', *Cytometry. Part A : the journal of the International Society for Analytical Cytology*, 83(1), pp. 134–40.

Zingaretti, M. C. *et al.* (2009) 'The presence of UCP1 demonstrates that metabolically active adipose tissue in the neck of adult humans truly represents brown adipose tissue', *The FASEB Journal*, 23(9), pp. 3113–3120.

Zuk, P. a. *et al.* (2002) 'Human adipose tissue is a source of multipotent stem cells', *Molecular biology of the cell*. Edited by M. Raff. The American Society for Cell Biology, 13(12), pp. 4279–4295.

Zuk, P. A. *et al.* (2001) 'Multilineage Cells from Human Adipose Tissue: Implications for Cell-Based Therapies', *Tissue Engineering*, 7(2), pp. 211–228.

Zuk, P. A. (2010) 'The Adipose-derived Stem Cell: Looking Back and Looking Ahead', *Mol.Biol.Cell*, 21(1939-4586 (Electronic)), pp. 1783–1787.

Erklärung über den Eigenanteil an den Veröffentlichungen

Alle aufgeführten Studien sind in Erstautorenschaft meiner Person entstanden. Alle Co-Autoren haben die Manuskripte der Veröffentlichungen begutachtet und freigegeben.

Studie I - ***Isolation and differentiation potential of human mesenchymal stem cells from adipose tissue harvested by water jet-assisted liposuction***

1. 80 % Durchführung der Datenerhebung im Labor (Live/Dead-Färbung Fettgewebe, Mikroskopie, Zellisolation und Kultur, Kristallviolett-, Bodipy-, Alkalische Phosphatase und Kresolphthalein-Quantifizierung)
2. 100 % Statistische Datenauswertung und Erstellen von Tabellen und Abbildungen
3. 80 % Diskussion und Interpretation der Daten
4. 80 % Entwurf und Verfassen der Manuskripte inkl. Literaturrecherche

Studie II - ***Human adipocytes and CD34$^+$ cells from the stromal vascular fraction of the same adipose tissue differ in their energy metabolic enzyme configuration***

1. 100 % Durchführung der Datenerhebung im Labor (Isolation Adipozyten und CD34$^+$-Zellen, Live/Dead-Färbung, Zellpräparation für und Quantifizierung von Enzymaktivitäten, Bestimmung DNA-Menge, Färbung für Durchflusszytometrie)
2. 100 % Statistische Datenauswertung und Erstellen von Tabellen und Abbildungen
3. 80 % Diskussion und Interpretation der Daten
4. 80 % Entwurf und Verfassen der Manuskripte inkl. Literaturrecherche

Studie III - ***Energy metabolic capacities of human adipose-derived mesenchymal stromal cells in vitro and their adaptations in osteogenic and adipogenic differentiation***

1. 100 % Durchführung der Datenerhebung im Labor (Zellisolation und Kultur, Live/Dead-Färbungen, Mikroskopie, Kristallviolett-, Bodipy-, Alkalische Phosphatase-Quantifizierung, Zellpräparation für und Quantifizierung von Enzymaktivitäten, Bestimmung DNA-Menge, RNA-Isolation und Expressionsanalyse Enzymisotypen, Mitochondrienisolation und -quantifizierung)
2. 100 % Statistische Datenauswertung und Erstellen von Tabellen und Abbildungen
3. 90 % Diskussion und Interpretation der Daten
4. 80 % Entwurf und Verfassen der Manuskripte inkl. Literaturrecherche

_____ _____

Ort, Datum Unterschrift - Juliane Meyer

_____ _____

Ort, Datum Unterschrift – PD Dr. Kirsten Peters (Betreuerin)

Selbstständigkeitserklärung

Ich versichere, die vorliegende Arbeit zum Thema „Energy metabolic configuration of human adipose tissue-derived cells and its changes due to *in vitro* culture with osteogenic and adipogenic differentiation“ selbständig und ohne die Hilfe Dritter verfasst zu haben. Stellen, die anderen Werken in Wortlaut oder Sinn entnommen sind, habe ich durch die Angabe der entsprechenden Quellen kenntlich gemacht.

Ich erkläre, meine wissenschaftliche Arbeit nach den Prinzipien der guten wissenschaftlichen Praxis gemäß der gültigen „Satzung der Universität Rostock zur Sicherung guter wissenschaftlicher Praxis“ angefertigt zu haben.

_____ _____

Ort, Datum Unterschrift - Juliane Meyer

Danksagung

Außerordentlicher Dank gilt meiner Gutachterin und Betreuerin PD Dr. Kirsten Peters. Durch ihre Anleitung aber auch den Freiraum, den sie mir in der Gestaltung meiner wissenschaftlichen Arbeit hat zukommen lassen, habe ich es gelernt selbstständig wissenschaftlich zu arbeiten und dabei immer nach ehrlicher Erkenntnis und hoher wissenschaftlicher Qualität zu streben.

Besonderer Dank gilt ebenso meinem Gutachter und Betreuer Prof. Dr. Fritz-Olaf Lehmann. Er bot mir stets ein offenes Ohr und seinen Blick auf das große Ganze, um meine Arbeit eigenständig in die Welt der Wissenschaft einordnen zu können.

Ich möchte den Kollegen des AMP-Lab Mainz, Ullrich Knollmann, Sebastian Mispagel und Tanja May, ganz speziell aber Prof. Dr. Günter Kamp danken. Die geduldige Betreuung und fachliche Zusammenarbeit tragen bis heute ihre Früchte.

Ich möchte allen Kollegen aus dem Arbeitsbereich Zellbiologie danken. Durch die freundliche, offene und absolut kollegiale Zusammenarbeit, die im Arbeitsbereich gepflegt wird, war die Arbeit nicht nur zu schaffen, sie hat auch Spaß gemacht.

Dank gilt ebenso meinen Kollegen der Firma Human Med AG und dem Lehrstuhl für Mikrofluidik der Universität Rostock. Ihre Kooperation ermöglichte meine Stelle an der Universitätsmedizin. Die Herausforderungen vor die wir uns gegenseitig gestellt und die wir gemeinsam gemeistert haben, haben mich viel über den Sinn und den Wert der interdisziplinären Zusammenarbeit gelehrt.

Ich danke meinen Freunden, von denen viele ebenfalls in der Promotions-situation waren. Geteilter Frust ist bekanntlich halber Frust und wir haben uns gegenseitig immer daran erinnert, dass auch für andere Dinge Platz sein muss und kann.

Meinem Freund danke ich für seine immerwährende, geduldige Unterstützung und dafür, dass er mich an den richtigen Stellen motiviert und an den richtigen Stellen zu Pausen überredet hat.

Zu Letzt aber am aller meisten danke ich meinen Eltern und meinem Bruder. Ihr habt immer an mich geglaubt, auch wenn ich es mal nicht konnte. Ohne euch wäre es nicht gegangen.

Lebenslauf

Persönliche Daten

Name	Juliane Meyer
Geburtsdatum	31.07.1986
Familienstand	ledig

Beruflicher Werdegang

seit 03|2018	Human Med AG – Angestellte Medical Affairs
2011-2018	Universitätsmedizin Rostock, Arbeitsbereich Zellbiologie – wissenschaftliche Mitarbeiterin

Studium

10|2005-12|2011	Diplomstudium der Biologie an der Universität Rostock Hauptfach: Tierphysiologie Nebenfach 1: Genetik Nebenfach 2: Mikrobiologie Nebenfach 3: Medizinische Mikrobiologie Diplomarbeit: „Effekte der osteogenen und adipogenen Differenzierung auf den Energiestoffwechsel humaner, mesenchymaler Stammzellen in vitro“

Reprints of Publications included in this Dissertation

1. Isolation and differentiation potential of human mesenchymal stem cells from adipose tissue harvested by water jet-assisted liposuction
2. Human adipocytes and CD34+ cells from the stromal vascular fraction of the same adipose tissue differ in their energy metabolic enzyme configuration
3. Energy metabolic capacities of human adipose-derived mesenchymal stromal cells *in vitro* and their adaptations in osteogenic and adipogenic differentiation

Aesthetic Surgery Journal Advance Access published May 24, 2015

Research

Isolation and Differentiation Potential of Human Mesenchymal Stem Cells From Adipose Tissue Harvested by Water Jet-Assisted Liposuction

Aesthetic Surgery Journal
2015, 1–10

DOI: 10.1093/asj/sjv075
www.aestheticsurgeryjournal.com
OXFORD UNIVERSITY PRESS

Juliane Meyer, MSc; Achim Salamon, PhD; Nicole Herzmann, MSc; Stefanie Adam; Hans-Dieter Kleine, MD; Inge Matthiesen, PhD; Klaus Ueberreiter, MD; and Kirsten Peters, PhD

Abstract

Background: In recent years the therapeutic application of extracted adipose tissue for autologous fat grafting and the application of adipose tissue-derived mesenchymal stem cells (adMSC) isolated thereof has progressed. Water-jet assisted liposuction (WAL) is 1 procedure for harvesting adipose tissue and provides a favorable aesthetic outcome combined with high tissue protection. Tissue aspirated by WAL has been successfully applied in grafting procedures.

Objectives: The aims of this study were to confirm the tissue viability and to understand the abundance and mesenchymal differentiation capacity of stem cells within the tissue.

Methods: We analyzed tissue integrity of WAL tissue particles via fluorescence microscopy. The adMSC content was determined by isolating the cells from the tissue. The mesenchymal differentiation capacity was confirmed with cytochemical staining methods.

Results: The stromal vascular fraction of WAL tissue showed high viability and contained an average of 2.6 × 105 CD34-positive cells per milliliter of tissue. Thus WAL tissue contains a high number of stem cells. Furthermore adMSC isolated from WAL tissue showed typical mesenchymal differentiation potential.

Conclusions: WAL of adipose tissue is well suited for autologous fat grafting because it retains tissue viability. Furthermore it is a valid source for the subsequent isolation of adMSC with multipotent differentiation potential.

Level of Evidence: 3

Therapeutic

Accepted for publication April 6, 2015.

Through the therapeutic application of extracted adipose tissue for autologous fat grafting, liposuction has become an important issue.[1,2] In this context the properties of the aspirated tissue, like tissue particle size, viability, adipocytes number, and other adipose-resident cell types or functional structures (eg, blood vessels) need to be investigated in closer detail.

Adipose tissue is composed of various cell types (adipocytes, endothelial cells, fibroblasts, blood and blood-derived cells, and adipose tissue-derived mesenchymal stem cells [adMSC]).[3-6] Enzymatic digestion of the adipose tissue and depletion of adipocytes yields the so-called stromal vascular fraction (SVF), which already has successfully been used in

Mrs Meyer and Mrs Herzmann are PhD Students, Dr Salamon is a Post-doctoral Fellow, Mrs Adam is a Technical Assistant, and Dr Peters is Head of the Stem Cell Biology Group, Department of Cell Biology, Rostock University Medical Center, Rostock, Germany. Dr Kleine is on the Executive Board of Seracell Stammzelltechnologie GmbH, Rostock, Germany. Dr Matthiesen is Head of the Department of Medical Affairs, human med AG, Schwerin, Germany. Dr Ueberreiter is a Plastic Surgeon in private practice in Birkenwerder, Germany.

Corresponding Author:
Dr Kirsten Peters, Department of Cell Biology, Rostock University Medical Center, Schillingallee 69, 18057 Rostock, Germany.
E-mail: kirsten.peters@med.uni-rostock.de

different clinical approaches such as supplementation of fat grafts and treatment of urinary incontinence and chronic wounds.[7-10]

Zuk et al were the first to describe adMSC.[6] By their intrinsic capacity for self-renewal and multipotent mesenchymal differentiation, adMSC are important in tissue homeostasis and regeneration.[11] Human adMSC were shown to directly differentiate into osteoblasts and endothelial cells in a nonunion fracture model.[12] In case studies, human adMSC were already successfully used to treat critical-size calvaria[13] and maxilla defects.[14] Furthermore, adMSC were demonstrated to engraft at long-term at the transplantation site.[15,16]

Compared with bone marrow, adipose tissue can be harvested in higher amounts, with a higher abundance of stem cells and less donor-site morbidity.[17] adMSC are present at a concentration of roughly 50,000 cells per mL adipose tissue (approximately 7% of the cells found in enzyme-dissolved adipose tissue),[18,19] which is 100-fold higher than found for mesenchymal stem cells (MSC) isolated from bone marrow.[17] Also, the use of adult stem cells does not entail the ethical concerns that the use of embryonic stem cells does. Finally adMSC fulfill all MSC characteristics defined by the International Society for Cellular Therapy, the International Federation of Adipose Therapeutics and Sciences, and others.[20,21]

Adipose tissue can be harvested by various methods, such as resection, conventional liposuction, syringe-aspiration, and others.[2] The specific liposuction methodology applied may impact the viability of cells present in the harvested tissue.[22,23] Water jet-assisted liposuction (WAL) is a liposuction procedure that applies the tumescent solution as a thin, fan-shaped, targeted, pulsating jet.[24,25] The cannula used during the operation comprises 2 channels that make it possible to infiltrate the tumescent solution and aspirate the emerging water and fat suspension at the same time. Thus, the amount of fluid infiltrated into the patient is much lower than during conventional liposuction procedures, which lowers the risk of cardiovascular side effects. This aims at ensuring the desired aesthetic outcome and safety of the patient as well as protecting the harvested adipose tissue. Our examinations assure quality of autologous fat grafts obtained by WAL and show differentiation reliability of mesenchymal stem cells isolated from WAL tissue. To this end, we examined the viability, number and adipogenic or osteogenic differentiation potential of adMSC isolated from WAL-harvested adipose tissue.

METHODS

If not stated otherwise, all plastic-ware was from Greiner Bio-One (Frickenhausen, Germany) and all reagents were from Sigma-Aldrich (Steinheim, Germany).

Donors

This study examined 13 consecutive patients (1 man and 12 women) over a 27-month period from August 2012 to October 2014. The patients gave written informed consent that they were willing to take part in this study. The study was approved by the ethics committee of Rostock University Medical Center under the registration number A2013-0112, and it complies with the ethical standards defined by the World Medical Association Declaration of Helsinki.

Aspiration of Human Adipose Tissue

The liposuction procedure was carried out according to the BEAULI protocol described by Ueberreiter et al.[26] Briefly, a pulsating water jet was applied for infiltration with simultaneous suction. For infiltration the ranges 1 to 3 are available, ranging from 90 mL/minutes ± 15% to 130 mL/minutes ± 15%. The infiltration solution used was classical Klein's tumescence solution that was prewarmed to 37 to 38°C. The cannulas for harvesting have an outer diameter of 38 mm and bear sharp tips. After the first infiltration, there was no required waiting period before the suction could be commenced. The negative pressure for the suction was adjusted to 500 mbar.

Viability Assessment of the WAL-Isolated Tissue

In order to evaluate the viability of the aspirated tissue, a live/dead staining was performed as described previously.[27] Therefore, the aspirated tissue was incubated for 10 minutes with cell culture medium (Dulbecco's Modified Eagle Medium (DMEM), Life Technologies, Darmstadt, Germany) supplemented with 3 µM Hoechst 33342 (Bis-benzimide H33342 trihydrochloride), 500 nM propidium iodide, and 1 µM calcein acetoxymethyl ester (both Life Technologies). The tissue was then analyzed by fluorescence microscopy (Carl Zeiss Microscopy GmbH, Göttingen, Germany) using the blue, green, and red emission filters. Emission maxima of the dyes are 460 nm (Hoechst 33342), 516 nm (calcein), and 617 nm (propidium iodide). Excitation maxima are 360 nm (Hoechst 33342), 496 nm (calcein), and 535 nm (propidium iodide).

Isolation and Culture of adMSC

As described previously,[28] adipose tissue was digested using 1.6 mg/mL Collagenase NB4 (SERVA, Heidelberg, Germany), a mixture of a neutral protease and the collagenases I and II in phosphate-buffered saline (PBS) with calcium and magnesium (PAA Laboratories, Coelbe, Germany). Through a series of steps of washing in PBS with 10% fetal calf serum (FCS; PAN Biotech, Aidenbach,

Germany) and centrifugation, the SVF was separated from the adipose tissue remains. At this point the SVF cell number and content of CD34-positive cells were determined with flow cytometry (see Flow Cytometric Analysis section). The cells liberated from the digested tissue were incubated for 24 hours under standard cell culture conditions (5% CO_2 and 37°C in a humidified atmosphere). CD34-positive cells were isolated from total plastic-adherent cells using a magnetic bead depletion system (Life Technologies). During this selection procedure, the number of cells that were plastic adherent after 24 hours and the number of cells that were plastic adherent and CD34 positive were determined using the Scepter cell counter (Merck KGaA, Darmstadt, Germany). Since the bead depletion is a standard procedure to attain the cells used for the experiments, we desisted from the reapplication of flow cytometry. After 3 passages, adMSC were seeded into experimentation at 20,000 cells per cm^2. Absence of *Mycoplasma* species was confirmed microscopically after DNA staining.

AdMSC were cultured in standard culture medium, adipogenic differentiation stimulating medium, and osteogenic differentiation-stimulating medium. Standard culture medium was DMEM, high glucose, GlutaMAX-I, supplemented with 1% penicillin/streptomycin (100 U/mL and 100 µg/mL; both Life Technologies), and 10% FCS. For adipogenic stimulation, 500 µM 3-isobutyl-1-methylxanthin (SERVA), 10 µM insulin, 1 µM dexamethasone, and 200 µM indomethacin (Fluka, Seelze & Buchs, Germany) were added to standard culture medium. For osteogenic stimulation, standard culture medium was supplemented with 0.25 g/L ascorbic acid, 1 µM dexamethasone, and 10 µM β-glycerophosphate (Fluka). At confluence, cultivation in standard and differentiation-inducing media began, termed day 0, and took up to 35 days. Change of medium was done every 2 to 3 days.

Flow Cytometric Analysis

In order to quantify the CD34 positive cell population of the SVF, isolated cell-suspension specimens from 7 patients were stained using a CD34 single platform staining kit (Stem-Kit, Beckman-Coulter, Krefeld, Germany). The Stem-Kit Reagents consist of a 2-color fluorescent (CD45-FITC/CD34-PE) murine monoclonal antibody reagent, a 2-color murine fluorescent (CD45-FITC/isoclonic control-PE) reagent to check the non-specific binding of the CD34-PE monoclonal antibody, a nucleic acid viability dye (7-amino-actinomycin-D/7-AAD), a reagent (ammonium chloride) to lyse erythrocytes, and Stem-Count fluorospheres for absolute count determination of CD34-positive cells. Therefore, tubes were prefilled with 20 µL of a mixture of CD45-FITC (clone J33) and CD34-PE (clone 581) and 20 µL of 7-AAD-solution. 100 µL of cell suspension was added and incubated for 15 minutes at room temperature (20°C) in the dark. A second incubation for 10 minutes was done after addition of 2 mL lysis reagent. 100 µL Stem-Count fluorospheres were added to the cell suspension directly before measurement. The flow cytometer FC500 Flow Cytometer (Beckman-Coulter) was equipped with a 20 mW argon-ion-laser providing excitation at a wavelength of 488 nm.

Analysis was done following a modified ISHAGE protocol[29] for single platform analysis.[30] Cells were gated for CD45 and 7-AAD-negative cells to exclude leucocytes and dead cells. Viable CD34-positive cells and fluorospheres were counted using the CXP analysis software (Beckman-Coulter). The stem cell concentration was then calculated on the basis of the fluorosphere concentration provided by the test kit.

Quantification of Cell Number

The cell number in tissue from 8 individuals was determined by crystal violet staining as described previously.[28] Crystal violet stains the negatively charged cellular DNA via ionic attraction[31] in a linear fashion.[32]

Analysis of Mesenchymal Differentiation

Analysis of Adipogenic Differentiation

Intracellular accumulation of lipids in the isolated adMSC of 5 individuals was detected by fluorescence staining of lipid vacuoles after 14 days of culture as described previously.[33] To this end the cells were washed with PBS and fixed in 4% paraformaldehyde (PFA). After washing with PBS, the cells were incubated in the Bodipy staining solution (1 µg/mL 150 mM NaCl, Life Technologies) in the dark. The cells were then washed with PBS and H_2O. The fluorescence intensity was measured in a fluorescence microplate reader (TECAN, Crailsheim, Germany) using an excitation wavelength of 480 nm and an emission wavelength of 515 nm. Fluorescence microscopy was done to document the formation of lipid vacuoles within the cells using an Axiocam MRc fitted to an Axio Scope.A1 (Carl Zeiss Microscopy GmbH).

Analysis of Osteogenic Differentiation

Quantification of alkaline phosphatase (ALP) activity in the isolated adMSC of 6 patients and the extracellular matrix (ECM) calcium content in the isolated adMSC of 4 patients were used to detect osteogenic differentiation of the cells as previously described.[28] For photo documentation of ALP (liver/bone/kidney isoenzyme) activity, cells were stained with a solution of 67 mM 2-Amino-2-methyl-1.3-propanediol (AMPED), 2.7 mM Naphtol AS-MX phosphate, and 2.7 mM Fast Red Violet LB Salt in H_2O. Quantification of ALP activity was done after 21 days of culture by washing cells with Tris-buffered saline and permeabilizing lysis buffer (1% Tween 20 and 100 mM phenylmethanesulfonyl fluoride in H_2O) and incubating with ALP substrate solution (10 mM para-nitrophenylphosphate (pNPP), 100 mM AMPED, and 5 mM $MgCl_2$ in H_2O for 1 hour under standard culture

conditions. To stop ALP activity, 2 M NaOH was added. The absorbance of the supernatant was quantified in a microplate reader (anthos Mikrosysteme) at 405 nm.

For the visual documentation of the calcium deposition in the ECM, the cells were stained with 30 mM Alizarin Red S dissolved in H_2O. Pictures were taken with the camera AxioCam ICc1 fitted to an Axiovert 25 (Carl Zeiss Microscopy GmbH). Quantification of ECM calcium content based on Ca^{2+} complexation by *ortho*-cresolphthalein was done after 35 days. Briefly, after washing cells with PBS and fixation with 4% PFA pre-warmed to 37°C, cells were washed with H_2O, and cresolphthalein buffer (0.1 mg/mL *ortho*-cresolphthalein complexon, 1 mg/mL 8-hydroxy quinoline, and 6% of 37% HCl in H_2O) was added. After incubation for 5 minutes at room temperature (19°C to 21°C), AMP buffer (15% 2-Amino-2-methyl-1-propanol [AMP] in H_2O, pH 10.7) was added and incubated for 15 minutes at room temperature (20°C). The optical density of the supernatant was quantified in a microplate reader (anthos Mikrosysteme) at 580 nm.

Data Illustration and Statistics

All measurements were performed in triplicate. Data are illustrated as bar and line charts as well as box plots and were created using the R software environment for statistical computing and graphics.[34] The data displayed are the medians with positive and negative error bars representing the third and first quartile, respectively. Since the data obtained were in most cases not normally distributed, testing for significance in the difference between 2 datasets was done using the nonparametric Mann-Whitney *U* test. The level of significance was set to a *P*-value of lower or equal to .05 ($P \leq .05$) and calculated using R.

RESULTS

The average patient age was 42 years (range, 24-59 years). All patients were healthy adults seeking contouring of one or more of the following areas: arms, hips, buttocks, upper and lower abdomen, upper and lower back, flanks, inner thighs, and outer thighs. The patients had an average body mass index of 25.8 (range, 21-35). The time from tissue harvest to cell isolation was less than 20 hours.

Viability of the Aspirated Tissue

The combined live/dead staining of WAL tissue resulted in a comprehensive green fluorescence emission of the tissue and thus indicates its viability, while the nuclei of all cells are stained in blue (Figure 1A). A thin green circumferential fluorescent line reflects the spherical shape of the mature adipocytes. The biggest part of the adipocytes is filled by

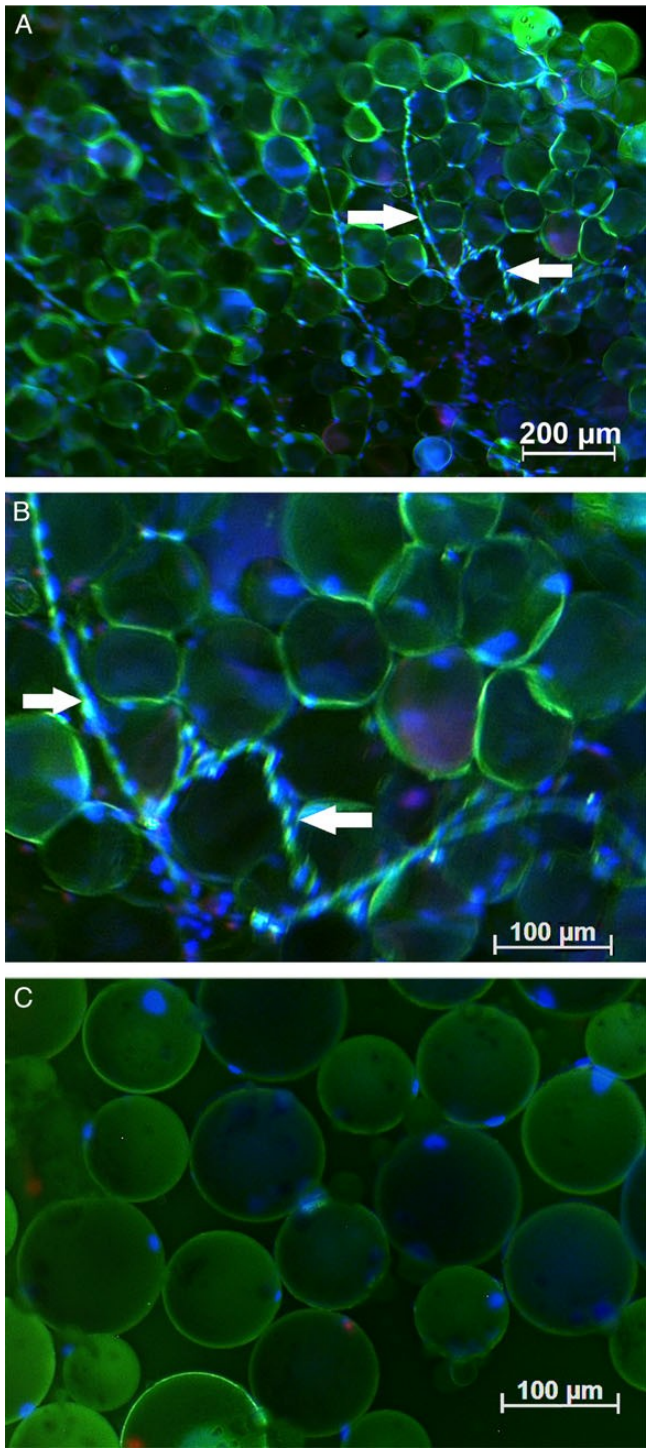

Figure 1. Live/dead-stained adipose tissue directly after the isolation by WAL (A; green: viable cells, red: dead cells, blue: nuclei); detail from isolated tissue showing vasculature-like structures (B); single cell suspension resulting from enzymatic digestion of the tissue (C). Most cells showed an intensive green staining and were thus identified as viable. A number of blood vessel-like structures were detectable (arrows). Only a few dead cells (red fluorescence) were found.

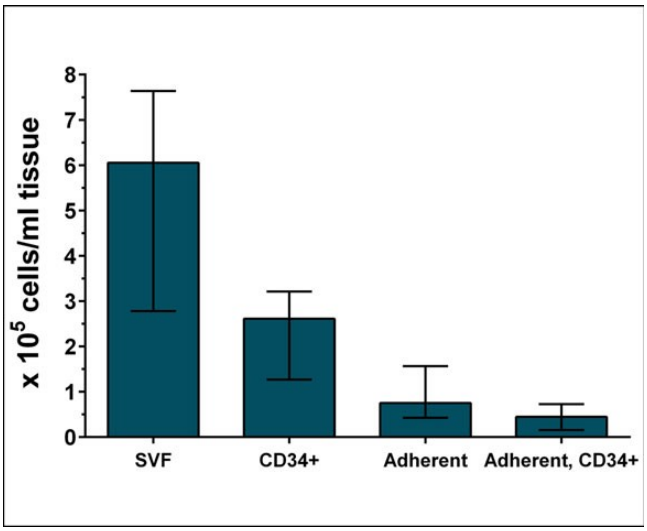

Figure 2. Quantification of cell amounts after different steps of isolation (cell concentration in the SVF; concentration of CD34-positive cells within the SVF; concentration of plastic-adherent cells after 24 hours of culture; concentration of plastic-adherent and CD34-positive cells after 24 hours of culture; n = 7). The SVF on average contains 6.1×10^5 cells per mL harvested adipose tissue and an average of 2.6×10^5 cells per mL tissue was positive for CD34. After 24 hours of cultivation, an average of 0.8×10^5 cells per mL tissue was plastic adherent, and thereof 0.45×10^5 cells per mL tissue, on average, were positive for CD34.

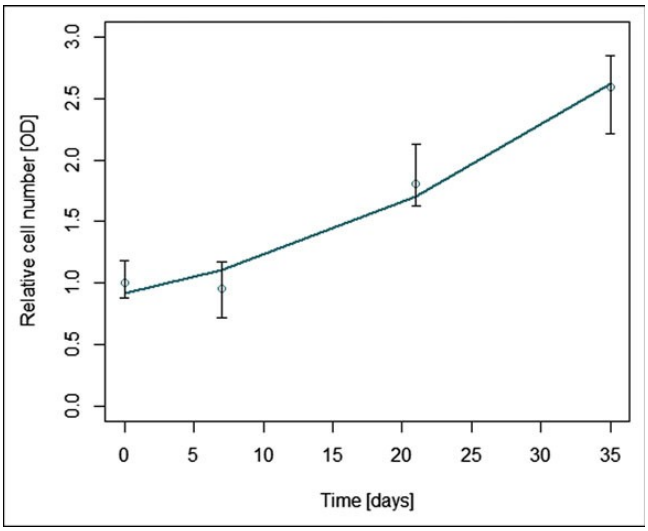

Figure 3. Proliferation of adMSC under steady state cultivation conditions; adMSC were cultured for 35 days. Cell numbers were determined at 0, 7, 21, and 35 days. All values were normalized to the 0 day value. Cells show continuous proliferation, ie, 2.5-fold increase of cell number over 35 days of culture (n = 8).

a unilocular lipid vacuole that is unstained, due to an organelle-inherent lack of esterase activity required for fluorophore activation. Only a few dead cells were detected (Figure 1B, red fluoresecence). Furthermore, blood vessel-like structures were detectable throughout the WAL-derived tissue (white arrows, Figure 1A and B). Collagenase treatment of WAL-isolated tissue led to a single cell suspension of mostly viable cells (Figure 1C).

Number of Cells in Aspirated Tissue

After preparation of a single cell suspension, the SVF was obtained by removal of adipocytes. The SVF on average contained 6.1×10^5 cells per mL aspirated tissue. Almost half of that fraction was identified as CD34 positive (averaging 43%, about 2.6×10^5 cells per mL aspirated tissue). Moreover, an average of 18% of the SVF (0.8×10^5 cells per mL aspirated tissue) was adherent after 24 hours of standard cell culture, roughly half of this portion was adherent and CD34 positive (0.45×10^5 cells per mL aspirated tissue from the SVF) (Figure 2).

Proliferation of adMSC In Vitro

To evaluate the proliferation behavior of WAL-isolated adMSC during cultivation and under differentiation conditions, cells were seeded into steady state conditions and the relative cell numbers were determined after 0, 7, 21, and 35 days of cultivation. We found a continuous increase in cell number and thus continuous proliferation of adMSC (Figure 3).

Mesenchymal Differentiation Potential

Adipogenic Differentiation

After 14 days of adipogenic stimulation, the formation of lipid-filled vacuoles in adMSC was detectable, whereas no lipid vacuoles were found in adMSC under control conditions (Figure 4A,B). Quantification of the amount of accumulated intracellular lipid revealed a significant 3-fold increase under adipogenic differentiation conditions (Figure 4C).

Osteogenic Differentiation

To evaluate the degree of osteogenic differentiation, the activity of the enzyme ALP and the amount of calcium phosphate deposited to the ECM were determined. In contrast to the control cultures showing a mild red staining (Figure 5A), osteogenically stimulated adMSC showed a distinct red staining for ALP after 21 days of cultivation (Figure 5B). After 35 days of osteogenic stimulation, calcium phosphate deposits were found, which was not true for the unstimulated control cultures (Figure 5D,E). Quantification of these differentiation markers confirmed distinct changes in the cellular phenotypes: after 21 days in osteogenic differentiation medium, cells displayed a more than 4-fold higher activity of ALP than cells that had been cultured under standard conditions

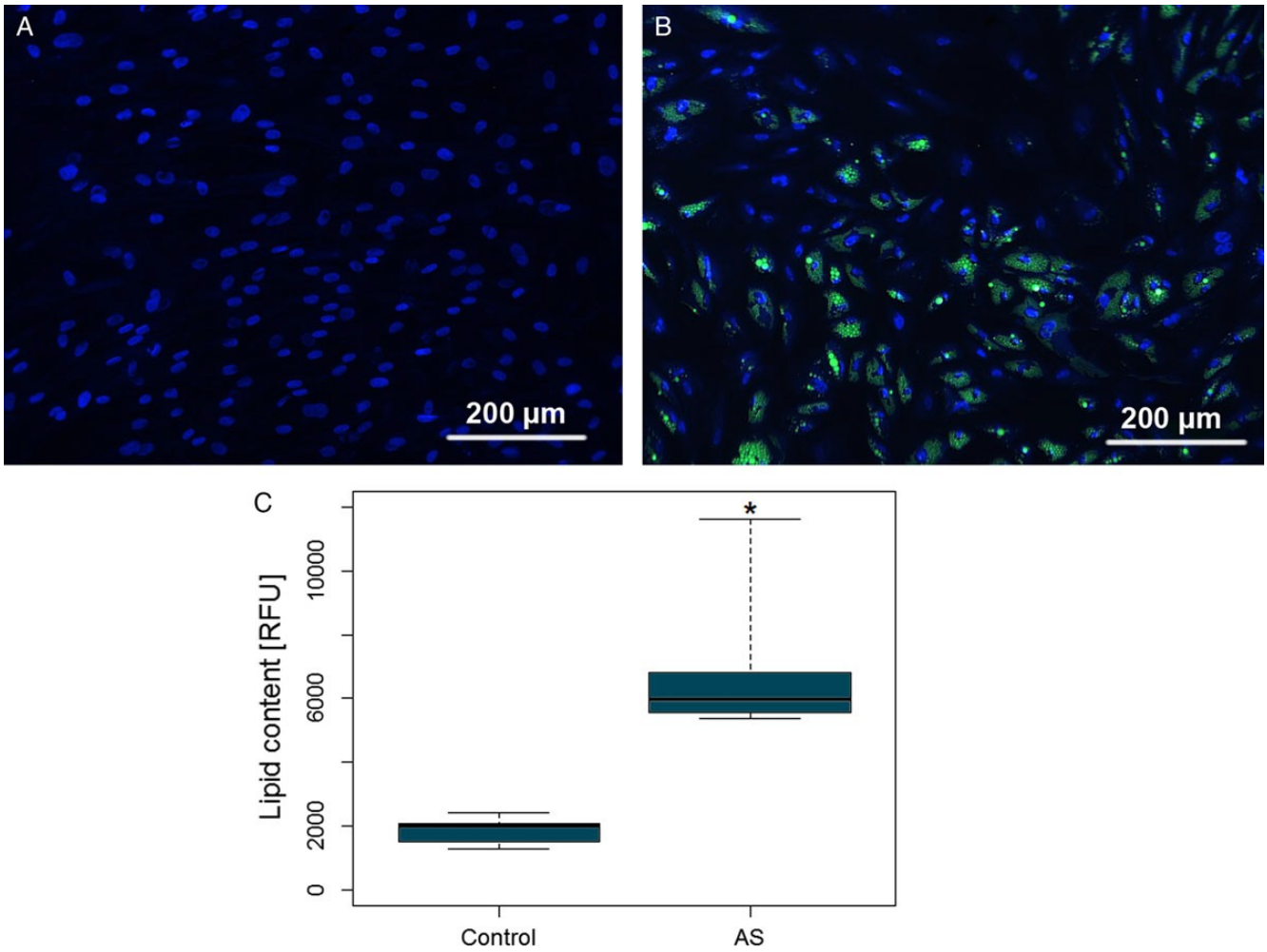

Figure 4. Adipogenic differentiation degree of adMSC. Staining of lipid vacuoles (green) and nuclei (blue) in unstimulated control cultures (A) and adipogenically stimulated adMSC (AS) after 14 days (B). Quantification of lipid content (C, quantification of fluorescence intensity; n = 5; Mann-Whitney *U* test). Only adipogenically stimulated adMSC showed lipid accumulation.

(Figure 5C). Calcium phosphate deposition by adMSC stimulated osteogenically for 35 days was almost 100-times higher than found for cells in the control cultures, which showed almost no calcium phosphate deposition (Figure 5F).

DISCUSSION

WAL is a liposuction procedure that provides a favorable aesthetic outcome combined with high tissue protection and lower risk of cardiovascular side effects due to lowered amount of infiltrated fluid compared with conventional liposuction procedures.[24,25,35,36] Moreover tissue aspirated by WAL has already been successfully applied in grafting procedures.[26,37] Peltoniemi et al proposed that WAL is a preferable technique for autologous fat grafting because it yields a transplant rich in stem cells and enables easy injection without pressure, thus preventing damage to cells.[38]

To confirm the high viability and abundance of stem cells in adipose tissue aspirated by WAL, we analyzed WAL tissue particles regarding integrity, adMSC yield, and mesenchymal differentiation capacity. The scope of this study did not include the examination of other liposuction techniques, such as a direct comparison of tissue harvested from the same patient in the same operation but with 2 different techniques, which would have been a more direct approach for the evaluation of the WAL technique. Nonetheless using data from current publications, the WAL procedure can be put into context with other liposuction techniques. Through visual evaluation, we can show that WAL aspiration results in viable tissue with intact vasculature-like structures. This is consistent with previous findings revealing that WAL tissue consists of intact cell aggregates and small blood vessels.[35] The assessment of the overall cell content and consecutive quantification of dead and viable cells could be a subject of future studies. We

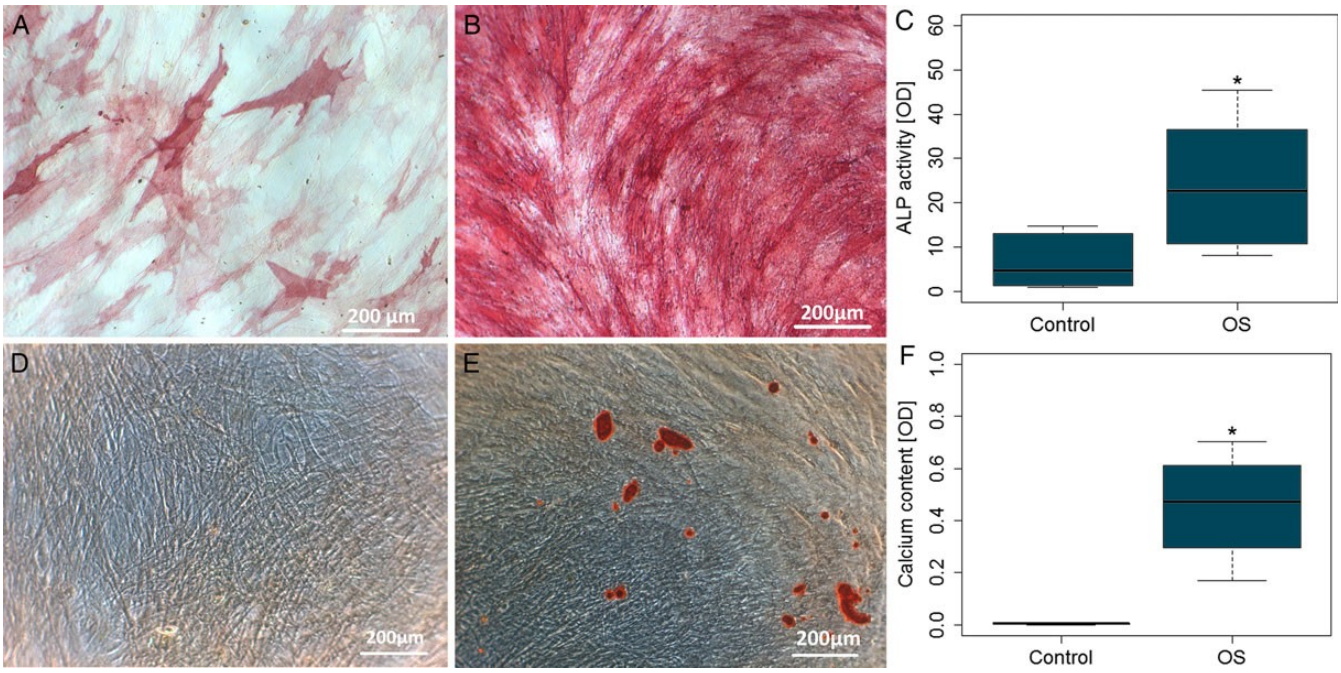

Figure 5. Osteogenic differentiation degree of adMSC. ALP-staining (red) in control cultures (A) and in osteogenically stimulated cultures (OS) after cultivation for 21 days (B). Quantification of ALP activity (C; n = 6; Mann-Whitney *U* test). Staining of ECM calcium deposition in control cultures (D) and osteogenically induced cultures after cultivation for 35 days (E). Quantification of ECM calcium content (F, cresolphthalein staining; n = 4; Mann-Whitney *U* test). Compared with non-stimulated control cultures, osteogenically stimulated cultures showed a 4-fold increase in ALP activity after 21 days and a 100-fold higher calcium deposition in the ECM after 35 days.

found that the enzymatic digestion procedure yields a single cell suspension consisting of adipocytes and an SVF with an average of 6.1×10^5 cells per mL WAL tissue. Differences in cell number of the SVF have been found for different tissue harvesting methods. For example an average of 3×10^5 SVF cells per mL tissue was found after liposuction not performed by WAL,[39] 6×10^5 after ultrasound-assisted liposuction and 7×10^5 after adipose tissue resection.[40] Since the SVF is a heterogeneous mixture of cells and thus the SVF cell content is not a direct measure of stem cell content, we have analyzed the presence of CD34-positive cells within the SVF. CD34 was first identified in stromal precursors in normal human adult bone marrow,[41] and the Stro-1 antibody frequently used for prospective isolation of MSC was consequently generated using CD34-positive MSC.[42] Subsequently, CD34 was found to be expressed also by hematopoietic stem cells in activated state and thus cycling in the blood stream, while hematopoietic stem cells in quiescent state and residing to the bone marrow are CD34 negative.[43] Subsequently, the panel of CD34-expressing cells was even more extended to muscle satellite cells, interstitial cells, epithelial, and endothelial progenitors[44] and is currently thought to be expressed by all perivascular cells in situ,[45] though not always at constant level, as reported for MSC whose CD34-expression level declines upon passaging in vitro.[46] The SVF from WAL tissue contained an average of 2.6×10^5 CD34-positive cells per mL tissue (an average of 43% of SVF). Results from other groups are an average of 22.5%[17] and 15% to 40% cells per mL tissue.[5] Following the statements made above, 1 portion of the CD34-positive cells is of hematopoietic origin while the other is adMSC. This was confirmed by Bourin et al by detecting a CD34-positive, but CD45-negative population of cells within the SVF of adipose tissue because hematopoietic precursors would be positive for both surface markers.[20] The 2 cell populations could be separated by selecting them for adherence to standard tissue culture polystyrene because adMSC are plastic adherent[47] whereas hematopoietic stem cells are not.[48,49] Thus, the CD34-positive and plastic-adherent population of 0.45×10^5 cells per mL tissue (8% of the SVF and 18.9% of the CD34-positive cells) that we isolated from the SVF 24 hours after tissue digestion represents a homogenous population of adMSC. Other groups have found 6.3% ± 1.8% to be functional adMSC residing in the SVF of resected adipose tissue, 1.9% ± 1.3% functional adMSC in the SVF of tissue obtained by tumescent liposuction, and 0.4% ± 0.1% functional adMSC in the SVF of tissue obtained by ultrasound-assisted liposuction.[40] A wide range of adMSC

content in the SVF is discernible comparing a single patient's material. While the average is 8%, as mentioned above, the range varied from 2.3% to 17.9%. Philips et al, in experiments where tissue was harvested with the Coleman technique, found this range to vary from 4% to 37%.[50] The differences between the study outcomes result from the fact that the methods used for the analysis of adMSC content in adipose tissue differ between almost every single research group. In this case not only the aspiration method was different but also the adMSC content was determined by flow cytometric analysis of the SVF, while in our study the absolute adMSC content was determined after 24 hours of plastic adherence.

Supportingly adipogenic stimulation of the isolated adMSC led to intracellular lipid accumulation, which proves the adipogenic differentiation potential of the adMSC obtained from WAL tissue. Also, the osteogenic differentiation potential could be shown after specific stimulation by means of differentiation markers ALP activity and ECM calcification. Thus, adMSC from WAL tissue show mesenchymal differentiation potential. It has been shown that the stem cell content in harvested tissue may be a positive measure for the long-term survival and retention of fat grafts.[50] Thus, not only does WAL represent a very gentle operation technique concerning the patient comfort and the viability of the harvested tissue,[24,38] but the possibility of enriching fat grafts with autologous stem cells isolated from the same tissue represents a promising clinical application. Another important point will be the future application of stem cells in the treatment of, eg, degenerative arthritis, and a possible wide variety of other clinical indications. The comparative examination of tissues from the same patient harvested by WAL and other liposuction techniques would be an interesting prospect for future studies.

CONCLUSIONS

WAL is a liposuction procedure that provides favorable results concerning patient comfort and aesthetic outcome. We show that WAL tissue is a valid source of adMSC, yielding numbers of cells that lie within the range of cell numbers isolatable from adipose tissue harvested with other techniques. The adMSC isolated from WAL tissue are viable and possess mesenchymal differentiation potential. In this respect WAL tissue may be used for autologous fat grafting and is an appropriate source for adMSC isolation.

Disclosures

Dr Kleine is on the Executive Board of Seracell Stammzelltechnologie GmbH (Rostock, Germany) Dr Matthiesen is an employee of human med AG (Schwerin, Germany). The other authors have no financial disclosures to report.

Funding

This work was financially supported by the federal state Mecklenburg-Vorpommern and by the European Union [ESF/IV- WM-B34-0013/11]. This funding was used for the employment of scientific personnel, lab equipment, conference fees, and travel expenses. The funders had no role in the study design, data collection and analysis, decision to publish, or preparation of the manuscript.

REFERENCES

1. Hsu VM, Stransky CA, Bucky LP, Percec I. Fat grafting's past, present, and future: why adipose tissue is emerging as a critical link to the advancement of regenerative medicine. *Aesthet Surg J*. 2012;32(7):892-899.
2. Kakagia D, Pallua N. Autologous Fat Grafting: In Search of the Optimal Technique. *Surg Innov*. 2014;21(3):327-336.
3. Astori G, Vignati F, Bardelli S, et al. "In vitro" and multicolor phenotypic characterization of cell subpopulations identified in fresh human adipose tissue stromal vascular fraction and in the derived mesenchymal stem cells. *J Transl Med*. 2007;5:55.
4. Gimble JM, Guilak F, Bunnell BA. Clinical and preclinical translation of cell-based therapies using adipose tissue-derived cells. *Stem Cell Res Ther*. 2010;1(2):19.
5. Yoshimura K, Shigeura T, Matsumoto D, et al. Characterization of freshly isolated and cultured cells derived from the fatty and fluid portions of liposuction aspirates. *J Cell Physiol*. 2006;208(1):64-76.
6. Zuk PA, Zhu M, Mizuno H, et al. Multilineage cells from human adipose tissue: implications for cell-based therapies. *Tissue Eng*. 2001;7(2):211-228.
7. Sterodimas A, de Faria J, Nicaretta B, Boriani F. Autologous fat transplantation versus adipose-derived stem cell-enriched lipografts: a study. *Aesthet Surg J*. 2011;31(6):682-693.
8. Yamamoto T, Gotoh M, Kato M, et al. Periurethral injection of autologous adipose-derived regenerative cells for the treatment of male stress urinary incontinence: Report of three initial cases. *Int J Urol*. 2012;19(7):652-659.
9. Akita S, Yoshimoto H, Akino K, et al. Early experiences with stem cells in treating chronic wounds. *Clin Plast Surg*. 2012;39(3):281-292.
10. Zhu M, Zhou Z, Chen Y, et al. Supplementation of fat grafts with adipose-derived regenerative cells improves long-term graft retention. *Ann Plast Surg*. 2010;64(2):222-228.
11. Majka SM, Barak Y, Klemm DJ. Concise review: adipocyte origins: weighing the possibilities. *Stem Cells*. 2011;29(7):1034-1040.
12. Shoji T, Ii M, Mifune Y, et al. Local transplantation of human multipotent adipose-derived stem cells accelerates fracture healing via enhanced osteogenesis and angiogenesis. *Lab Invest*. 2010;90(4):637-649.
13. Lendeckel S, Jodicke A, Christophis P, et al. Autologous stem cells (adipose) and fibrin glue used to treat widespread traumatic calvarial defects: case report. *J Craniomaxillofac Surg*. 2004;32(6):370-373.
14. Mesimaki K, Lindroos B, Tornwall J, et al. Novel maxillary reconstruction with ectopic bone formation by GMP

adipose stem cells. *Int J Oral Maxillofac Surg*. 2009;38 (3):201-209.
15. Toupet K, Maumus M, Peyrafitte JA, et al. Long-term detection of human adipose-derived mesenchymal stem cells after intraarticular injection in SCID mice. *Arthritis Rheum*. 2013;65(7):1786-1794.
16. Nowacki M, Pietkun K, Pokrywczynska M, et al. Filling Effects, Persistence, and Safety of Dermal Fillers Formulated With Stem Cells in an Animal Model. *Aesthet Surg J*. 2014;34(8):1261-1269.
17. James AW, Zara JN, Zhang X, et al. Perivascular stem cells: a prospectively purified mesenchymal stem cell population for bone tissue engineering. *Stem Cells Transl Med*. 2012;1(6):510-519.
18. Levi B, Longaker MT. Concise review: adipose-derived stromal cells for skeletal regenerative medicine. *Stem Cells*. 2011;29(4):576-582.
19. Shi Y, Niedzinski JR, Samaniego A, Bogdansky S, Atkinson BL. Adipose-derived stem cells combined with a demineralized cancellous bone substrate for bone regeneration. *Tissue Eng Part A*. 2012;18(13-14):1313-1321.
20. Bourin P, Bunnell BA, Casteilla L, et al. Stromal cells from the adipose tissue-derived stromal vascular fraction and culture expanded adipose tissue-derived stromal/stem cells: a joint statement of the International Federation for Adipose Therapeutics and Science (IFATS) and the International Society for Cellular Therapy (ISCT). *Cytotherapy*. 2013;15 (6):641-648.
21. Dominici M, Le Blanc K, Mueller I, et al. Minimal criteria for defining multipotent mesenchymal stromal cells. The International Society for Cellular Therapy position statement. *Cytotherapy*. 2006;8(4):315-317.
22. Lalikos JF, Li YQ, Roth TP, Doyle JW, Matory WE, Lawrence WT. Biochemical assessment of cellular damage after adipocyte harvest. *J Surg Res*. 1997;70 (1):95-100.
23. Schreml S, Babilas P, Fruth S, et al. Harvesting human adipose tissue-derived adult stem cells: resection versus liposuction. *Cytotherapy*. 2009;11(7):947-957.
24. Man D, Meyer H. Water jet-assisted lipoplasty. *Aesthet Surg J*. 2007;27(3):342-346.
25. Steinert M. [Physical lipolysis]. *Hautarzt*. 2010;61 (10):856-863.
26. Ueberreiter K, von Finckenstein JG, Cromme F, Herold C, Tanzella U, Vogt PM. [BEAULI--a new and easy method for large-volume fat grafts]. *Handchir Mikrochir Plast Chir*. 2010;42(6):379-385.
27. Salamon A, van Vlierberghe S, van Nieuwenhove I, et al. Gelatin-Based Hydrogels Promote Chondrogenic Differentiation of Human Adipose Tissue-Derived Mesenchymal Stem Cells In Vitro. *Materials*. 2014;7(2): 1342-1359.
28. Salamon A, Jonitz-Heincke A, Adam S, et al. Articular cartilage-derived cells hold a strong osteogenic differentiation potential in comparison to mesenchymal stem cells in vitro. *Exp Cell Res*. 2013;319(18):2856-2865.
29. Sutherland DR, Anderson L, Keeney M, Nayar R, Chin-Yee I. The ISHAGE guidelines for CD34+ cell determination by flow cytometry. International Society of Hematotherapy and Graft Engineering. *J Hematother*. 1996;5(3):213-226.
30. Keeney M, Chin-Yee I, Weir K, Popma J, Nayar R, Sutherland DR. Single platform flow cytometric absolute CD34+ cell counts based on the ISHAGE guidelines. International Society of Hematotherapy and Graft Engineering. *Cytometry*. 1998;34(2):61-70.
31. Noeske K. [The binding of crystal violet on deoxyribonucleic acid. Cytophotometric studies on normal and tumor cell nuclei]. *Histochemie*. 1966;7(3):273-287.
32. Gillies RJ, Didier N, Denton M. Determination of cell number in monolayer cultures. *Anal Biochem*. 1986;159 (1):109-113.
33. Fiedler T, Salamon A, Adam S, Herzmann N, Taubenheim J, Peters K. Impact of bacteria and bacterial components on osteogenic and adipogenic differentiation of adipose-derived mesenchymal stem cells. *Exp Cell Res*. 2013;319(18):2883-2892.
34. R_Core_Team. R: A Language and Environment for Statistical Computing. Vienna, Austria: R_Core_Team, 2013.
35. Stutz JJ, Krahl D. Water jet-assisted liposuction for patients with lipoedema: histologic and immunohistologic analysis of the aspirates of 30 lipoedema patients. *Aesthetic Plast Surg*. 2009;33(2):153-162.
36. Stabile M, Ueberreiter K, Schaller HE, Hoppe DL. Jet-assisted fat transfer to the female breast: preliminary experiences. *Eur J Plast Surg*. 2014;37(5):267-272.
37. Sasaki GH. Water-assisted liposuction for body contouring and lipoharvesting: safety and efficacy in 41 consecutive patients. *Aesthet Surg J*. 2011;31(1):76-88.
38. Peltoniemi HH, Salmi A, Miettinen S, et al. Stem cell enrichment does not warrant a higher graft survival in lipofilling of the breast: a prospective comparative study. *J Plast Reconstr Aesthet Surg*. 2013;66(11):1494-1503.
39. Mitchell JB, McIntosh K, Zvonic S, et al. Immunophenotype of human adipose-derived cells: temporal changes in stromal-associated and stem cell-associated markers. *Stem Cells*. 2006;24(2):376-385.
40. Oedayrajsingh-Varma MJ, van Ham SM, Knippenberg M, et al. Adipose tissue-derived mesenchymal stem cell yield and growth characteristics are affected by the tissue-harvesting procedure. *Cytotherapy*. 2006;8(2):166-177.
41. Simmons PJ, Torok-Storb B. CD34 expression by stromal precursors in normal human adult bone marrow. *Blood*. 1991;78(11):2848-2853.
42. Simmons PJ, Torok-Storb B. Identification of stromal cell precursors in human bone marrow by a novel monoclonal antibody, STRO-1. *Blood*. 1991;78(1):55-62.
43. Lin CS, Ning H, Lin G, Lue TF. Is CD34 truly a negative marker for mesenchymal stromal cells? *Cytotherapy*. 2012;14(10):1159-1163.
44. Sidney LE, Branch MJ, Dunphy SE, Dua HS, Hopkinson A. Concise Review: Evidence for CD34 as a Common Marker for Diverse Progenitors. *Stem Cells*. 2014;32(6):1380-1389.
45. Crisan M, Corselli M, Chen WC, Peault B. Perivascular cells for regenerative medicine. *J Cell Mol Med*. 2012;16 (12):2851-2860.

46. Kaiser S, Hackanson B, Follo M, et al. BM cells giving rise to MSC in culture have a heterogeneous CD34 and CD45 phenotype. *Cytotherapy*. 2007;9(5):439-450.
47. Rada T, Reis RL, Gomes ME. Distinct stem cells subpopulations isolated from human adipose tissue exhibit different chondrogenic and osteogenic differentiation potential. *Stem Cell Rev*. 2011;7(1):64-76.
48. Glimm H, Eaves CJ. Direct evidence for multiple self-renewal divisions of human in vivo repopulating hematopoietic cells in short-term culture. *Blood*. 1999;94 (7):2161-2168.
49. Handgretinger R, Gordon PR, Leimig T, et al. Biology and plasticity of CD133+ hematopoietic stem cells. *Ann N Y Acad Sci*. 2003;996:141-151.
50. Philips BJ, Grahovac TL, Valentin JE, et al. Prevalence of endogenous CD34+ adipose stem cells predicts human fat graft retention in a xenograft model. *Plast Reconstr Surg*. 2013;132(4):845-858.

Experimental Cell Research 380 (2019) 47–54

Contents lists available at ScienceDirect

Experimental Cell Research

journal homepage: www.elsevier.com/locate/yexcr

Human adipocytes and CD34$^+$ cells from the stromal vascular fraction of the same adipose tissue differ in their energy metabolic enzyme configuration

Juliane Meyer[a], Robby Engelmann[b], Günter Kamp[c], Kirsten Peters[a,*]

[a] Department of Cell Biology, University Medicine Rostock, Schillingallee 69, 18057 Rostock, Germany
[b] Institute of Immunology & Core Facility for Cell Sorting & Cell Analysis, University Medicine Rostock, Schillingallee 70, 18057 Rostock, Germany
[c] AMP-Lab GmbH, Mendelstraße 11, 48149 Münster, Germany

ARTICLE INFO

Keywords:
Adipose tissue
Adipocytes
Adipose tissue-derived mesenchymal stem/stroma cells
Energy metabolism
Pentose phosphate pathway
Glycolysis
Gluconeogenesis
Dehydrogenases
Fatty acid oxidation

ABSTRACT

Adipose tissue plays a role in energy storage and metabolic balance and is composed of different cell types. The metabolic activity of the tissue itself has been a matter of research for a long time, but comparative data about the energy metabolism of different cell types of human subcutaneous adipose tissue are sparse. Therefore, we compared the activity of major energy metabolic pathways of adipocytes and CD34$^+$ cells from the stromal vascular fraction (SVF) separated from the same tissue. This CD34$^+$ cell fraction is enriched with adipose tissue-derived mesenchymal progenitors, as they account for the largest proportion of CD34$^+$ cells of the SVF. Adipocytes displayed significantly higher mitochondrial enzyme capacities compared to CD34$^+$ SVF-cells, as shown by the higher activities of isocitrate dehydrogenase and ß-hydroxyacyl-CoA dehydrogenase. Inversely, the CD34$^+$ SVF-cells showed higher capacities for cytosolic carbohydrate metabolism, represented by the activity of glycolysis and the pentose phosphate pathway. Thus, the CD34$^+$ SVF-cells may ensure the provision of pentose phosphates and reduction equivalents for the replication of DNA during proliferation. The data indicate that these two cell fractions of the human adipose tissue vary in their metabolic configuration adapted to their physiological demands regarding proliferation and differentiation *in vivo*.

1. Introduction

The view of adipose tissue as an organ of mere energy storage has been amended with its role in the whole body energy balance [1]. Adipose tissue varies in its cellular composition and metabolic task depending on the developmental stage of the individual and the tissue source. A distinction can be made between white, brite/beige and brown adipose tissue. These various adipose tissues differ regarding specific energy metabolic characteristics: white adipose tissue stores and releases energy by turning over lipids [2], whereas brite/beige and brown adipose tissue dissipates energy directly as heat by uncoupling oxidative phosphorylation from adenosine triphosphate (ATP) production [3,4].

White adipose tissue is composed of a variety of cell types besides the tissue-characteristic adipocytes. The size and number of adipocytes in subcutaneous white adipose tissue is highly variable and dependent on the individual energy balance [5]. All cells of the adipose tissue that are not adipocytes are called 'stromal vascular fraction' (SVF) as they can be conjointly collected via centrifugation during the technical process of adipose tissue dissociation and cell isolation. The SVF includes cells like, adipose tissue-derived mesenchymal stromal cells (ASC), the progenitors of adipocytes, endothelial cells, and blood-derived cells such as leukocytes and macrophages [6–8]. One large subfraction of the SVF expresses the transmembrane phosphoglycoprotein CD34 on its surface [6–9]. Relatively little is known about the function and intracellular ligands of CD34 in the SVF of the adipose tissue [10,11]. CD34 has been proposed to both promote proliferation and migration and to block differentiation [12,13]. In the SVF of adipose tissue, CD34$^+$ cells include the ASC, the adipocyte progenitor cells, the endothelial cells and their progenitors, and hematopoietic progenitors [7,8,11,14]. Approximately 60–85% of the CD34$^+$ SVF- cells are ASC [15–19].

Earlier examinations of adipose tissue metabolism by enzyme activity measurement were carried out on whole adipose tissue homogenates [20–23]. In general, enzymes of the glycolytic and related pathways were examined. The enzyme activities in the total adipose tissue homogenates indicated a low glycolytic activity since the activities of the rate-determining enzyme phosphofructokinase (PFK) were low compared to other tissues like skeletal muscle [20]. Furthermore, a low capacity for gluconeogenesis was indicated in total adipose tissue

* Corresponding author.
E-mail address: kirsten.peters@med.uni-rostock.de (K. Peters).

https://doi.org/10.1016/j.yexcr.2019.04.018
Received 14 December 2018; Received in revised form 26 March 2019; Accepted 15 April 2019
Available online 16 April 2019
0014-4827/

homogenates due to the comparably low activities of fructose-1,6-bisphosphatase (FBPase) [20,22].

The knowledge about the energy metabolism of cell types separated from human subcutaneous adipose tissue is limited. Overall adipocytes are shown to demonstrate a continuous turnover of their stored lipids [2]. Kheterpal et al. compared energy metabolic aspects of human adipocytes with the mixed cell population of SVF cells from the same tissue. They found proteins involved in glycolysis and gluconeogenesis, lipid metabolism and oxidative stress defense to be differentially regulated in adipocytes compared to SVF cells [24].

The quantification of enzyme activities can be used for characterizing the metabolic state of tissues [25,26]. Therefore, in this study we have analyzed and compared marker enzyme activities of major energy metabolic pathways of human adipocytes with those of the $CD34^+$ cell population from SVF which is enriched in ASC content. Thus, we compared marker enzyme activities of mature adipocytes with those of an enriched fraction of adipose tissue-derived mesenchymal progenitors. Since the isolation of these cell fractions took place without further cell cultivation, these enzyme activities had not been influenced by *in vitro* conditions.

2. Materials and methods

2.1. Tissue donation

The study was approved by the ethics committee of Rostock University Medical Center [http://www.ethik.med.uni-rostock.de/], registration number A2013-0112 and it complies with the ethical standards defined by the World Medical Association Declaration of Helsinki. The patients gave informed consent for the use of their tissue in a scientific study.

Material from 8 patients was used for this study. Three of these patients were male, five female. The patients were on average 44 years old (ranging from 18 to 65) and had an average BMI of 29.5 (ranging from 25.9 to 34.4) and were thus mildly obese but not diabetic.

2.2. Collection of $CD34^+$ SVF-cells and adipocytes

The adipose tissue was attained by liposuction either using a tumescent or a water-jet assisted procedure. The time between the tissue harvest and the cell isolation was between 3 and 20 h. During this time, the tissue was stored at room temperature. The digestion of two times 30 ml of adipose tissue was based on a previously established isolation protocol [27]; each of the 30 ml tissue portions were exposed to a digestion with an end concentration of 0.12 U/ml collagenase (NB4, Serva). Incubation took place for 30 min, shaking at 37 °C. After filtration through a 100 µm strainer (Greiner), the digested tissue was washed with 10 ml Ringer solution (B. Braun Melsungen) with 4% human albumin (Behring). After 10 min of sedimentation the tissue was centrifuged for 10 min at 400 × g at room temperature. After centrifugation the lipid portion of the tissue consisted of an oily phase on top and a phase with single cell adipocytes relieved from cells of the SVF below. 1 ml of single cell adipocyte suspension was taken and shock frozen in liquid nitrogen. The samples were stored at −80 °C until the measurement of the enzyme activities.

The rest of the supernatant was discarded. The cell pellets were each resuspended in 10 ml Ringer solution with 4% human albumin, filtered through a 40 µm strainer and again centrifuged for 10 min at 400 × g at room temperature. The cell pellets of both 30 ml tissue portions were then pooled in 10 ml Dulbecco's Modified Eagle Medium (DMEM, Thermo Fisher Scientific) containing 10% FCS and antibiotics (100 U/ml penicillin, 100 mg/ml streptomycin, Thermo Fisher Scientific). After the addition of 80 µl magnetic Dynabeads™ from the CD34 positive Isolation Kit (Thermo Fisher Scientific) the cells were incubated on a roll mixer at 4 °C for 30 min. The cells were then attached to a magnet. After the removal of cell culture medium, the cells were resuspended in 10 ml Ringer solution with 4% human albumin. After 10 min of washing on the roll mixer at 4 °C, the cells were again attached to the magnet and finally resuspended in 1.5 ml of sodium phosphate buffer (100 mM Na_2HPO_4, 100 mM NaH_2PO_4, 1 mM EDTA, 1 mM DTT, 1 mM PMSF). 1 ml of cell suspension was shock frozen in liquid nitrogen. The samples were stored at −80 °C until the measurement of the enzyme activities.

2.3. Preparation of adipocytes for enzyme activity measurement

The 1 ml adipocyte fractions were thawed on ice, and 500 µl of sodium phosphate buffer and 1 µl of 100 mM PMSF (Applichem) were added (final PMSF concentration: 66.7 µM). The adipocyte fractions were disintegrated on ice via ultrasonication with a Branson sonifier (3 × 10 s, duty cycle constant, level 1, Heinemann Ultraschall-und Labortechnik). The disintegrated adipocyte solutions were then centrifuged at 10,000 × g for 6 min at 4 °C. The aqueous infranatant was used for the measurement of the enzyme activities.

2.4. Preparation of $CD34^+$ SVF-cells for enzyme activity measurement

The 1 ml $CD34^+$ SVF fractions were thawed on ice and 1 µl of 100 mM PMSF were added. The cells were disintegrated on ice via ultrasonication with a Branson sonifier for 3 × 10 s, duty cycle constant, level 1. The solutions with the entirely disintegrated cells were then centrifuged at 400 × g for 5 min at 4 °C. The supernatant was used for the measurement of the enzyme activities.

2.5. Enzyme activity measurement

Enzyme assays were performed with aliquots of the cell homogenates. The enzyme activities were traced spectrophotometrically in a microplate reader (TECAN), measuring the light absorption at 340 nm (37 °C) using NAD(P)H + H^+ as indicator. The activities were given as international units per mg DNA (1 U = 1 µmol substrate transformed per min at 37 °C). The assays for phosphofructokinase (PFK; EC 2.7.1.11), glyceraldehyde 3-phosphate dehydrogenase (GAPDH, EC 1.2.1.12), lactate dehydrogenase (LDH; EC 1.1.1.27), glucose 6-phosphate dehydrogenase (G6PDH, EC 1.1.1.49), fructose-1,6-bisphosphatase (FBPase, EC 3.1.3.11), glutathione disulfide reductase (GSR; EC 1.8.1.7), NAD^+-dependent isocitrate dehydrogenase (NAD-IDH; EC 1.1.1.41), $NADP^+$-dependent isocitrate dehydrogenase (NADP-IDH; EC 1.1.1.42), ß-hydroxyacyl-CoA dehydrogenase (HOADH; EC 1.1.1.35) and creatine kinase (CK; EC 2.7.3.2) were performed as previously described [28].

2.6. Determination of DNA content

The Qubit™ dsDNA BR Assay Kit and the Qubit® 2.0 Fluorometer (Thermo Fisher Scientific) were used according to the manufacturer's instructions to determine the DNA content in the homogenates. The Qubit™ dsDNA BR Assay Kit detects double-stranded DNA.

2.7. Flow cytometry

The isolated SVF was immediately analyzed via the Stem-Kit™ Reagents test kit (Beckman Coulter). The kit includes the CD45-FITC (clone J33)/CD34-PE (clone 581) Reagent (CD45/CD34), the CD45-FITC/IsoClonic Control-PE Reagent, Stem-Count Fluorospheres, 7AAD Viability dye and 10× NH_4Cl Lysing solution. Staining was done according to the manufacturer's instructions. For the quantification of the amount of nucleated cells, Hoechst 33342 was added in a concentration of 5 µg/ml 10 min before measuring. First the analyzed cell solution was gated on Hoechst-positive and thus nucleated cells. The nucleated cells were further gated on $CD34^+CD45^-$ and $CD34^+CD45^+$ cells. Viability of cells was assessed by 7-AAD staining. The data were acquired with a

FACS Aria II machine (BD Biosciences, Germany) and analyzed using FACS Diva Software (Version 6.1.2).

2.8. Fluorescent staining

All staining solutions were prepared in cell culture medium (see 2.2). The staining of the adipose tissue and adipocytes was performed with Calcein AM (5 µg/ml, ABD Biosciences) and Hoechst 33342 (5 µg/ml, Sigma-Aldrich). After 10 min of incubation in the dark under cautious agitation, fluorescence microscopy images were acquired using an Axiocam MRc fitted to an Axio Scope.A1 (Carl Zeiss).

The staining of the SVF and the $CD34^+$ SVF-cells was performed after centrifugation of the cells at 400 × g. The resulting cell pellet was resuspended in the staining solution containing Calcein-AM and Hoechst 33342 in a concentration of 5 µg/ml each. After 10 min of incubation in the dark, the images were obtained as described above.

2.9. Statistical analysis

The numbers of donors are included in the figure and table legends. Excel 2013 and R software environment (version 3.3.1) for statistical computing and graphics [29] were used for calculations and statistical analysis (homogeneity of variances for the enzyme activity data, *U* test according to Mann and Whitney ($p < 0.05$)). The graphs were generated with GraphPad Prism version 7.02 for Windows (GraphPad Software) and display medians and the interquartile range.

3. Results

3.1. Processing of the human lipoaspirate and characterization of the resulting cell types after tissue dissociation

The processing of the human adipose tissue and the isolation of the two cell fractions was as follows (schematically depicted in Fig. 1I): Aspirated adipose tissue which consists of small lobules (Fig. 1I, top) was subjected to an enzymatic dissociation which led to a single-cell suspension. After steps of washing, filtration and centrifugation the lipid phase was separated from the aqueous phase, leading to the two populations of adipocytes and the SVF (Fig. 1I, middle). By means of a magnetic bead system, the $CD34^+$ fraction was separated from the remainder of the SVF (Fig. 1I, bottom).

These different steps of the processing and cell separation were traced microscopically (Fig. 1II). The aspirated human liposuction tissue consists of small lobules and showed large adipocytes filled with a monolocular lipid vacuole. The adipocytes were embedded in a vascularized tissue structure (Fig. 1IIA). After enzymatic dissociation, the cells from the lipid phase of the preparation were recognizable as adipocytes in suspension due to their monolocular vacuole (Fig. 1IIB). The lipid phase was void of further tissue structures and non-adipocytic cells. Surrounding lipid droplets could be distinguished from the adipocytes by the lack of a nucleus (Fig. 1IIB). The cells of the aqueous phase of the adipose tissue preparation were a mixture of single cells of diverse morphology, defined as the SVF cells. The SVF fraction is free of adipocytes due to the fractionation of the lipid and aqueous phase (Fig. 1IIC). The following CD34 magnetic bead selection resulted in a $CD34^+$ fraction of the SVF (named $CD34^+$ SVF-cells) (Fig. 1IID and E).

Flow cytometry revealed that 36.9% of the isolated SVF cells were $CD34^+$ (Fig. 2). Within the SVF population only 0.9% of the cells were positive for CD34 as well as for CD45. Thus, within the $CD34^+$ SVF, 97.6% of the cells were CD45-negative.

3.2. Analysis of maximum catalytic capacities of major energy metabolic pathways

Important energy-metabolic pathways were examined by measuring the maximum catalytic activities of several marker enzymes in freshly isolated adipocytes and the $CD34^+$ SVF-cells of the SVF from the same adipose tissue (Fig. 3). These analyses revealed that the rate-limiting enzyme of glycolysis, the phosphofructokinase (PFK), is detectable in low activities in adipocytes (0.21 U/mg DNA), whereas $CD34^+$ SVF-cells showed 4.5-fold higher PFK-activities (0.95 U/mg DNA) (Fig. 3A).

The glycolytic enzymes glyceraldehyde 3-phosphate dehydrogenase (GAPDH) and lactate dehydrogenase (LDH) displayed the highest activities in both cell populations (Fig. 3B and C). The GAPDH activity was, with 10.8 U/mg DNA, approximately 1.7-fold higher in adipocytes than in the $CD34^+$ SVF-cells (6.37 U/mg DNA). The LDH activity in adipocytes was, with 25.3 U/mg DNA, approximately 2.3-fold higher than in the $CD34^+$ SVF-cells (6.37 U/mg DNA).

The activity of the marker enzyme of the pentose phosphate pathway, the glucose-6-phosphate dehydrogenase (G6PDH), was over 5-fold less in adipocytes (0.19 U/mg DNA) compared with the $CD34^+$ SVF-cells at 0.98 U/mg DNA (Fig. 3D).

A marker enzyme of the gluconeogenesis, the fructose 1.6-bisphosphatase (FBPase), was represented in low activities in both cell populations: the activity of FBPase was, with 0.04 U/mg DNA, 4-fold higher in adipocytes than in the $CD34^+$ SVF-cells with 0.01 U/mg DNA (Fig. 3E).

The antioxidant defense enzyme glutathione reductase (GSR) showed nearly similar activities in adipocytes and the $CD34^+$ SVF-cells (0.65 U/mg DNA in adipocytes and 0.58 U/mg DNA in $CD34^+$ cells) (Fig. 3F).

The enzymes NAD^+-dependent isocitrate dehydrogenase (NAD-IDH), $NADP^+$-dependent isocitrate dehydrogenase (NADP-IDH) and ß-hydroxyacyl-CoA dehydrogenase (HOADH) are connected to oxygen-dependent energy metabolism which is located in the mitochondria. These enzymes showed significantly higher activities in adipocytes than in the $CD34^+$ SVF-cells. The activity of the NAD-IDH was, with 0.44 U/mg DNA, 3.1-fold higher in adipocytes compared with the $CD34^+$ SVF-cells with 0.14 U/mg DNA. The activity of the NADP-IDH with 1.63 U/mg DNA was 2.6-fold higher in adipocytes than in the $CD34^+$ SVF-cells with 0.63 U/mg DNA. The activity of the HOADH with 4.93 U/mg DNA in adipocytes was 5.4-fold higher than in the $CD34^+$ SVF-cells with 0.92 U/mg DNA (Fig. 3G, H and I).

The phosphocreatine/creatine kinase reaction is part of the energy metabolism of many cell types and can work without oxygen. The activity of the creatine kinase (CK) was 2.8-fold higher in adipocytes with 5.11 U/mg DNA compared with the $CD34^+$ SVF-cells with 1.82 U/mg DNA (Fig. 3J).

4. Discussion

Mature adipocytes have been demonstrated to execute a continuous turnover of their stored lipids [2] and are considered to be incapable of proliferation [30]. In contrast, a majority of the $CD34^+$ SVF-cells have a precursor status and are potentially able to proliferate and differentiate depending on their physiological needs [30–33]. Therefore, adipocytes and $CD34^+$ SVF-cells face different physiological demands that might be reflected in their metabolic capacities.

4.1. Preparation of adipocytes and $CD34^+$ SVF-cells

The isolation of adipocytes and the SVF is well-established [34,35]. We have extended a known isolation protocol by a magnetic bead-based isolation of a $CD34^+$ SVF-cell population. Our flow cytometric data revealed that 36.9% of the nucleated cell fraction was positive for CD34. The $CD34^+$ SVF-cell population includes endothelial cells, endothelial progenitors, hematopoietic progenitors the ASC and the adipocyte progenitors [11,14]. Between 13.3% and 15.4% of the cells in the SVF were found to be $CD45^-/CD34^+$ and positive for CD31 as well. These cells are considered to be mature endothelial cells and endothelial progenitors [18,19]. According to our data only 0.9% of the nucleated SVF cells co-expressed CD45 and CD34 and may thus be

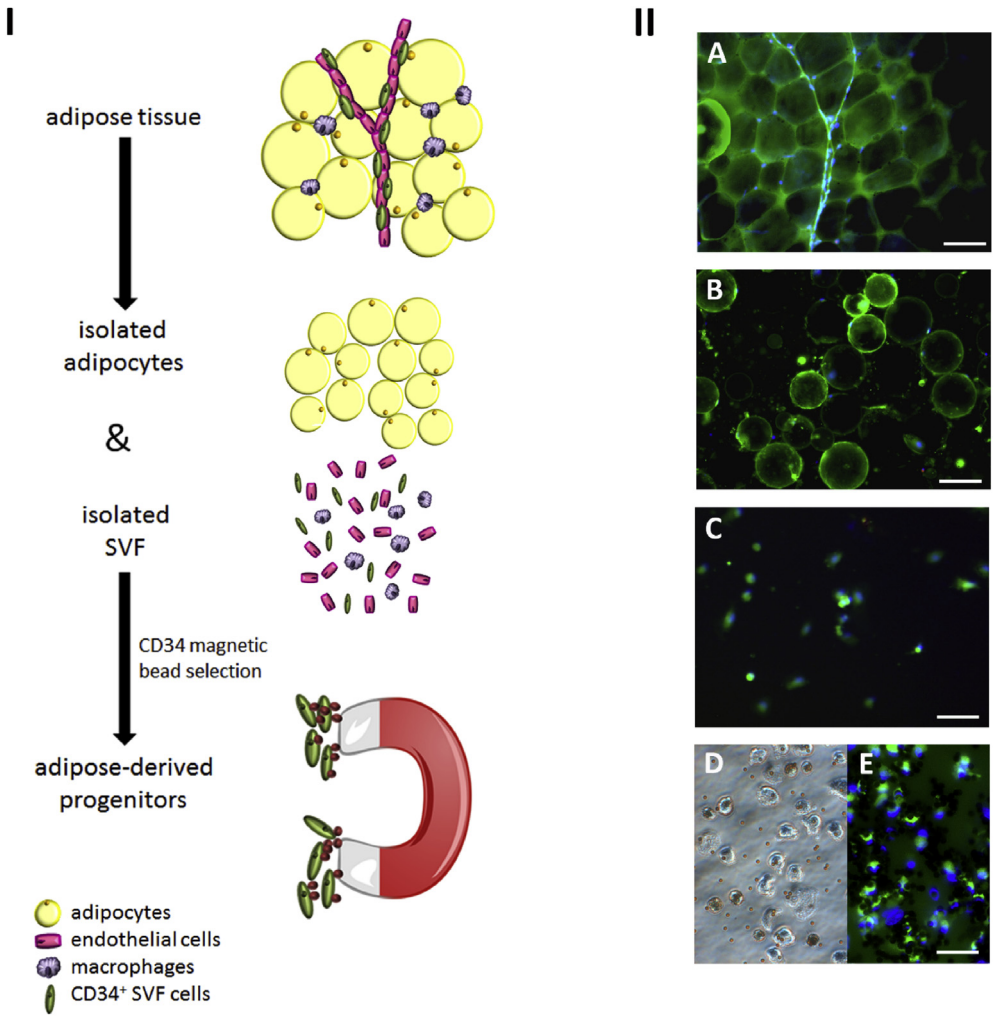

Fig. 1. I: Schematic depiction of the adipose tissue processing and II: microscopic depiction of the tissue and cell fractions during processing by combined vital and nuclear staining and phase contrast. A) Aspirated adipose tissue, (B) adipocytes from the lipid phase of the tissue preparation, (C) SVF after separation, (D) phase contrast micrograph of $CD34^+$ SVF-cells, (E) vital/nuclear stain of the $CD34^+$ SVF-cells from the SVF (green: vital stain, blue: nuclei, scale bar = 100 µm in A and B; 50 µm in C, D and E). (For interpretation of the references to colour in this figure legend, the reader is referred to the Web version of this article.)

considered hematopoietic precursors [36]. Other studies have found 2–4% of the SVF cells to co-express CD34 and CD45 [37,38]. From our data and the literature, we can thus conclude that approximately 60–85% of the cells isolated with the $CD34^+$-selection used in this study were ASC [15–19].

4.2. Differences in the energy metabolic configuration of the cell populations separated from human adipose tissue.

4.2.1. Glycolysis and gluconeogenesis

The activities of the glycolysis-related enzymes PFK, GAPDH and LDH could be detected in both cell populations, and thus indicate the capacity for glycolysis [20,39]. GAPDH and LDH activities were significantly higher than PFK in both cell populations. This is in agreement with Shonk et al. who detected PFK, GAPDH and LDH activities in

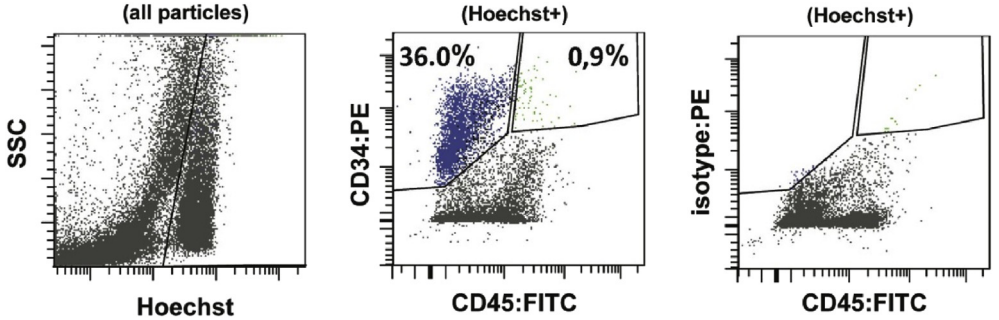

Fig. 2. Flow cytometry of freshly isolated SVF cells. Representative plots of A) nucleated cells, B) nucleated cells gated on $CD34^+CD45^-$ and $CD34^+CD45^+$ and C) isotype control. Numbers in the dot plots indicate the mean percentages of the particular cell populations (n = 4).

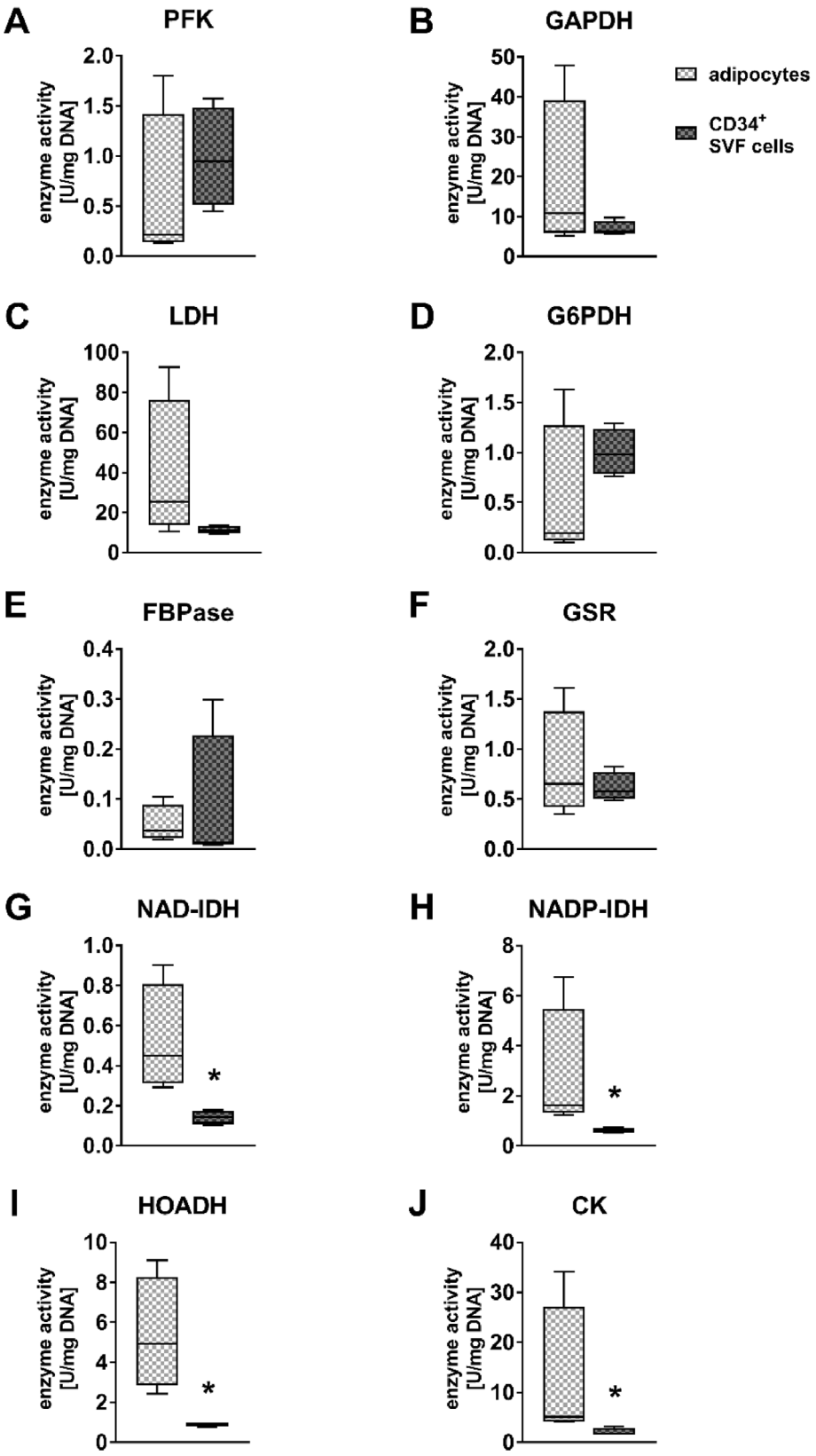

Fig. 3. Marker enzyme activities in adipocytes and the CD34$^+$ SVF-cells; (A) PFK; (B) GAPDH; (C) LDH; (D) G6PDH; (E) FBPase; (F) GSR; (G) NAD-IDH; (H) NADP-IDH; (I) HOADH and (J) CK; activities were normalized to the overall DNA content of the cells (n = 4 *significantly different; Mann-Whitney *U* Test, $p < 0.05$).

human whole adipose tissue homogenates [22]. The proportions of the glycolysis-related enzymes differ clearly between the examined cell populations: Whereas the GAPDH and LDH activities were approximately twice as high in adipocytes, the activities of PFK were approximately four times lower in adipocytes compared to the CD34$^+$ SVF-cells.

PFK catalyzes the flux-determining, the non-equilibrium reaction of glycolysis, while the reaction catalyzed by GAPDH happens at near equilibrium [25]. The inverse behavior of PFK and GAPDH appears contradictory since both enzymes are part of the same pathway. Comparative studies of adipocytes and the mixed SVF revealed contradictory results as well: Kheterpal et al. found a higher GAPDH protein amount in adipocytes compared with the SVF, but simultaneously lower protein amounts of triosephosphate isomerase [24]. Both enzymes are part of the glycolytic pathway. One explanation for this inverse behavior could be anaplerosis of the glycolytic pathway from glycerol. In this context the substrate of GAPDH, i.e. 3-phosphoglyceraldehyde, might not only emerge from the PFK product fructose-1,6-bisphosphate, but also from glycerol by the activities of the enzymes glycerol kinase, glycerol-3-phosphate dehydrogenase and triose phosphate isomerase [40], which can each be found in white adipose tissue or adipocytes respectively [24,41–43].

Glycolytic metabolism is thought to be increased in actively proliferating cells [44]. In contrast to adipocytes, CD34$^+$ SVF-cells have been identified to possess proliferative potential [2]. ASC *in vitro* that do not proliferate displayed a decrease in glycolytic capacity, whereas the highly proliferative ASC displayed an increase in glycolytic capacity [28].

Among the analyzed enzymes, the marker enzyme of gluconeogenesis, FBPase, showed the lowest capacities. In contrast, in ASC *in vitro* the FBPase activities were below the detection limits [28]. This difference could represent an adaptation to the *in vitro* conditions with plentiful glucose available. The culture medium used in this study contains 4.5 g/l glucose, which is about 4-fold higher than the normal blood glucose level [45]. Thus, it can be suggested the gluconeogenic capacity is downregulated *in vitro* since the necessity for glucose recovery becomes obsolete. Therefore, it is suggested that *in vivo* adipocytes and ASC from the same tissue possess a metabolic flexibility to be able to facilitate gluconeogenesis when needed.

4.2.2. Pentose phosphate pathway

A pathway branching off intermediate products from glycolysis is the pentose phosphate pathway [46]. Its rate-limiting marker enzyme is the G6PDH. In our study the measured activities of PFK and G6PDH suggest a similar capacity for the pentose phosphate pathway and glycolysis. The pentose phosphate pathway delivers pentoses for RNA or DNA synthesis and NADPH for the cytosolic regeneration of glutathione, protecting the redox status [40]. High G6PDH activity has been associated with increased proliferation of various cell lines *in vitro* [47]. The low G6PDH activity described in this study for adipocytes that do not proliferate substantially [48], compared with CD34$^+$ SVF-cells, confirms these observations.

4.2.3. Mitochondria-related metabolism

The enzymes involved in mitochondrial metabolism showed significantly higher activities in adipocytes than in CD34$^+$ SVF-cells, indicating a distinguished role of mitochondrial and lipid metabolism respectively in differentiated human adipocytes. While mitochondrial proteins represent only 4.8% of the total human proteome in adipocytes [49], 22% of the proteins were identified as of mitochondrial origin [50]. In this study, the significance of the mitochondrial metabolism in adipocytes becomes evident by the measured capacity of the NAD-IDH, which is 3-fold higher when compared with the capacity measured in CD34$^+$ SVF-cells.

The most striking difference in activity was obvious for HOADH, the enzyme indicating the capacity for β-oxidation, which was about 5-fold higher in adipocytes. Fain et al. described an enrichment of mRNAs encoding enzymes involved in the turnover of lipids in adipocytes when compared with the SVF of human omental adipose tissue [51]. Interestingly, when comparing the capacities of HOADH in *in vitro*-cultured ASC with and without adipogenic stimulation, we observed the same behavior [28].

In mitochondria, the NADP-IDH plays a major role for the NADPH supply for the antioxidative defense catalyzed by the GSR [52]. Since no difference was measured in GSR activity, the higher activity measured for NADP-IDH in adipocytes might originate from the cytosolic isoform that delivers reduction equivalents for lipid synthesis [52]. The comparatively low NADP-IDH activities measured in CD34$^+$ SVF-cells which do not synthesize lipids in substantial amounts indicate a low demand for glutathione regeneration and thus a low need for antioxidative defense. However, the antioxidative defense system is complex, so this issue needs further investigation.

4.2.4. Phosphocreatine system

The CK catalyzes a near-equilibrium reaction and is found in cytoplasm and mitochondria (reviewed in Ref. [53]). The CK activity in adipocytes was almost three times higher than in CD34$^+$ SVF-cells. In adipocytes of white adipose tissue, the CK activity cannot be linked to a role in thermogenesis as it is done in brown adipocytes [54]. Thus the following scenario could be possible: the CK activity in the adipocytes might be facilitated to overcome the limitation of a strictly diffusional exchange of ATP and ADP among gradients and thus spatial restrictions of energy transport [55]. The main volume of adipocytes is occupied by a monolocular lipid vacuole that is encompassed by a thin layer of cytoplasm. It appears thus likely that CK ensures the subcellular ATP homeostasis, improving energy transport from ATP-producing to ATP-consuming reactions [56]. When comparing the capacities of CK in *in vitro*-cultured ASC with and without adipogenic stimulation, we found the similar behavior [28].

4.2.5. Overall view of energy metabolic characteristics

In principle, the differences in the methods of isolation and preparation as well as analysis of the cell populations discussed in this study might lead to limitations regarding the comparability and interpretation of results. Further examinations will be necessary to illuminate the metabolism of the different cell types of adipose tissue. Interestingly, the statistical deviations of the data collected for adipocytes were overall higher than those found for the relatively heterogeneous CD34$^+$ SVF-cell population. These deviations might be of interest, since the adipocyte amount and differentiation degree is dependent on the nutritional state of the donor [57]. Thus, for future experiments it will be of interest to pay also attention to specific patient parameters like body mass index.

In conclusion, we found considerable differences in the metabolic phenotype of adipocytes and CD34$^+$ SVF-cells from the same tissue. The enzymes related to mitochondrial and lipid metabolism showed a higher representation in adipocytes, whereas the activity of the rate-limiting enzyme of glycolysis was higher in the CD34$^+$ SVF-cells. These energy metabolic differences can be interpreted as an adaptation to their physiological demands and might correlate with the potential of CD34$^+$ SVF-cells to be able to proliferate and differentiate, whereas adipocytes do not proliferate after final differentiation. These data might allow conclusions regarding the distinct physiological demands of differentiated adipocytes and the CD34$^+$ SVF-cells in the human adipose tissue *in vivo*.

Disclosure statement

None of the authors has to declare any conflicts of interest.

Acknowledgements

The authors thank Dr. med. habil. Jürgen Weber (Ästhetikklinik Rostock, Germany), Dr. med. Klaus Ueberreiter (Park-Klinik Birkenwerder, Germany) and their patients for kindly providing liposuction tissue. Furthermore, we thank the University Medicine Rostock for the provision of the Core Facility for Cell Sorting & Cell Analysis (head of department: Prof. Dr. Brigitte Müller-Hilke).

This work was financially supported by the European Union (EFRE) and the Federal State of Mecklenburg-Vorpommern („Entwicklung eines Systems zur automatisierten Zellfraktionierung aus humanem Fettgewebe für neuartige regenerative Anwendungen und Therapien (ARENA)", TBI-V-003-VBU-001).

References

[1] E.D. Rosen, B.M. Spiegelman, Adipocytes as regulators of energy balance and glucose homeostasis, Nature 444 (2006) 847–853, https://doi.org/10.1038/nature05483.
[2] A. Strawford, F.S. Antelo, M. Christiansen, M.K. Hellerstein, Adipose tissue triglyceride turnover, de novo lipogenesis, and cell proliferation in humans measured with 2H2O, AJP Endocrinol. Metab. 286 (2004) E577–E588, https://doi.org/10.1152/ajpendo.00093.2003.
[3] B. Cannon, J. Nedergaard, Brown adipose tissue: function and physiological significance, Physiol. Rev. 84 (2004) 277–359.
[4] M.T. Hyvönen, K.L. Spalding, Maintenance of white adipose tissue in man, Int. J. Biochem. Cell Biol. 56 (2014) 123–132, https://doi.org/10.1016/j.biocel.2014.09.013.
[5] V. Van Harmelen, T. Skurk, K. Röhrig, Y.M. Lee, M. Halbleib, I. Aprath-Husmann, H. Hauner, Effect of BMI and age on adipose tissue cellularity and differentiation capacity in women, Int. J. Obes. 27 (2003) 889–895, https://doi.org/10.1038/sj.ijo.0802314.
[6] P. Bourin, B. a Bunnell, L. Casteilla, M. Dominici, A.J. Katz, K.L. March, H. Redl, J.P. Rubin, K. Yoshimura, J.M. Gimble, Stromal cells from the adipose tissue-derived stromal vascular fraction and culture expanded adipose tissue-derived stromal/stem cells: a joint statement of the International Federation for Adipose Therapeutics and Science (IFATS) and the International So, Cytotherapy 15 (2013) 641–648, https://doi.org/10.1016/j.jcyt.2013.02.006.
[7] L. Zimmerlin, V.S. Donnenberg, M.E. Pfeifer, E.M. Meyer, Stromal vascular progenitors in adult human adipose tissue, Cytometry. A 77 (2010) 22–30, https://doi.org/10.1002/cyto.a.20813.Stromal.
[8] T. Tallone, C. Realini, A. Böhmler, T. Moccetti, S. Bardelli, G. Soldati, Adult human adipose tissue contains several types of multipotent cells, J. Cardivascular Transl. Res. 4 (2011) 200–210, https://doi.org/10.1007/s12265-011-9257-3.
[9] J.B. Mitchell, K. McIntosh, S. Zvonic, S. Garrett, Z.E. Floyd, A. Kloster, Y. Di Halvorsen, R.W. Storms, B. Goh, G. Kilroy, X. Wu, J.M. Gimble, Immunophenotype of human adipose-derived cells: temporal changes in stromal-associated and stem cell-associated markers, Stem Cell. 24 (2006) 376–385, https://doi.org/10.1634/stemcells.2005-0234.
[10] A. Scherberich, N. Di Maggio, K.M. Mcnagny, A familiar stranger: CD34 expression and putative functions in SVF cells of adipose tissue, World J. Stem Cell. 5 (2013) 1–8, https://doi.org/10.4252/wjsc.v5.i1.World.
[11] S.G.B. Furness, K. McNagny, Beyond mere markers: functions for CD34 family of sialomucins in hematopoiesis, Immunol. Res. 34 (2006) 13–32, https://doi.org/10.1385/IR:34:1:13.
[12] B.D.S. Krause, M.J. Fackler, C.I. Civin, W.S. May, CD34: structure, biology and clinical utility, Blood 87 (1996) 1–13.
[13] J.S. Nielsen, K.M. Mcnagny, Novel functions of the CD34 family, J. Cell Sci. 121 (2008) 3683–3692, https://doi.org/10.1242/jcs.03504.
[14] L.E. Sidney, M.J. Branch, S.E. Dunphy, H.S. Dua, A. Hopkinson, Concise review: evidence for CD34 as a common marker for diverse progenitors, Stem Cell. 32 (2014) 1380–1389, https://doi.org/10.1002/stem.1661.
[15] V. Feisst, A.E.S. Brooks, C.-J.J. Chen, P.R. Dunbar, Characterization of mesenchymal progenitor cell populations directly derived from human dermis, Stem Cell. Dev. 23 (2014) 631–642, https://doi.org/10.1089/scd.2013.0207.
[16] G. Lin, M. Garcia, H. Ning, L. Banie, Y.-L. Guo, T.F. Lue, C.-S. Lin, Defining stem and progenitor cells within adipose tissue, Stem Cell. Dev. 17 (2008) 1053–1063, https://doi.org/10.1089/scd.2008.0117.
[17] A.S. Klar, S. Güven, J. Zimoch, N.A. Zapiórkowska, T. Biedermann, S. Böttcher-Haberzeth, C. Meuli-Simmen, I. Martin, A. Scherberich, E. Reichmann, M. Meuli, Characterization of vasculogenic potential of human adipose-derived endothelial cells in a three-dimensional vascularized skin substitute, Pediatr. Surg. Int. 32 (2016) 17–27, https://doi.org/10.1007/s00383-015-3808-7.
[18] L. Zimmerlin, V.S. Donnenberg, J.P. Rubin, A.D. Donnenberg, Mesenchymal markers on human adipose stem/progenitor cells Ludovic, Cytometry A. 83 (2013) 134–140, https://doi.org/10.1002/cyto.a.22227.
[19] H. Eto, H. Suga, D. Matsumoto, K. Inoue, N. Aoi, H. Kato, J. Araki, K. Yoshimura, Characterization of structure and cellular components of aspirated and excised adipose tissue, Plast. Reconstr. Surg. 124 (2009) 1087–1097, https://doi.org/10.1097/PRS.0b013e3181b5a3f1.
[20] P. Schwandt, H.W. Doerr, W. Krone, S. Werner, Aktivitätsbestimmung von Schlüsselenzymen im menschlichen Fettgewebe, Klin. Wochenschr. 48 (1970) 224–227, https://doi.org/10.1007/BF01485063.
[21] F.W. Schmidt, E. Schmidt, Enzym-muster menschlicher Gewebe, Klin. Wochenschr. 38 (1960) 957–961.
[22] C.E. Shonk, B.J. Koven, H. Majima, G.E. Boxer, Enzyme patterns in human tissues. II. Glycolytic enzyme patterns in nonmalignant human tissues, Canc. Res. 24 (1964) 709–721.
[23] P. Schwandt, H.W. Doerr, W. Krone, Enzymaktivitäten im Fettgewebe, Klin. Wochenschr. 49 (1971) 358–360.
[24] I. Kheterpal, G. Ku, L. Coleman, G. Yu, A.A. Ptitsyn, E. Floyd, J.M. Gimble, Proteome of human subcutaneous adipose tissue stromal vascular fraction cells vs. mature adipocytes based on DIGE, J. Proteome Res. 10 (2011) 1519–1527, https://doi.org/10.1021/pr100887r.Proteome.
[25] E.A. Newsholme, C. Start, Regulation des Stoffwechsels. Homöostase im menschlichen und tierischen Organismus: Amazon.de: Eric A. Newsholme, Carole Start: Bücher, 1. Verlag Chemie, Weinheim, 1983.
[26] D. Pette, Zellphysiologie des Stoffwechsels, twelfth ed., Konstanzer Universitätsverlag, Konstanz, 1970.
[27] J. Meyer, A. Salamon, N. Herzmann, S. Adam, H.-D. Kleine, I. Matthiesen, K. Ueberreiter, K. Peters, Isolation and differentiation potential of human mesenchymal stem cells from adipose tissue harvested by water jet-assisted liposuction, Aesthet. Surg. J. 35 (2015) 1–10, https://doi.org/10.1093/asj/sjv075.
[28] J. Meyer, A. Salamon, S. Mispagel, G. Kamp, K. Peters, Energy metabolic capacities of human adipose-derived mesenchymal stromal cells in vitro and their adaptations in osteogenic and adipogenic differentiation, Exp. Cell Res. 370 (2018) 632–642, https://doi.org/10.1016/j.yexcr.2018.07.028.
[29] R. R Development Core Team, R: a language and environment for statistical computing, R Found. Stat. Comput. 1 (2011) 409, https://doi.org/10.1007/978-3-540-74686-7.
[30] D.B. Hausman, M. DiGirolamo, T.J. Bartness, G.J. Hausman, R.J. Martin, The biology of white adipocyte proliferation, Obes. Rev. 2 (2001) 239–254, https://doi.org/10.1046/j.1467-789X.2001.00042.x.
[31] P. a. Zuk, M. Zhu, P. Ashjian, D. a. De Ugarte, J.I. Huang, H. Mizuno, Z.C. Alfonso, J.K. Fraser, P. Benhaim, M.H. Hedrick, Human adipose tissue is a source of multipotent stem cells, Mol. Biol. Cell 13 (2002) 4279–4295, https://doi.org/10.1091/mbc.E02.
[32] M.C. Yoder, Human endothelial progenitor cells, Cold Spring Harb. Perspect. Med. 2 (2012) a006692, https://doi.org/10.1101/cshperspect.a006692.
[33] M. Ogawa, Differentiation and proliferation of hematopoietic stem cells, Blood 81 (1993) 2844–2853.
[34] P.A. Zuk, M. Zhu, H. Mizuno, J. Huang, J.W. Futrell, A.J. Katz, P. Benhaim, H.P. Lorenz, M.H. Hedrick, Multilineage cells from human adipose tissue: implications for cell-based therapies, Tissue Eng. 7 (2001) 211–228, https://doi.org/10.1089/107632701300062859.
[35] M. Rodbell, Metabolism of isolated fat cells: I. Effects of hormones on glucose metabolism and lipolysis, J. Biol. Chem. 239 (1964) 375–380.
[36] M. Tavian, L. Coulombel, D. Luton, H.S. Clemente, F. Dieterlen-lievre, B. Peault, Aorta-associated CD34+ hematopoietic cells in the early human embryo, Blood 87 (1996) 67–72, https://doi.org/10.1109/HAPTICS.2014.6775502.
[37] G. Astori, F. Vignati, S. Bardelli, M. Tubio, M. Gola, V. Albertini, F. Bambi, G. Scali, D. Castelli, V. Rasini, G. Soldati, T. Moccetti, 'In vitro' and multicolor phenotypic characterization of cell subpopulations identified in fresh human adipose tissue stromal vascular fraction and in the derived mesenchymal stem cells, J. Transl. Med. 5 (2007) 55, https://doi.org/10.1186/1479-5876-5-55.
[38] L.C. Rose, D.K. Kadayakkara, G. Wang, A. Bar-Shir, B.M. Helfer, C.F. O'Hanlon, D.L. Kraitchman, R.L. Rodriguez, J.W.M. Bulte, Fluorine-19 labeling of stromal vascular fraction cells for clinical imaging applications, Stem Cells Transl. Med. 4 (2015) 1472–1481.
[39] M.C. Scrutton, M.F. Utter, The regulation of glycolysis and gluconeogenesis in animal tissues, Annu. Rev. Biochem. 37 (1968) 249–302.
[40] D.L. Nelson, M.M. Cox, Principles of Biochemistry, fifth ed., (2011), https://doi.org/10.1007/s11655-011-0820-1 Tenney, Sara, New York.
[41] K. Chakrabarty, B. Chaudhuri, H. Jeffay, Glycerokinase activity in human brown adipose tissue, J. Lipid Res. 24 (1983) 381–390 http://www.ncbi.nlm.nih.gov/pubmed/6304216%5Cnhttp://www.jlr.org/content/24/4/381.full.pdf.
[42] J. Swierczynski, L. Zabrocka, Enhanced glycerol 3-phosphate dehydrogenase activity in adipose tissue of obese humans, Mol. Cell. Biochem. 254 (2003) 55–59.
[43] T. Sledzinski, J. Korczynska, E. Goyke, T. Stefaniak, M. Proczko-Markuszewska, L. Kaska, J. Swierczynski, Association between cytosolic glycerol 3-phosphate dehydrogenase gene expression in human subcutaneous adipose tissue and BMI, Cell. Physiol. Biochem. 32 (2013) 300–309, https://doi.org/10.1159/000354438.
[44] M.G. Vander Heiden, L.C. Cantley, C.B. Thompson, Understanding the Warburg Effect: the metabolic requirements of cell proliferation, Science 80– (324) (2009) 1029–1033, https://doi.org/10.1126/science.1160809.Understanding.
[45] R.A.M. Cunha, M.R. Bentes, V.H. Araú, M.C. Souza, M.V. Noleto, A.A. Soares Jr., A.M. Lehnen, Changes in blood glucose among trained normoglycemic adults during a mini-trampoline exercise session, J. Sports Med. Phys. Fitness. 56 (2016) 1547–1553.
[46] N.S. Chandel, Navigating Metabolism, first ed., Inglis, John, Cold Spring Harbor, 2015.
[47] W. Tian, L.D. Braunstein, J. Pang, K.M. Stuhlmeier, Q. Xi, X. Tian, R.C. Stanton, Importance of glucose-6-phosphate dehydrogenase activity for cell growth, J. Biol. Chem. 273 (1998) 10609–10617.
[48] Y. Si, J. Yoon, K. Lee, Flux profile and modularity analysis of time-dependent metabolic changes of de novo adipocyte formation, Am. J. Physiol. Metab. 292 (2007) E1637–E1646, https://doi.org/10.1152/ajpendo.00670.2006.

[49] C. Guda, E. Fahy, S. Subramaniam, MITOPRED: a genome-scale method for prediction of nucleus-encoded mitochondrial proteins, Bioinformatics 20 (2004) 1785–1794, https://doi.org/10.1093/bioinformatics/bth171.
[50] X. Xie, Z. Yi, B. Bowen, C. Wolf, C.R. Flynn, S. Sinha, L.J. Mandarino, C. Meyer, Characterization of the human adipocyte proteome and reproducibility of protein abundance by one-dimensional gel electrophoresis and HPLC-ESI-MS/MS, J. Proteome Res. 9 (2010) 4521–4534, https://doi.org/10.1038/jid.2014.371.
[51] J.N. Fain, B. Buehrer, S.W. Bahouth, D.S. Tichansky, A.K. Madan, Comparison of messenger RNA distribution for 60 proteins in fat cells vs the nonfat cells of human omental adipose tissue, Metabolism 57 (2008) 1005–1015, https://doi.org/10.1016/j.metabol.2008.02.019.
[52] H.J. Koh, S.M. Lee, B.G. Son, S.H. Lee, Z.Y. Ryoo, K.T. Chang, J.W. Park, D.C. Park, B.J. Song, R.L. Veech, H. Song, T.L. Huh, Cytosolic NADP + -dependent isocitrate dehydrogenase plays a key role in lipid metabolism, J. Biol. Chem. 279 (2004) 39968–39974, https://doi.org/10.1074/jbc.M402260200.
[53] T. Wallimann, T. Schnyder, J. Schlegel, M. Wyss, G. Wegmann, A.M. Rossi, W. Hemmer, H.M. Eppenberger, A.F. Quest, Subcellular compartmentation of creatine kinase isoenzymes, regulation of CK and octameric structure of mitochondrial CK: important aspects of the phosphoryl-creatine circuit, Prog. Clin. Biol. Res. 315 (1989) 159–176.
[54] T. Wallimann, W. Hemmer, 111-2 Creatine kinase in non-muscle tissues and cells, Mol. Cell. Biochem. 133 (1994) 193–220.
[55] P.P. Dzeja, A. Terzic, Phosphotransfer networks and cellular energetics, J. Exp. Biol. 206 (2003) 2039–2047, https://doi.org/10.1242/jeb.00426.
[56] T. Wallimann, M. Wyss, D. Brdiczka, K. Nicolay, H.M. Eppenberger, Intracellular compartmentation, structure and function of creatine kinase isoenzymes in tissues with high and fluctuating energy demands: the 'phosphocreatine circuit' for cellular energy homeostasis, Biochem. J. 281 (1992) 21–40, https://doi.org/10.1042/bj2810021.
[57] A. Englhardt, F.A. Gries, H. Liebermeister, K. Jahnke, Size, lipid and enzyme content of isolated human adipocytes in relation to nutritional state, Diabetologia 7 (1971) 51–58, https://doi.org/10.1007/BF00443881.

Experimental Cell Research 370 (2018) 632–642

Contents lists available at ScienceDirect

Experimental Cell Research

journal homepage: www.elsevier.com/locate/yexcr

Energy metabolic capacities of human adipose-derived mesenchymal stromal cells *in vitro* and their adaptations in osteogenic and adipogenic differentiation

Juliane Meyer[a], Achim Salamon[a], Sebastian Mispagel[b], Günter Kamp[b], Kirsten Peters[a,*]

[a] Department of Cell Biology, University Medicine Rostock, Schillingallee 69, 18057 Rostock, Germany
[b] AMP-Lab GmbH, Mendelstraße 11, 48149 Münster, Germany

ARTICLE INFO

Keywords:
Energy metabolism
Mesenchymal stromal/stem cells (MSC)
Adipose tissue
Proliferation
Cell differentiation
Pentose phosphate pathway
Glycolysis
Tricarboxylic acid cycle
Beta-oxidation

ABSTRACT

Mesenchymal stromal/stem cells (MSC) are important in tissue homeostasis and regeneration due to their ability for self-renewal and multipotent differentiation. Differentiation, as well as proliferation, requires adaptations in the cell metabolism. However, only few data exist concerning the energy metabolism of non-differentiating and differentiating MSC. In this study we compared capacities of major energy metabolic pathways of MSC from human adipose tissue (adMSC*) in vitro* in the non-differentiated state with those of osteogenically or adipogenically differentiating adMSC. To this end we quantified the proliferation and differentiation status of adMSC and analyzed maximum enzyme capacities and several enzyme isoforms of major energy metabolic pathways regarding their activity and gene expression. We could show that non-differentiating and osteogenic cultivation conditions induced proliferation and showed increasing capacities of the glycolytic marker enzyme phosphofructokinase as well as the marker enzyme of the pentose phosphate pathway glucose-6-phosphate dehydrogenase. Adipogenic stimulation, which was accompanied by the absence of proliferation, reduced the glycolytic capacity (*e.g.* decreased glyceraldehyde 3-phosphate dehydrogenase capacity) and induced an increase in mitochondrial enzyme capacities. These changes in energy metabolism might represent an adaptation of adMSC to the high energy demand during proliferation and to the specific cellular functions during osteogenic or adipogenic differentiation respectively.

1. Introduction

Mesenchymal stromal/stem cells (MSC) from human adipose tissue (adipose-derived MSC/adMSC) have gained increasing attention for therapeutic applications as a possible alternative to other stem cell types like bone marrow MSC (bmMSC) [1–3]. Zuk et al. were the first to characterize adMSC [4,5]. adMSC are important in tissue homeostasis and regeneration due to their capacity for self-renewal and multipotent differentiation [6]. adMSC have been shown to possess potential for mesenchymal (*e.g.* adipocytes, osteocytes, chondrocytes *in vitro)* [4,5] and non-mesenchymal (*e.g.* neuron-like morphology) [7] differentiation. It has been suggested that the number of MSC in adipose tissue is higher than in bone marrow [8]. The feasibility and safety of therapeutic applications of adMSC have been examined in animals and humans [9–11].

The energy and substrates for biosynthesis are provided by the cellular metabolism. Enzymes and metabolites of the cellular metabolism participate in cell signaling and gene expression [12–14]. Cell fates such as differentiation and proliferation can cause changes in metabolism and can also be dependent on them [15,16]. Different cells show varying demands on energy supply, dependent on their function and environment [17,18]. Short-term changes in energy demand require adaptation within seconds (*e.g.* in the active muscle). This can be realized by modifications of regulatory enzymes. The modifications can be of a covalent (*e.g.* phosphorylation) or non-covalent nature (allosteric regulation). Long term adaptations of energy metabolism to specific environments or cell functions are indicated by changes of enzyme concentrations [19]. The participation of different metabolic pathways in energy metabolism can be assessed by measuring the maximum activities of marker enzymes which catalyze irreversible or flux-limiting reactions of the respective pathways [20,21].

Only few data concerning the energy metabolism of MSC *in vitro* have been published so far. It has been shown that bmMSC mainly metabolize glucose to lactate (glycolysis), rather than using oxidative

* Corresponding author.
E-mail address: kirsten.peters@med.uni-rostock.de (K. Peters).

https://doi.org/10.1016/j.yexcr.2018.07.028
Received 20 March 2018; Received in revised form 4 July 2018; Accepted 18 July 2018
Available online 20 July 2018
0014-4827/

phosphorylation [22]. Furthermore it has been demonstrated that non-differentiating bmMSC and osteogenically differentiating bmMSC exhibit a mixed metabolism, with a significant glycolytic component [23]. The differentiation of MSC is shown to be regulated by mitochondrial function [24,25].

Since it is known that MSC show variations in their proliferation behavior and phenotype depending on their differentiation status, we hypothesized that the process of differentiation in adMSC is accompanied by diverging energy demands. These divergences might induce differences in their energy metabolism. To support this hypothesis, we analyzed major metabolic pathway capacities in undifferentiated and differentiating adMSC. With these new data we were able to reveal fundamental energy metabolic characteristics of adMSC and their adaptations during osteogenic and adipogenic differentiation.

2. Materials and methods

Unless stated otherwise, the chemicals, enzymes, antibiotics and biological factors were supplied by Sigma-Aldrich. Cell culture plastics were from Nunc and Greiner.

2.1. Tissue donation

The patients gave informed consent to a donation of their tissue. The study was approved by the ethics committee of the Rostock University Medical Center [http://www.ethik.med.uni-rostock.de/] under the registration number A2013-0112. It complies with the ethical standards of the World Medical Association Declaration of Helsinki.

The material for the different analyses was retrieved from 15 patients. The data, as supplied by the surgeons, show 1 male and 14 female patients. The patients were on average 41.8 years old (ranging from 29 to 54) and had a BMI of 24.2 (ranging from 19.5 to 27.4); this corresponds to a normal average weight. The liposuction procedure was performed by the water-jet assisted liposuction or tumescent suction technique.

2.2. Isolation and culture of adMSC

adMSC isolation was performed as previously described [26] with some variations. Briefly, the tissue was digested for 30 min, shaken with Collagenase (SERVA) dissolved in PBS (with Ca^{2+} and Mg^{2+}, PAN Biotech) at a concentration of 0.24 U/mL. The tissue was filtered through a 100 µm strainer (BD) and washed with 10 mL of PBS containing 10% fetal calf serum (FCS, PAN Biotech). After a sedimentation time of 10 min, the infranatant was filtered through a 40 µm strainer (BD). After centrifugation for 10 min at 400 × *g*, the pellets were pooled in 10 mL PBS containing 10% FCS and centrifuged for 5 min at 400 × *g*. The final cell pellet was then resuspended in 12 mL Dulbecco's Modified Eagle Medium (DMEM, 4.5 g/L glucose, 0.862 g/L glutamine; Thermo Fisher Scientific) containing 10% FCS and antibiotics (100 U/ml penicillin, 100 mg/mL streptomycin, Thermo Fisher Scientific) (hereinafter called proliferation medium), seeded into 75 cm^2 cell culture flasks and cultivated at 37 °C and 5% CO_2 in a humidified atmosphere. This selection for plastic adherent cells after 24 h of incubation was amended by a selection of a CD34-positive subpopulation with the Dynal CD34 progenitor cell isolation system (Thermo Fisher Scientific). The cells so attained were declared as the passage 1 culture.

Seeding of the cells for experimentation was done in the fourth passage at 20,000 cells/cm^2 into 6- and 96-well plates. After seeding, adMSC were cultured until confluence was reached (2–3 d) and then stimulated to differentiate using an osteogenic differentiation stimulating medium (OS: proliferation medium plus 0.25 g/L ascorbic acid, 1 µM dexamethasone and 10 mM β-glycerophosphate) or adipogenic differentiation stimulating medium (AS: proliferation medium plus 1 µM dexamethasone, 500 µM IBMX, 200 µM indomethacin, 10 µM insulin). US indicates the proliferation medium only containing 1% penicillin/streptomycin and 10% FCS and no specific differentiation factors; this was used for the non-stimulated adMSC cultures. The start of stimulation is termed day zero of experimentation.

2.3. Cell number quantification

Quantification of the adMSC number under the distinct experimental conditions was done indirectly using the basic dye crystal violet. Due to its positive charge, crystal violet binds negatively charged cellular macromolecules, most of which consist of DNA, *via* ionic attraction [27]. Due to a linear correlation, cell numbers can indirectly be determined quantifying the optical density (OD) of the re-solubilized dye [28]. The staining was done according to a previously established protocol [29].

2.4. Detection of differentiation

Microscopic depiction of osteogenic differentiation – Osteogenic differentiation was visualized by the staining of the alkaline phosphatase (ALP) activity after 21 days (using Naphtol AS-MX phosphate and Fast Red Violet LB); staining of the extracellular matrix mineralization was performed after 35 days (using alizarin red S). Both protocols were described previously [30]. The images were recorded with an AxioCam ICc1 camera fitted to an Axiovert 25 (Carl Zeiss Microscopy GmbH).

Quantification of alkaline phosphatase activity – Osteogenic differentiation was analyzed by the quantification of ALP. ALP catalyzes the hydrolysis of an arylphosphate residue of its synthetic substrate para-nitrophenyl phosphate (pNPP) into the colored product para-nitrophenol [31]. Quantification the optical density of the colored product generated over time yields a measurement of ALP activity. The staining was done according to a previously established protocol [29].

Microscopic depiction and quantification of cellular lipid content – Cellular lipid content was determined using an unmodified lipophilic boron dipyromethene dye (Bodipy) which dissolves well in cellular neutral lipids– most of which are triglycerides– which form the core of lipid droplets and are surrounded by a monolayer of phospholipids [32]. The staining and analysis was done according to a previously established protocol [30]. The fluorescence intensity within the cells is measured in relative fluorescence units (RFU). Fluorescence microscopy was performed using an Axiocam MRc fitted to an Axio Scope.A1 (Carl Zeiss Microscopy GmbH).

2.5. Enzyme activity assays

The adMSC layers were washed once with PBS, and afterwards 85 µL/cm^2 extraction buffer (100 mM Na_2HPO_4 (Merck), 100 mM NaH_2PO_4 (Merck), 1 mM dithiothreitol (Roche), 1 mM ethylenediaminetetraacetic acid (EDTA), 0.1 mM Phenylmethylsulfonyl fluoride (PMSF, Applichem)) was added. Subsequently, the cell layers were mechanically detached with a cell scraper (Sarstedt). The resulting cell suspension was frozen in liquid nitrogen and stored at − 80 °C. For the enzyme activity assays, the frozen cell suspension was slowly thawed. 0,1 mM PMSF was added and the suspension was homogenized with a sonifier (3 × 10 s, at 4 °C, G. Heinemann Ultraschall-und Labortechnik). Enzyme assays were performed with aliquots of adMSC homogenates. The enzyme activities were measured in a microplate reader (TECAN), tracing the light absorption at 340 nm (37 °C) with NAD(P)H + H^+ as indicator. The activities are displayed as international units per mg DNA (1 U = 1 µmol substrate transformed per min at 37 °C). The assays for phosphofructokinase (PFK; EC 2.7.1.11), lactate dehydrogenase (LDH; EC 1.1.1.27), NAD^+-dependent isocitrate dehydrogenase (NAD-IDH; EC 1.1.1.41), $NADP^+$-dependent isocitrate dehydrogenase (NADP-IDH; EC 1.1.1.42) and glutathione disulfide reductase (GSR; EC 1.8.1.7) have been described [33] and were adapted as described in Peters et al. [34]. The following assays were further modified:

Glyceraldehyde 3-phosphate dehydrogenase (GAPDH, EC 1.2.1.12):

50 mmol L^{-1} triethanolamine buffer (TRAP), 4 mmol L^{-1} $MgCl_2$ (Merck, Darmstadt, Germany), 1 mmol L^{-1} ATP (Roche, Mannheim, Germany), 1 mmol L^{-1} EDTA, 2.4 mmol L^{-1} glutathione, 7 mmol L^{-1} 3-phosphoglycerate, 0.2 mmol L^{-1} NADH + H^+, 10 U mL^{-1} phosphoglycerate kinase (EC 2.7.2.3); pH 7.6.

ß-Hydroxyacyl-CoA dehydrogenase (HOADH; EC 1.1.1.35): 100 mmol L^{-1} triethanolamine buffer (TRAP), 5 mmol L^{-1} EDTA, 0.2 mmol L^{-1} NADH + H^+; 0,3 mmol L^{-1} acetoacetyl coenzyme A, pH 7.6.

Creatine kinase (CK; EC 2.7.3.2): 100 mmol L^{-1} triethanolamine buffer (TRAP), 8 mmol L^{-1} $MgCl_2$, 2 mmol L^{-1} EDTA, 1 mmol L^{-1} ADP, 25 µmol L^{-1} diadenosine pentaphosphate, 30 mmol L^{-1} phosphocreatine, 2 mmol L^{-1} $NADP^+$, 20 mmol L^{-1} glucose, 2 U mL^{-1} glucose 6-phosphate dehydrogenase (G6PDH, EC 1.1.1.49), 3 U mL^{-1} hexokinase (HK, EC 2.7.1.1); pH 7.6.

Glucose 6-phosphate dehydrogenase (G6PDH, EC 1.1.1.49): 50 mmol L^{-1} triethanolamine buffer (TRAP), 5 mmol L^{-1} EDTA, 0.4 mmol L^{-1} $NADP^+$, 2 mmol L^{-1} glucose 6-phosphate; pH 7.6.

Fructose-1,6-bisphosphatase (FBPase, EC 3.1.3.11): 100 mmol L^{-1} triethanolamine buffer (TRAP), 5 mmol L^{-1} EDTA, 80 mmol L^{-1} $MgCl_2$, 0.4 mmol L^{-1} fructose 1,6-bisphosphate, 0.4 mmol L^{-1} $NADP^+$, 0.7 U mL^{-1} G6PDH (EC 1.1.1.49), 2.8 U ml^{-1} phosphoglucose isomerase (PGI, EC 5.3.1.9); pH 7.5.

2.6. DNA quantification

The DNA quantification was performed using the Qubit™ dsDNA BR Assay Kit and the Qubit® 2.0 Fluorometer (Thermo Fisher Scientific) according to the manufacturer's instructions with aliquots from the sonicated adMSC homogenates that were used for the enzyme activity assays (for the preparation of these homogenates refer to section "Enzyme activity assays"). The Qubit™ dsDNA BR Assay Kit is selective for double-stranded DNA.

2.7. Quantification of the expression of different isoforms of LDH, NADP-IDH and CK

The quantification of LDH isoforms LDHA and LDHB; the NADP-IDH isoforms IDH1, IDH2 and IDH3A and the CK isoforms CKB, CKM, CKMT1B and CKMT2 was done using a real-time reverse transcriptase polymerase chain reaction (real-time RT PCR). The cells were homogenized on QIAshredder columns (Qiagen). The RNA was isolated from the lysate with the innuPREP RNA Mini Kit (Analytik Jena) following the manufacturer's instructions. The RNA was then transcribed into cDNA using the QuantiTect Reverse Transcription Kit (Qiagen). Specific PCR templates were identified with the help of the reference sequence collection "Gene", accessible on the NCBI web page. After identifying the different existing isoforms of the enzymes concerned, a transcript variant was chosen as a sequence template for the primers. The design of the corresponding primer was done with the Primer-BLAST tool on NCBI (see Table 1). Potential binding to residual genomic DNA was tested for. The primers were purchased from Sigma-Aldrich. With the 7500 Real Time PCR system (Applied Biosystems), Real-time PCR of transcribed samples was subsequently performed utilizing the Power SYBR Green PCR Master Mix (Thermo Fisher Scientific). The collected data were evaluated with the SDS 7500v 2.3 Software. Gene expression levels were calculated with the ΔCT method with normalization to human-specific 18S RNA and corrected for primer efficiency that was determined with the Real-time PCR Miner algorithm [35].

2.8. Isolation and quantification of adMSC mitochondria content

After 7 and 14 d in control and differentiation cultures in 6-well plates, the cells were harvested. Their mitochondrial content was isolated with the Mitochondria Isolation Kit (Miltenyi Biotech) and quantified with the FluoroProfile® Protein Quantification Kit. Isolation as well as quantification was done according to manufacturer's instructions. The mitochondrial isolate was disrupted by ultrasonication for 30 s. Quantification of the protein content in the mitochondrial homogenate was done with a fluorimetric assay based on epicocconone [36]. The amount of mitochondria was then normalized to the cell number that was determined *via* crystal violet staining. Enzyme activities of presumably cytoplasmic-only (GAPDH) and mitochondrial-only (HOADH) enzymes were measured in the mitochondrial isolates as an internal control for the quality of the mitochondria isolation. As had been shown before, the isolation procedure of mitochondria with paramagnetic beads renders a population of pure and functional mitochondria [37]. In the same study no GAPDH could be found in mitochondrial isolates harvested by the described method.

Table 1
qPCR primers used in this study.

Primer	Sequence	Target gene
18S_fw	ATGGCCGTTCTTAGTTGGTG	18S ribosomal RNA
18S_re	CGCTGAGCCAGTCAGTGTAG	
LDHA_fw	CTGTTCCACTTAAGGCCCCTC	Homo sapiens lactate
LDHA_re	GGAACCAAAAGGAATCGGGAATG	dehydrogenase A
LDHB_fw	CTCATTGCACCAGTTGCGG	Homo sapiens lactate
LDHB_re	TCAGCCAGAGACTTTCCCAG	dehydrogenase B
IDH1_fw	CTGCCCACGGGACTGTAAC	Homo sapiens isocitrate
IDH1_re	AGGCAAAAATGGAAGCAATGGG	dehydrogenase 1 (NADP+), soluble (IDH1)
IDH2_fw	AGTGTACAACTTCCCCGCAG	Homo sapiens isocitrate
IDH2_re	ATAGTGCTTGTCAAAGATCTCCTGG	dehydrogenase 2 (NADP+), mitochondrial (IDH2)
IDH3A_fw	ACTGGTGGTGTTCAGACAGTAAC	Homo sapiens isocitrate
IDH3A_re	CCACTGAATAGGTGCTTTGGC	dehydrogenase 3 (NAD+) alpha
CKM_fw	CGACCTGGACCCTAACTACG	Homo sapiens creatine
CKM_re	GTCAGGCTGTTGAGAGCTTCC	kinase, muscle type
CKB_fw	AGCTCATCGACGACCACTTC	Homo sapiens creatine
CKB_re	GTCATTGTGCCAGATACCGC	kinase, brain type
CKMT1B_fw	CCTGTCCATCTAACCTGGGC	Homo sapiens creatine
CKMT1B_re	TGGGAAGCGGCTATCTTTGC	kinase, mitochondrial 1B
CKMT2_fw	CTCCAAGCGCAGACTACCC	Homo sapiens creatine
CKMT2_re	GGTGTCACCTTGTTGCGAAG	kinase, mitochondrial 2 (sarcomeric)

2.9. Statistical analysis

Numbers of donors are mentioned in the Figure and Table legends. The data for one single donor was measured in a technical triplicate (cell amount, ALP activity, lipid content) or duplicate (enzyme activity, amount of DNA, expression of enzyme isoforms, mitochondrial protein). Calculations and statistical analyses were carried out with the Excel 2013 and R software environment for statistical computing and graphics [38] as well as GraphPad Prism version 7.02 for Windows (GraphPad Software). The normality of the data distribution was tested with the Shapiro-Wilk normality test. The homogeneity of variance of enzyme activity data, cell culture analysis data, RNA expression data und mitochondrial protein quantification was analyzed with a *U*-test according to Mann and Whitney ($p < 0.05$). All diagrams were created with the GraphPad software. The data displayed are medians with the interquartile range.

3. Results

3.1. Investigation of osteogenically and adipogenically differentiating adMSC

Fluorescence microscopic images of the live/dead staining of all culture conditions were taken after 21 d. These images displayed no impairment of the cell vitality as the vital staining revealed regular cell

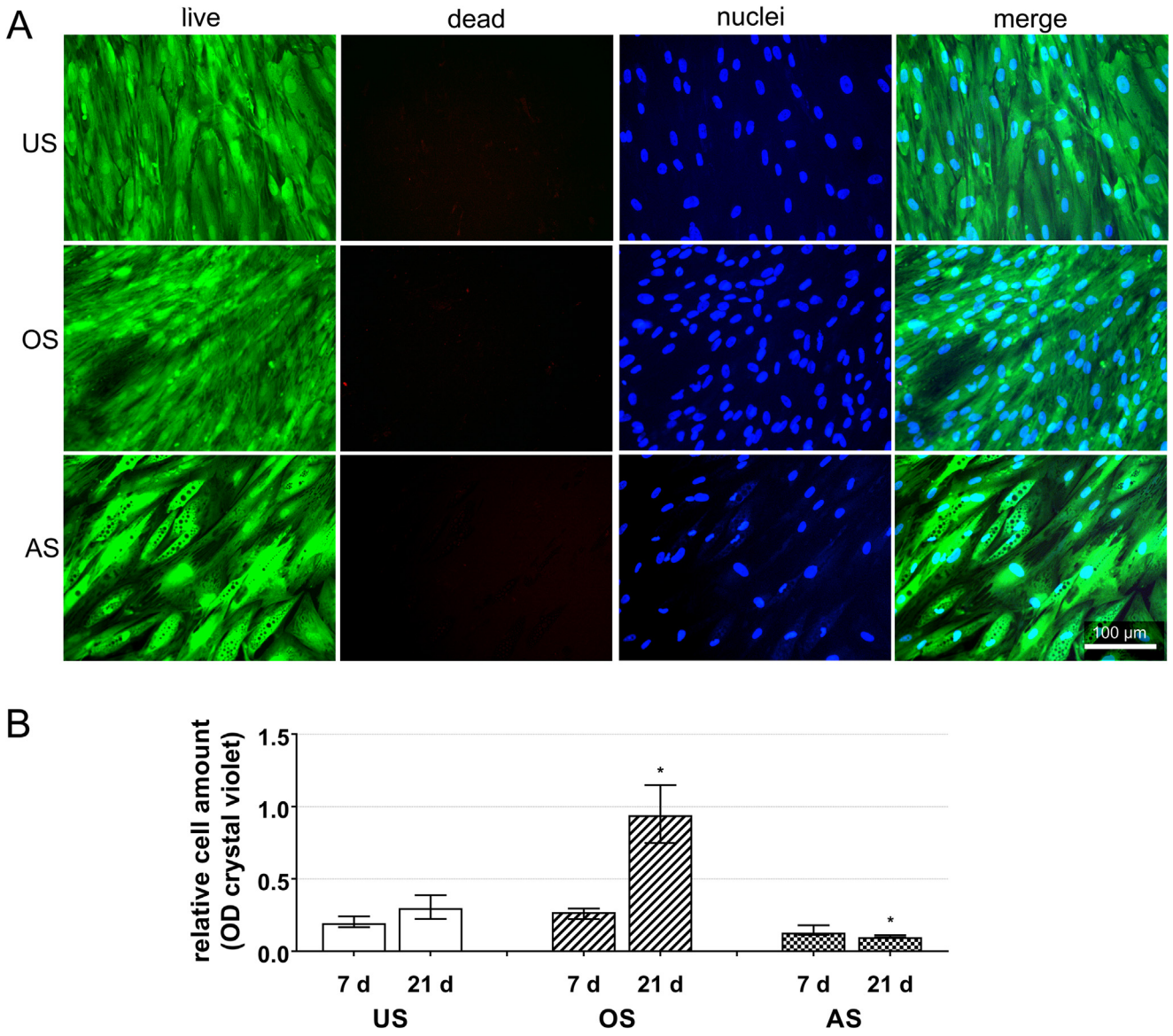

Fig. 1. Monitoring of adMSC vitality and relative cell amount in non-stimulated cultures (US), osteogenically stimulated cultures (OS) and adipogenically stimulated cultures (AS). (A) live/dead staining after 21 d (green: cytoplasm of vital cells; red: nuclei of dead cells; blue: nuclei; scale bar: 100 µm); (B) relative cell amount quantified after 7 and 21 d (n = 4; * significantly different from US cultures at the respective time point; Mann-Whitney *U*-Test; $p < 0.05$).

growth and the staining indicative of dead cells rarely occurred (Fig. 1A). Furthermore, the nuclear staining indicated an obvious difference in the amount of cells after 21 d as the nuclei number appeared highest in osteogenic-stimulated adMSC. This observation was confirmed by the quantification of the relative cell amount (Fig. 1B). In non-stimulated adMSC cultures a 1.3-fold increase in cell number occurred from day 7 to day 21. After 7 d of osteogenic stimulation the amount of cells was 1.4-fold higher than in non-stimulated adMSC. After 21 d in osteogenic culture the amount of cells had increased 3.7-fold compared to non-stimulated adMSC. In contrast, the cell numbers of adipogenically stimulated adMSC did not change significantly over the cultivation period of 21 d (Fig. 1B). The viability of the cells was further verified by testing the metabolic activity at all time points of measurement (Supplemental information S1). This assay showed no impairment of vitality and is in agreement with the live/dead staining and the cell number quantification.

Osteogenic differentiation is characterized by the upregulation of bone-specific molecules and enzymes like alkaline phosphatase (ALP) as well as the mineralization of their extracellular matrix. Non-stimulated adMSC did not show a specific osteogenic differentiation since only few cells show a slight ALP-positivity (Fig. 2A); osteogenic stimulation led to a distinct positivity for ALP-activity (Fig. 2B). Matrix mineralization did not occur in unstimulated adMSC cultures (Fig. 2C), whereas osteogenically stimulated adMSC showed a large number of mineralization nodules (Fig. 2D). Adipogenic differentiation is characterized by the formation of multilocular, lipid-filled vacuoles. Whereas in non-stimulated adMSC no lipid accumulation was detectable (Fig. 2E), adipogenically stimulated adMSC showed numerous lipid-filled vacuoles (Fig. 2F).

The quantification of ALP activity revealed its 5-fold increase by cultivation of adMSC with osteogenic stimulation for 21 d compared to non-stimulated cultures (Fig. 3A). In contrast, the ALP activity of adipogenically stimulated adMSC was 6-fold lower than the ALP activity in osteogenically stimulated adMSC over the same period. The quantification of the lipid accumulation in adipogenically stimulated cultures showed 5–6-fold increased values compared to non-stimulated and osteogenic cultures (Fig. 3B).

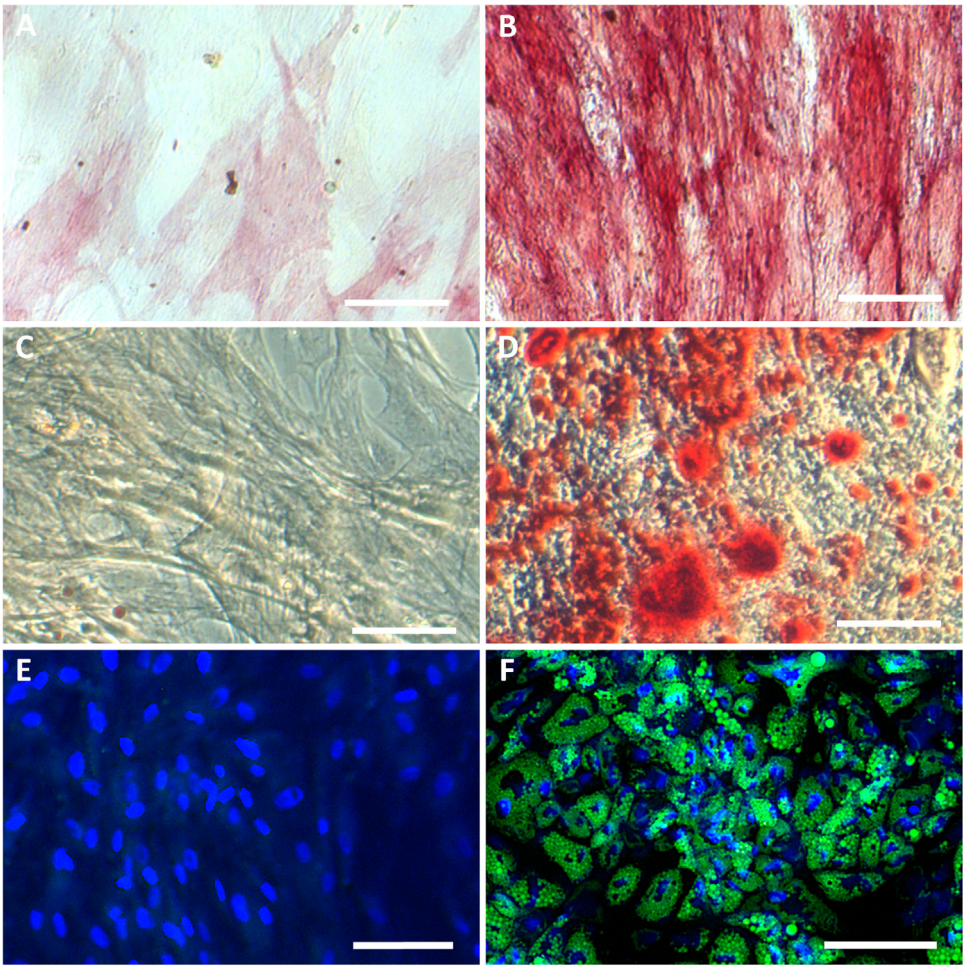

Fig. 2. Detection of differentiation in adMSC. (A) staining for ALP activity in non-stimulated adMSC and (B) in osteogenically stimulated adMSC after 21 d; (C) staining of extracellular matrix mineralization in non-stimulated adMSC and (D) in osteogenically stimulated adMSC after 35 d; (E) lipid staining in non-stimulated adMSC and (F) in adipogenically stimulated adMSC after 14 d (blue: nuclei, green: lipid), (scale bar: 100 μm).

3.2. Enzyme activities of adMSC and differentiation-dependent changes

Important energy-metabolic pathways were examined by measuring the maximum catalytic activities of several marker enzymes in non-differentiating adMSC cultures and osteogenically or adipogenically differentiating cultures (Fig. 4).

The regulatory enzyme of glycolysis is the PFK. In non-differentiating cultures, PFK activity increased with advanced cultivation period (0.25 U/mg DNA and 0.5 U/mg DNA after 7 and 21 d) (Fig. 4A). GAPDH and LDH (Fig. 4B and C) showed the highest activities of all enzymes tested (*e.g.* 48 U/mg DNA and 7 U/mg DNA respectively after 7 d). The GAPDH and LDH activities were increased 1.6 and 2.3-fold after 21 d (75 U/mg DNA and 16 U/mg DNA respectively). In osteogenically differentiating adMSC, the total increase of maximum PFK activity was much higher compared to GAPDH and LDH (13-fold from 0.5 U/mg DNA after 7 d to 6.5 U/mg DNA after 21 d). Maximum GAPDH activities of adMSC in osteogenic differentiation were only slightly higher than in non-differentiating adMSC cultures (55 U/mg DNA and 101 U/mg DNA after 7 and 21 d). LDH activity rose 4-fold in osteogenic cultures (8 U/mg DNA and 35 U/mg DNA after 7 and 21 d) compared to a 2.3-fold rise in non-differentiating cultures. Therefore, in osteogenically differentiating cultures the ratio GAPDH/PFK was 15 after 21 d, which is 15-fold lower than in the non-differentiating cultures. In adipogenically differentiating cultures the maximum activities

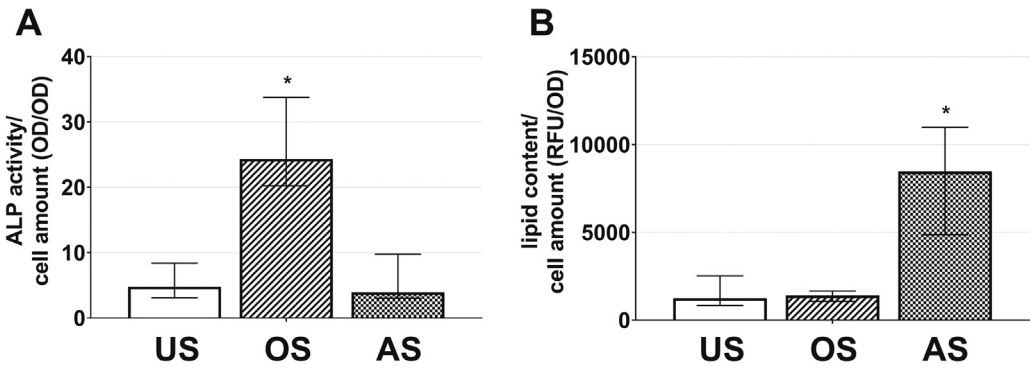

Fig. 3. Quantification of osteogenic or adipogenic differentiation in non-stimulated cultures (US), in osteogenically stimulated cultures (OS) and in adipogenically stimulated cultures (AS). (A) ALP activity after 21 d; (B) quantification of lipid accumulation after 21 d (US, OS, AS, n = 4, * significantly different from US; Mann-Whitney *U*-Test, $p < 0.05$).

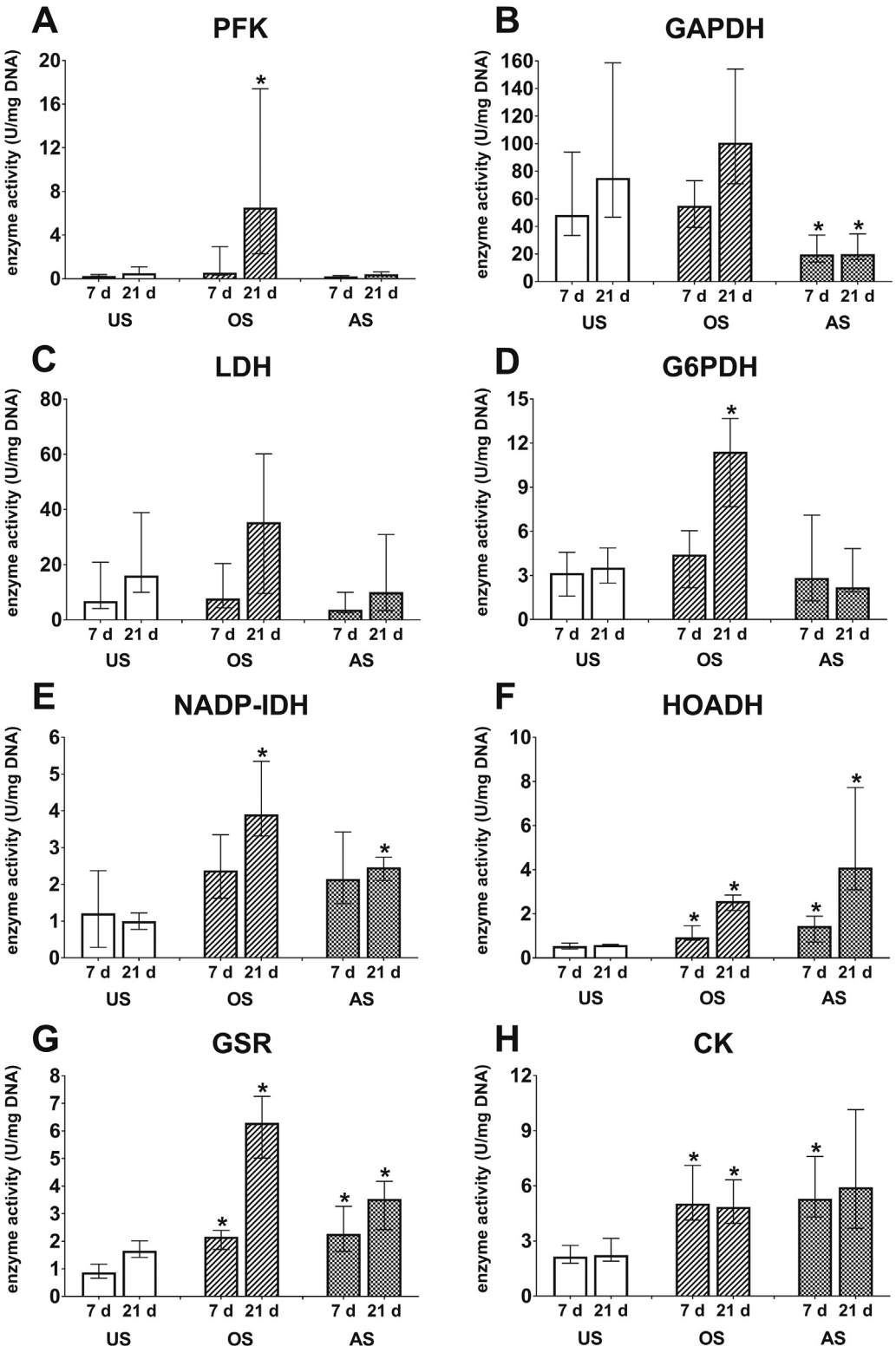

Fig. 4. Marker enzyme activities in non-differentiating (US), and osteogenically (OS) or adipogenically (AS) differentiating adMSC cultures after 7 and 21 d, (A) PFK, (B) GAPDH, (C) LDH, (D) G6PDH, (E) NADP-IDH, (F) HOADH, (G) GSR, (H) CK; Activities were normalized to the overall DNA content of the cells (n = 8, * significantly different from US cultures at the respective time point; Mann-Whitney *U*-Test, $p < 0.05$).

of PFK, GAPDH and LDH were lower than in the non-differentiating cultures. PFK activity increased 2-fold with adipogenic stimulation (0.2 U/mg DNA after 7 d and 0.4 U/mg DNA after 21 d), while GAPDH activity did not change within the adipogenic cultivation period (20 U/mg DNA after 7 and 21 d). LDH activities increased 2.7-fold by adipogenic differentiation (3.7 U/mg DNA after 7 d and 10 U/mg DNA after 21 d). The ratio GAPDH/PFK was 135 after 7 d and 61 after 21 d.

The marker enzyme of the pentose phosphate pathway (PPP), G6PDH, displays relatively constant capacities in non-differentiating cells with 3.1 U/mg DNA after 7 d and 3.5 U/mg DNA after 21 d

(Fig. 4D). Osteogenic differentiation induced a 2.6-fold increase of G6PDH activity (4.4 U/mg DNA after 7 d and 11.4 U/mg DNA after 21 d). Under adipogenic differentiation the G6PDH activity was below the activities in non-differentiating cultures and did not significantly change within the adipogenic cultivation period (2.8 U/mg DNA after 7 d and 2.2 U/mg DNA after 21 d).

In order to assess the relevance of the citric acid cycle in adMSC *in vitro,* the capacities of the marker enzymes NAD-IDH and NADP-IDH were measured. Whereas NAD-IDH activity was not detectable at any point of time in any cultivation condition, NADP-IDH activity was evident (Fig. 4E). Non-differentiating cultures showed a low capacity of the NADP-IDH that did not significantly change during cultivation (1.2 U/mg DNA after 7 d and 1.0 U/mg DNA after 21 d). In osteogenically and adipogenically differentiating adMSC cultures the NADP-IDH activities were significantly higher after the 21 d cultivation period compared with the non-differentiating cultures (2.4 U/mg DNA and 2.1 U/mg DNA after 7 d respectively and 3.9 U/mg DNA and 2.5 U/mg DNA after 21 d respectively).

The mitochondrial marker enzyme of fatty acid oxidation, HOADH, showed low maximum activities under non-differentiating conditions (0.5 U/mg DNA and 0.6 U/mg DNA after 7 and 21 d, Fig. 4F). The HOADH activity in osteogenically differentiating cells was slightly higher after 7 d (0.9 U/mg DNA) and increased 2.9-fold to 2.6 U/mg DNA after 21 d. The overall highest HOADH activities were detected in adipogenically differentiating adMSC. After 7 d of adipogenic stimulation 1.4 U HOADH/mg DNA were detectable and HOADH activity also increased 2.9-fold to 4 U/mg DNA after 21 d.

The GSR, which is part of the antioxidative defense system, showed an increase over time under all cultivation conditions (Fig. 4G). Maximum activities in the non-differentiating cultures were comparatively low (0.9 U/mg DNA and 1.7 U/mg DNA after 7 and 21 d). After 7 d under osteogenic cultivation conditions, the capacity was already more than twice as high and increased further after 21 d under osteogenic stimulation (2.2 U/mg DNA and 6.3 U/mg DNA after 7 and 21 d). In adipogenically differentiating cultures the GSR showed a capacity similar to that in osteogenically differentiating cells after 7 d, but the increase in the following 14 d of culture was less pronounced (2.3 U/mg DNA and 3.5 U/mg DNA after 7 and 21 d).

CK activity, which is involved in buffering and recovery of ATP, was present in adMSC. In adMSC cultures without specific stimulation the maximum CK activities (Fig. 4H) were 2.1 U/mg DNA after 7 d and no significant changes appeared with advanced cultivation time (2.2 U/mg DNA after 21 d). In osteogenically differentiating cultures the CK capacities were higher than in non-differentiating cultures (4.1 U/mg DNA and 3.9 U/mg DNA after 7 and 21 d). The highest CK activities were found in adipogenically differentiating cultures (5.3 U/mg DNA after 7 d and 5.9 U/mg DNA after 21 d of culture). Activities of the marker enzyme of gluconeogenesis, FBPase, could not be detected.

3.3. Expression level of isoforms of LDH, IDH and CK

The necessity for the adaption of the gene expression for the different isoforms of LDH, IDH and CK was elucidated by determining their gene expression levels after 7 and 14 d of cultivation.

Among LDH isoforms, *LDHB* is the prevailingly expressed isoform in adMSC (Fig. 5A). The expression level is 100–1000 times higher than that of the *LDHA* isoform. The osteogenic and adipogenic differentiation induced no significant differences in the expression of *LDHB*.

The gene expression status of the *IDH* isoforms is more complex (Fig. 5B). Whereas in non-differentiating and osteogenic cultures the expression of *IDH2* (mitochondrial NADP-dependent isoform) is predominant, the *IDH1* (cytosolic NADP-dependent isoform) is strongly expressed in adipogenically differentiated cultures. *IDH1* expression was 8-fold higher in adipogenic differentiation than in the non-differentiating cultures after 14 d. Furthermore, the expression of *IDH2* also increased about 3-fold in adipogenic differentiation at both time points.

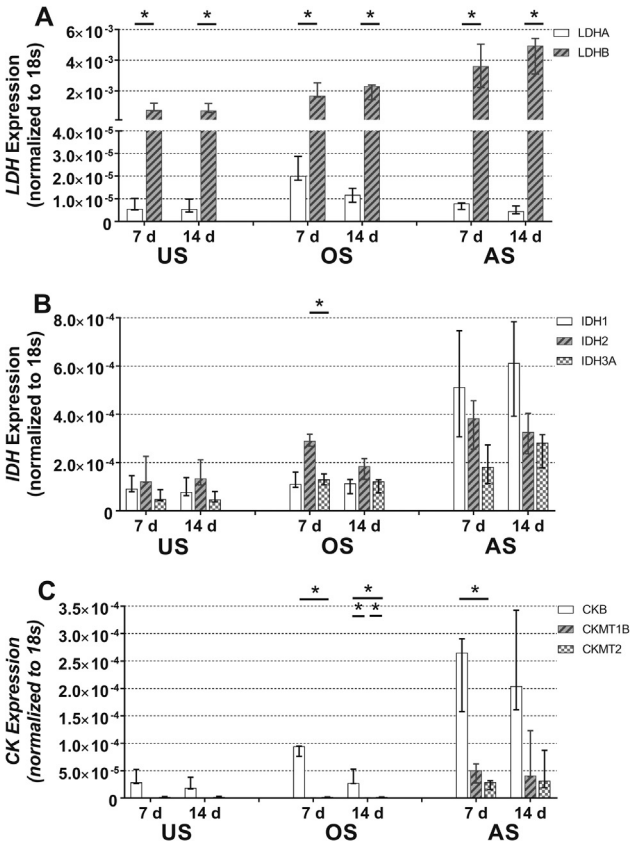

Fig. 5. Gene expression levels in non-differentiating (US) and osteogenically (OS) or adipogenically (AS) differentiating adMSC after 7 and 14 d (A) LDH isoforms *LDHA* and *LDH*B, (B) IDH isoforms *IDH1, IDH2* and *IDH3A,* (C) CK isoforms *CKB, CKMT1B* and *CKMT2*, normalized to 18s RNA-expression (n = 3, all culture conditions were compared within one time point, * indicate significant differences, level of significance: $p \leq 0.05$).

Osteogenic differentiation also induced an increase of *IDH2* (about 2-fold at 14 d). Interestingly, the gene expression of the mitochondrial NAD-dependent isoform *IDH3A*, which lacks activity on the protein level, was detectable under all culture conditions. It was expressed at a low level in non-differentiating cultures. The expression increased about 3-fold in osteogenic differentiation and up to 6-fold in adipogenic differentiation.

The predominantly expressed CK isoform in adMSC is the *CKB* (cytosolic brain type isoform, Fig. 5C). The *CKB* is expressed 50-fold and 600-fold higher than the mitochondrial isoforms *CKMT2* and *CKMT1B* at the start of the experiment, respectively (see Supplementary material Fig. S2). In non-differentiating adMSC cultures and osteogenically stimulated adMSC cultures the *CKB* expression decreased with cultivation time. Notably, the adipogenic differentiation induced a significantly increased expression of the mitochondrial isoforms *CKMT1B* and *CKMT2. CKMT1B* is 270- and 530-fold higher compared with non-differentiating cultures after 7 and 14 d, *CKMT2* is 12 and 34-fold higher after 7 and 14 d, respectively. Expression of the muscle type CK gene *CKM* could not be detected.

3.4. Evaluation of the mitochondrial mass of non-differentiating adMSC and adMSC under mesenchymal differentiation

To assess whether the changes in protein and RNA expression levels in mitochondrial enzymes were due to a specific increase of catalytic activity and its gene expression level or to an overall rise in mitochondrial mass, the amount of mitochondrial protein was quantified (Fig. 6).

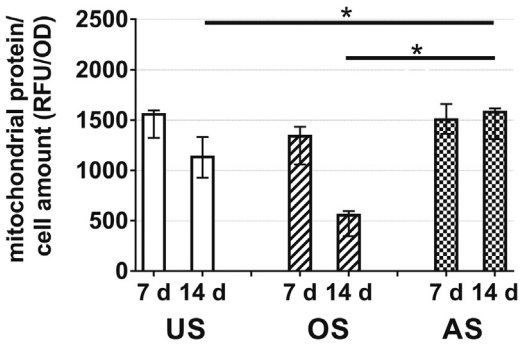

Fig. 6. Relative mitochondrial mass displayed as amount of mitochondrial protein normalized to cell number after 7 and 14 d in non-differentiating adMSC (US) and in osteogenic (OS) or adipogenic differentiation (AS). (n = 5, * indicate significant differences, level of significance: $p \leq 0.05$).

After 14 days of osteogenic differentiation, the mitochondrial mass per cell was 2-fold lower compared with non-differentiating cultures. At the same time the adMSC in adipogenically differentiating cultures had a significant, 1.4-fold higher amount of mitochondrial mass per cell compared to non-differentiating cultures. The efficiency of mitochondrial isolation was evaluated by the detection of the presence of the exclusively mitochondrial enzyme HOADH (see Supplementary material Table S1).

4. Discussion

In this study we analyzed the activity and gene expression of marker enzymes of energy metabolism in adMSC in non-differentiating adMSC *in vitro* and how it is influenced by osteogenic and adipogenic differentiation.

4.1. Proliferation and differentiation of adMSC

Moderate proliferative activity was shown to occur in the non-stimulated cultures, and high proliferative activity was induced in osteogenic differentiation over the 21 days of cultivation. On the other hand, the constant cell amount in the adipogenically differentiating adMSC over the experimentation period of 21 d indicates a lack of proliferative activity, as was previously shown [29].

By the detection of the osteogenic differentiation markers ALP activity and extracellular matrix mineralization [39], we could show that osteogenic stimulation of adMSC led to osteogenic differentiation. It was previously shown that the osteogenic differentiation of adMSC is accompanied by increased expression of the osteoblastogenic marker ZBTB16 (zinc finger and BTB domain containing 16) [40] and increased expression of osteocalcin and osteopontin [41,42]. The adipogenic differentiation of adMSC was also shown, as a pronounced lipid vacuole formation was detected in adipogenically stimulated cultures. The applied differentiation protocol is shown to induce adipogenic differentiation accompanied by the expression of leptin, glucose transporter GLUT4, PPARγ2 (peroxisome-proliferating activated receptor γ), LPL (lipoprotein lipase), and aP2 (adipocyte protein 2) [4,5,41,43].

We investigated the capacity of different energy metabolic pathways on the basis of these three *in vitro* approaches: 1) non-differentiating, slightly proliferating adMSC, 2) osteogenically differentiating, highly proliferative adMSC, and 3) adipogenically differentiating, non-proliferating adMSC.

4.2. Metabolism

The enzyme activities *in vivo* can diverge from maximum activities measured *in vitro* under optimal conditions. Therefore the maximum activities presented in this study represent a capacity of metabolic turnover and not the turnover *in vivo* in a specific metabolic state. However, previous studies have shown a good correlation of the capacities of energy pathway marker enzymes with their contribution to energy metabolism [44].

The glycolytic marker enzymes GAPDH and LDH showed the highest activities in adMSC at any time, suggesting a high capacity of carbohydrate catabolism. In non-differentiating adMSC, which showed moderate proliferation, GAPDH and LDH activities increased with cultivation time. The activity of the regulatory enzyme of glycolysis, PFK, is a magnitude lower compared to GAPDH as well as LDH. This has been shown before in endothelial cells [34] and might reflect the fact that GAPDH and LDH catalyze the reactions rather near the thermodynamic equilibrium of the reaction *in vivo*, in contrast to the regulatory enzyme PFK [20].

We could demonstrate that the osteogenic differentiation of adMSC is accompanied by a high cell division rate and characterized by an increase of all enzyme activities tested. This indicates an increased capacity for all energy metabolic pathways. Thus both the carbohydrate metabolism and the mitochondrial metabolism appeared enhanced in osteogenic differentiation. For both cell division and stem cell differentiation, a *de novo* synthesis of macromolecules is necessary [45,46]. In proliferating cell cultures, a preference for carbohydrate metabolism to lactate (glycolysis) under aerobic conditions is demonstrated [18,34]. This phenomenon is defined as the Warburg effect [47]. This less efficient energy pathway might be a way to increase the carbon flux through biosynthetic pathways [18]. However, the presence of the Warburg effect cannot be explicitly concluded by our data. Previous studies on the metabolism of MSC during differentiation have yielded controversial results. Pattappa et al. demonstrated a suppression of glycolysis in osteogenically differentiating bmMSC, suggesting a proportionate increase in oxidative phosphorylation [23]. Chen et al. reported a transition from glycolysis to oxidative phosphorylation in bmMSC upon osteogenic induction with a distinct decrease in glycolysis [48]. Shum et al. reported an induction of oxidative phosphorylation upon osteogenic differentiation of bmMSC, whereby the level of glycolysis was unchanged compared to undifferentiated bmMSC [49]. These results partially diverge from our findings which indicate the simultaneous increase of carbohydrate metabolism, oxidative phosphorylation and β-oxidation upon osteogenic differentiation. These controversial results may result from different analyzed targets and analytical methods as well as the fact that, in the other studies, mostly bmMSC were examined [50]. Furthermore, the large differences in cell culture conditions, *e.g.* as displayed in the differences of medium composition with partially supraphysiological levels of glucose, glutamine and pyruvate, might influence the cell metabolism [51]. Thus, further examinations will be necessary.

The presence of LDH activity and its increase within the cultivation period in all cultures indicates the capacity of adMSC for anaerobic energy production and/or the use of lactate as an aerobic substrate. The use of lactate for gluconeogenesis is improbable because no activity of the enzyme FBPase was detectable in adMSC. The striking dominance of the expression of the B subunit of LDH (heart type) indicates a preference for the conversion of lactate to the 3-carbon compound pyruvate [52]. On the other hand, a high consumption rate of glucose followed by a high discharge rate of lactate under standard cultivation conditions was shown for proliferating bmMSC and adMSC [22,53,54].

Adipogenically differentiated adMSC do not proliferate. Thus, the constant levels of GAPDH capacity during adipogenic differentiation simultaneous to the minor increase of PFK capacity may be caused by the ongoing lipid synthesis. During lipid synthesis, dihydroxyacetone phosphate is diverted from glycolysis and used for the anabolic pathway of lipid synthesis prior to the action of GAPDH in glycolysis [55]. The 2.7-fold increase of LDH within 2 weeks could imply the presence of the Warburg effect in adipogenically differentiating cells. But the Warburg effect has so far been detected in highly proliferating cells [55]. With the lack of proliferation, adipogenically differentiating

adMSC are missing this essential characteristic. Furthermore, as inferred from studies with white adipose tissue of rats, it has been suggested that in white adipocytes the main role of LDH may be the conversion of excess available glucose into the 3-carbon compound pyruvate in order to limit tissue self-utilization as a substrate [56]. This is supported by our data regarding the dominance of the expression of the LDH B subunit, which implies a preference for a lactate to pyruvate conversion.

G6PDH controls the flux of carbon through the PPP and competes with glycolysis for sugar metabolism. We could show a high G6PDH capacity in non-differentiating and differentiating adMSC. High G6PDH activities indicate the importance of the PPP for anabolism [34,57]. Strikingly, G6PDH activities were even higher than the control enzyme of glycolysis PFK. Thus the ratio of G6PDH to PFK is larger than 1. For example, in proliferating endothelial cells or carcinoma cells the ratios are lower (0.68 and 0.4–0.2, respectively). In frog skeletal muscle the values are actually below 0.001 [34]. Therefore a high ratio of G6PDH/PFK might be typical for proliferating and/or differentiating cells, as these are characterized by a relatively high anabolic metabolism.

The PPP delivers not only pentoses for the biosynthesis of macromolecules (*e.g.* nucleic acids) [12] but also reduction equivalents in the form of NAPDH + H^+ which are essential for biosynthesis (particularly lipogenesis) [58]. The regulation of the PPP capacity is strongly dependent on the regulation of lipid synthesis [59]. The high expression of the cytoplasm NADP-dependent IDH encoded by *IDH1* might be due to a high consumption of NADPH in the cytoplasm for lipid synthesis. Correspondingly, the expression level of *IDH1* prevails in adipogenically induced adMSC, where lipids are accumulated in vacuoles.

The enzyme activity measurements and mitochondria quantifications show that the HOADH activity and thus the capacity for ß-oxidation increases distinctly in adipogenic as well as in osteogenic differentiation *in vitro*. Consistent with our results, a constant mitochondrial mass during osteogenic differentiation [48,49] and a distinct increase in mitochondrial mass during adipogenic differentiation [25,60] have been found by others before. Ultimately, it is not known if the fatty acid synthesis and ß-oxidation occur simultaneously within one cell. Studies with white adipose tissue have shown that in the anabolic state, lipolysis is inhibited [12,61]. Whether this is a common regulatory mechanism remains to be elucidated since *e.g.* the conversion of white to brown adipocytes entails an upregulation of both fatty acid anabolic and catabolic pathways [62].

A mitochondrial NAD-dependent IDH activity could not be detected, thus a part of NADP-IDH might be located in the mitochondria because IDH is required for the citric acid cycle [19]. Correspondingly, the expression of *IDH2* in adMSC and its increase during osteogenesis and adipogenesis support the existence of mitochondrial NADP-IDH. At a lower but significant level, *IDH3A*, the catalytic NAD-IDH subunit, was also expressed in all adMSC. One explanation of this apparent discrepancy between the activity and the expression level could be that the expression of the catalytic α-subunit of *IDH3A* did not represent the total expression of NAD-IDH. In contrast to the homologous dimer NADP-IDH, the NAD-IDH contains two different regulatory subunits which allow allosteric regulation of the activity, particularly by cell energy charge (*e.g.* ADP/ATP) [63]. Translation to an active NAD-IDH can still be suppressed through alternatively spliced gene products of the regulatory subunits. NAD-IDH is particularly present in tissues with a high respiratory ATP turnover, like aerobic muscles, while in proliferating cells the NADP-IDH prevails [34]. It is being discussed that in proliferating and biosynthetically active cells most of the carbon that enters the TCA cycle is directed towards biosynthetic pathways rather than ATP production [45]. Thus *e.g.* for fatty acid synthesis, citrate could be removed from the TCA cycle prior to the action of NAD-dependent IDH. One reason the NADP-dependent IDH might be favoured in biosynthetically active cells is that, in contrast to the irreversible reaction of NAD-dependent conversion of isocitrate to oxoglutarate, the NADP-dependent reaction is reversible. This allows an anaplerotic pathway, forming isocitrate by glutaminolysis (reviewed in [64]). Using this pathway, glutamine can compensate for the lack of glucose not only for ATP-production but also for the supply of anabolic precursors [65].

The low GSR activities measured in non-differentiating, proliferating cells over the entire time of cultivation indicate a low activity of oxidative phosphorylation in the mitochondria of these cells. Low oxidative phosphorylation activity has also been shown for proliferating thymocytes [66]. The significant increase of GSR activity in osteogenically differentiating cells and the slight increase during adipogenic differentiation might be caused by the demand for regeneration of the detoxification system for reactive oxygen species during enhanced anabolism [67]. Furthermore, it has been reported that, upon adipogenic differentiation of bmMSC and adipose progenitors, the oxygen consumption increased [25,68]. Simultaneously, antioxidative defense enzymes were upregulated [25]. These data and our data suggest that the correlation of mitochondrial oxidative activity, enhanced anabolism and regulation of antioxidative defense need to be further elucidated.

High CK activity is found in the cytoplasm of cells with temporarily high or fluctuating energy demands (*e.g.* fast twitch muscle), where it regenerates ATP for seconds [69]. CK stimulates glycogenolysis by a multiple increase of the cytoplasmic, inorganic phosphate concentration [70]. This function is oxygen-independent, but the finding of a mitochondrial isozyme led to the idea of a functional coupling of CK with oxidative phosphorylation [69,71]. CK activities were found in all adMSC cultures but the gene expression data suggest that mitochondrial CKs were expressed particularly in adipogenically stimulated cells. This suggests that adipogenic stimulation shifted the energy metabolism towards a more oxidative metabolism than osteogenic stimulation did. The expression levels of CKB, CKMT1B and CKMT2 increasing with the progressing adipogenic differentiation imply an increasing role of a functional phosphocreatine-CK shuttle [69]. This shuttle has been found in human skin that was characterized as having high metabolic rates and energy turnover. In these cells the shuttle was mainly made up of the brain type CK and the ubiquitous mitochondrial CK [72]. Thus, although adipogenically induced cells do not proliferate, they show a metabolic phenotype that is characteristic for rapid ATP turnover.

In conclusion, the present data indicate that osteogenically differentiating adMSC *in vitro* showed a strongly proliferative phenotype that entails an increase in the capacity of all energy metabolic pathways tested (Fig. 7A). In contrast, the adipogenic differentiation of adMSC, associated with a lack of proliferation, is accompanied by a decreasing capacity for PPP and carbohydrate metabolism. At the same time, mitochondrial enzyme activities increase indicating a growing capacity for oxidative phosphorylation and β-oxidation (Fig. 7B). Thus, adipogenically differentiating adMSC *in vitro* indicate a shift of their energy metabolic capacity towards lipid metabolism.

While correlations between the proliferative state during osteogenic and adipogenic differentiation and metabolic rearrangements within the cells could be presented by this study, further investigations will be necessary to verify causal connections in proliferating and differentiating adMSC *in vitro* and *in vivo*.

Acknowledgments

The authors thank Dr. med. habil. Jürgen Weber (Ästhetikklinik Rostock, Germany), Dr. med. Klaus Ueberreiter (Park-Klinik Birkenwerder, Germany) and their patients for kindly providing liposuction tissue. Special thanks are also given to Steffi Adam for the technical assistance. This work was financially supported by the European Union (EFRE) and the Federal State of Mecklenburg-Vorpommern (SYNTERO, V-630-S-083-2010/245 and V-630-F-083-2010/248 and Jet Stem Cell Collector, V-630-S-120-2011/122 and V-630-F-120-2011/123), and the “ASCaffolds” project funded by the German Federal Ministry of Education and Research (ERA NET/EuroTransBio-7, Grant no. 031A244C).

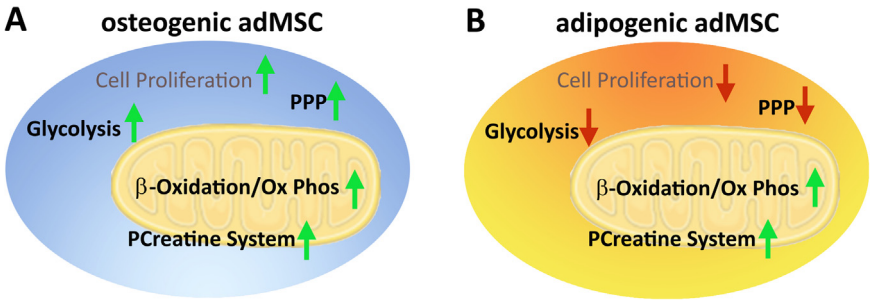

Fig. 7. Schematic depiction of the indicated metabolic rearrangements in adMSC during (A) osteogenic and (B) adipogenic differentiation in relation to non-differentiating adMSC (increased↑, decreased↓; Ox Phos: oxidative phosphorylation, PCreatine: phosphocreatine).

Disclosure statement

The authors declare that they have no conflicts of interest with the contents of this article.

Appendix A. Supplementary material

Supplementary data associated with this article can be found in the online version at doi:10.1016/j.yexcr.2018.07.028.

References

[1] R.H. Lee, B. Kim, I. Choi, H. Kim, H.S. Choi, K. Suh, Y.C. Bae, J.S. Jung, Characterization and expression analysis of mesenchymal stem cells from human bone marrow and adipose tissue, Cell. Physiol. Biochem. 14 (2004) 311–324.
[2] D. Peroni, I. Scambi, A. Pasini, V. Lisi, F. Bifari, M. Krampera, G. Rigotti, A. Sbarbati, M. Galie, Stem molecular signature of adipose-derived stromal cells, Exp. Cell Res. 314 (2008) 603–615.
[3] D. Spitkovsky, J. Hescheler, Adult mesenchymal stromal stem cells for therapeutic applications, Minim. Invasive Ther. Allied Technol. 17 (2008) 79–90.
[4] P.A. Zuk, M. Zhu, P. Ashjian, D.A. De Ugarte, J.I. Huang, H. Mizuno, Z.C. Alfonso, J.K. Fraser, P. Benhaim, M.H. Hedrick, Human adipose tissue is a source of multipotent stem cells, Mol. Biol. Cell 13 (2002) 4279–4295.
[5] P.A. Zuk, M. Zhu, H. Mizuno, J. Huang, J.W. Futrell, A.J. Katz, P. Benhaim, H.P. Lorenz, M.H. Hedrick, Multilineage cells from human adipose tissue: implications for cell-based therapies, Tissue Eng. 7 (2001) 211–228.
[6] M. Valtieri, A. Sorrentino, The mesenchymal stromal cell contribution to homeostasis, J. Cell. Physiol. 217 (2008) 296–300.
[7] D.A. De Ugarte, K. Morizono, A. Elbarbary, Z. Alfonso, P.A. Zuk, M. Zhu, J.L. Dragoo, P. Ashjian, B. Thomas, P. Benhaim, I. Chen, J. Fraser, M.H. Hedrick, Comparison of multi-lineage cells from human adipose tissue and bone marrow, Cells Tissues Organs 174 (2003) 101–109.
[8] A.W. James, J.N. Zara, X.L. Zhang, A. Askarinam, R. Goyal, M. Chiang, W. Yuan, L. Chang, M. Corselli, J. Shen, S. Pang, D. Stoker, B. Wu, K. Ting, B. Peault, C. Soo, Perivascular stem cells: a prospectively purified mesenchymal stem cell population for bone tissue engineering, Stem Cell Transl. Med. 1 (2012) 510–519.
[9] Z.M. MacIsaac, H. Shang, H. Agrawal, N. Yang, A. Parker, A.J. Katz, Long-term in-vivo tumorigenic assessment of human culture-expanded adipose stromal/stem cells, Exp. Cell Res. 318 (2012) 416–423.
[10] B. Fang, Y. Song, R.C. Zhao, Q. Han, Q. Lin, Using human adipose tissue-derived mesenchymal stem cells as salvage therapy for hepatic graft-versus-host disease resembling acute hepatitis, Transplant. Proc. 39 (2007) 1710–1713.
[11] K.S. Koh, T.S. Oh, H. Kim, I.W. Chung, K.W. Lee, H.B. Lee, E.J. Park, J.S. Jung, I.S. Shin, J.C. Ra, J.W. Choi, Clinical application of human adipose tissue-derived mesenchymal stem cells in progressive hemifacial atrophy (Parry-Romberg disease) with microfat grafting techniques using 3-dimensional computed tomography and 3-dimensional camera, Ann. Plast. Surg. 69 (2012) 331–337.
[12] N.S. Chandel, Navigating Metabolism, Cold Spring Harbor Laboratory Press, New York, 2015.
[13] A. Rupprecht, D. Sittner, A. Smorodchenko, K.E. Hilse, J. Goyn, R. Moldzio, A.E. Seiler, A.U. Brauer, E.E. Pohl, Uncoupling protein 2 and 4 expression pattern during stem cell differentiation provides new insight into their putative function, PLoS One 9 (2014) e88474.
[14] P.S. Ward, C.B. Thompson, Metabolic reprogramming: a cancer hallmark even warburg did not anticipate, Cancer Cell 21 (2012) 297–308.
[15] J.D. Ochocki, M.C. Simon, Nutrient-sensing pathways and metabolic regulation in stem cells, J. Cell Biol. 203 (2013) 23–33.
[16] N. Shyh-Chang, G.Q. Daley, Metabolic switches linked to pluripotency and embryonic stem cell differentiation, Cell Metab. 21 (2015) 349–350.
[17] T. Lonergan, B. Bavister, C. Brenner, Mitochondria in stem cells, Mitochondrion 7 (2007) 289–296.
[18] M.G. Vander Heiden, L.C. Cantley, C.B. Thompson, Understanding the Warburg effect: the metabolic requirements of cell proliferation, Science 324 (2009) 1029–1033.
[19] D.L. Nelson, M.M. Cox, Lehninger Principles of Biochemistry, W. H. Freeman, New York, 2013.
[20] E.A. Newsholme, C. Start, Regulation des Stoffwechsels. Homöostase im menschlichen und tierischen Organismus, Verlag Chemie, Weinheim, 1984.
[21] D. Pette, Zellphysiologie des Stoffwechsels, Konstanzer Universitätsverlag, Konstanz, 1970.
[22] D. Schop, F.W. Janssen, L.D. van Rijn, H. Fernandes, R.M. Bloem, J.D. de Bruijn, R. van Dijkhuizen-Radersma, Growth, metabolism, and growth inhibitors of mesenchymal stem cells, Tissue Eng. Part A 15 (2009) 1877–1886.
[23] G. Pattappa, H.K. Heywood, J.D. de Bruijn, D.A. Lee, The metabolism of human mesenchymal stem cells during proliferation and differentiation, J. Cell. Physiol. 226 (2011) 2562–2570.
[24] Q. Li, Z. Gao, Y. Chen, M.X. Guan, The role of mitochondria in osteogenic, adipogenic and chondrogenic differentiation of mesenchymal stem cells, Protein Cell 8 (2017) 439–445.
[25] Y. Zhang, G. Marsboom, P.T. Toth, J. Rehman, Mitochondrial respiration regulates adipogenic differentiation of human mesenchymal stem cells, PLoS One 8 (2013) e77077.
[26] K. Peters, A. Salamon, S. Van Vlierberghe, J. Rychly, M. Kreutzer, H.G. Neumann, E. Schacht, P. Dubruel, A new approach for adipose tissue regeneration based on human mesenchymal stem cells in contact to hydrogels – an in vitro study, Adv. Eng. Mater. 11 (2009) B155–B161.
[27] K. Noeske, The binding of crystal violet on deoxyribonucleic acid. Cytophotometric studies on normal and tumor cell nuclei, Histochemie 7 (1966) 273–287.
[28] R.J. Gillies, N. Didier, M. Denton, Determination of cell number in monolayer cultures, Anal. Biochem. 159 (1986) 109–113.
[29] A. Salamon, A. Jonitz-Heincke, S. Adam, J. Rychly, B. Muller-Hilke, R. Bader, K. Lochner, K. Peters, Articular cartilage-derived cells hold a strong osteogenic differentiation potential in comparison to mesenchymal stem cells in vitro, Exp. Cell Res. 319 (2013) 2856–2865.
[30] J. Meyer, A. Salamon, N. Herzmann, S. Adam, H.D. Kleine, I. Matthiesen, K. Ueberreiter, K. Peters, Isolation and differentiation potential of human mesenchymal stem cells from adipose tissue harvested by water jet-assisted liposuction, Aesthet. Surg. J. 35 (2015) 1030–1039.
[31] J. Montalibet, K.I. Skorey, B.P. Kennedy, Protein tyrosine phosphatase: enzymatic assays, Methods 35 (2005) 2–8.
[32] L.L. Listenberger, D.A. Brown, Fluorescent detection of lipid droplets and associated proteins, Curr. Protoc. Cell Biol. (2007) (Chapter 24, Unit 24.22).
[33] H.U. Bergmeyer, J. Bergmeyer, M. Grassl, Methods of Enzymatic Analysis, Verlag Chemie, Weinheim, 1983.
[34] K. Peters, G. Kamp, A. Berz, R.E. Unger, S. Barth, A. Salamon, J. Rychly, C.J. Kirkpatrick, Changes in human endothelial cell energy metabolic capacities during in vitro cultivation. The role of "aerobic glycolysis" and proliferation, Cell. Physiol. Biochem. 24 (2009) 483–492.
[35] S. Zhao, R.D. Fernald, Comprehensive algorithm for quantitative real-time polymerase chain reaction, J. Comput. Biol. 12 (2005) 1047–1064.
[36] P.J. Bell, P. Karuso, Epicocconone, a novel fluorescent compound from the fungus epicoccumnigrum, J. Am. Chem. Soc. 125 (2003) 9304–9305.
[37] H.T. Hornig-Do, G. Gunther, M. Bust, P. Lehnartz, A. Bosio, R.J. Wiesner, Isolation of functional pure mitochondria by superparamagnetic microbeads, Anal. Biochem. 389 (2009) 1–5.
[38] R.D.C. Team, R: A Language and Environment for Statistical Computing, R Found. Stat. Comput., Vienna, Austria, 2011.
[39] J.E. Aubin, Bone stem cells, J. Cell. Biochem. Suppl. 30–31 (1998) 73–82.
[40] A. Salamon, S. Adam, J. Rychly, K. Peters, Long-term tumor necrosis factor treatment induces NFkappaB activation and proliferation, but not osteoblastic differentiation of adipose tissue-derived mesenchymal stem cells in vitro, Int. J. Biochem. Cell Biol. 54 (2014) 149–162.
[41] G. Astori, F. Vignati, S. Bardelli, M. Tubio, M. Gola, V. Albertini, F. Bambi, G. Scali, D. Castelli, V. Rasini, G. Soldati, T. Moccetti, "In vitro" and multicolor phenotypic characterization of cell subpopulations identified in fresh human adipose tissue stromal vascular fraction and in the derived mesenchymal stem cells, J. Transl. Med. 5 (2007) 55.
[42] J.A. Lee, B.M. Parrett, J.A. Conejero, J. Laser, J. Chen, A.J. Kogon, D. Nanda, R.T. Grant, A.S. Breitbart, Biological alchemy: engineering bone and fat from fat-derived stem cells, Ann. Plast. Surg. 50 (2003) 610–617.

[43] T.M. Liu, M. Martina, D.W. Hutmacher, J.H. Hui, E.H. Lee, B. Lim, Identification of common pathways mediating differentiation of bone marrow- and adipose tissue-derived human mesenchymal stem cells into three mesenchymal lineages, Stem Cells 25 (2007) 750–760.
[44] E.A. Newsholme, A.R. Leech, Biochemistry for the Medical Sciences, J. Wiley and Sons, Chichester and New York, 1983.
[45] R.J. DeBerardinis, J.J. Lum, G. Hatzivassiliou, C.B. Thompson, The biology of cancer: metabolic reprogramming fuels cell growth and proliferation, Cell Metab. 7 (2008) 11–20.
[46] G. Musumeci, A. Mobasheri, F.M. Trovato, M.A. Szychlinska, A.C. Graziano, D. Lo Furno, R. Avola, S. Mangano, R. Giuffrida, V. Cardile, Biosynthesis of collagen I, II, RUNX2 and lubricin at different time points of chondrogenic differentiation in a 3D in vitro model of human mesenchymal stem cells derived from adipose tissue, Acta Histochem. 116 (2014) 1407–1417.
[47] O. Warburg, On the origin of cancer cells, Science 123 (1956) 309–314.
[48] C.T. Chen, Y.R. Shih, T.K. Kuo, O.K. Lee, Y.H. Wei, Coordinated changes of mitochondrial biogenesis and antioxidant enzymes during osteogenic differentiation of human mesenchymal stem cells, Stem Cells 26 (2008) 960–968.
[49] L.C. Shum, N.S. White, B.N. Mills, K.L. Bentley, R.A. Eliseev, Energy metabolism in mesenchymal stem cells during osteogenic differentiation, Stem Cells Dev. 25 (2016) 114–122.
[50] N. Quarto, D.C. Wan, M.D. Kwan, N.J. Panetta, S. Li, M.T. Longaker, Origin matters: differences in embryonic tissue origin and Wnt signaling determine the osteogenic potential and healing capacity of frontal and parietal calvarial bones, J. Bone Miner. Res. 25 (2010) 1680–1694.
[51] M.D. Brand, D.G. Nicholls, Assessing mitochondrial dysfunction in cells, Biochem. J. 435 (2011) 297–312.
[52] D.M. Dawson, N.O. Kaplan, T.L. Goodfriend, Lactic dehydrogenases – functions of two types – rates of synthesis of two major forms can be correlated with metabolic differentiation, Science 143 (1964) 929–933.
[53] K.E. Follmar, F.C. Decroos, H.L. Prichard, H.T. Wang, D. Erdmann, K.C. Olbrich, Effects of glutamine, glucose, and oxygen concentration on the metabolism and proliferation of rabbit adipose-derived stem cells, Tissue Eng. 12 (2006) 3525–3533.
[54] B.T. Mischen, K.E. Follmar, K.E. Moyer, B. Buehrer, K.C. Olbrich, L.S. Levin, B. Klitzman, D. Erdmann, Metabolic and functional characterization of human adipose-derived stem cells in tissue engineering, Plast. Reconstr. Surg. 122 (2008) 725–738.
[55] S.Y. Lunt, M.G. Vander Heiden, Aerobic glycolysis: meeting the metabolic requirements of cell proliferation, Annu. Rev. Cell Dev. Biol. 27 (2011) 441–464.
[56] S. Arriaran, S. Agnelli, D. Sabater, X. Remesar, J.A. Fernandez-Lopez, M. Alemany, Evidences of basal lactate production in the main white adipose tissue sites of rats. Effects of sex and a cafeteria diet, PLoS One 10 (2015) e0119572.
[57] W.N. Tian, L.D. Braunstein, J. Pang, K.M. Stuhlmeier, Q.C. Xi, X. Tian, R.C. Stanton, Importance of glucose-6-phosphate dehydrogenase activity for cell growth, J. Biol. Chem. 273 (1998) 10609–10617.
[58] B.L. Horecker, The biochemistry of sugars, Int. Z. fur Vitam.- und Ernahr. Beih. 15 (1976) 1–21.
[59] H. Kather, M. Rivera, K. Brand, Interrelationship and control of glucose metabolism and lipogenesis in isolated fat-cells. Control of pentose phosphate-cycle activity by cellular requirement for reduced nicotinamide adenine dinucleotide phosphate, Biochem. J. 128 (1972) 1097–1102.
[60] L. Wilson-Fritch, A. Burkart, G. Bell, K. Mendelson, J. Leszyk, S. Nicoloro, M. Czech, S. Corvera, Mitochondrial biogenesis and remodeling during adipogenesis and in response to the insulin sensitizer rosiglitazone, Mol. Cell. Biol. 23 (2003) 1085–1094.
[61] J.M. Rutkowski, J.H. Stern, P.E. Scherer, The cell biology of fat expansion, J. Cell Biol. 208 (2015) 501–512.
[62] V. Barquissau, D. Beuzelin, D.F. Pisani, G.E. Beranger, A. Mairal, A. Montagner, B. Roussel, G. Tavernier, M.A. Marques, C. Moro, H. Guillou, E.Z. Amri, D. Langin, White-to-brite conversion in human adipocytes promotes metabolic reprogramming towards fatty acid anabolic and catabolic pathways, Mol. Metab. 5 (2016) 352–365.
[63] D.T. Hartong, M. Dange, T.L. McGee, E.L. Berson, T.P. Dryja, R.F. Colman, Insights from retinitis pigmentosa into the roles of isocitrate dehydrogenases in the Krebs cycle, Nat. Genet. 40 (2008) 1230–1234.
[64] K. Smolkova, P. Jezek, The role of mitochondrial NADPH-dependent isocitrate dehydrogenase in cancer cells, Int. J. Cell Biol. 2012 (2012) 273947.
[65] M. Board, S. Humm, E.A. Newsholme, Maximum activities of key enzymes of glycolysis, glutaminolysis, pentose phosphate pathway and tricarboxylic acid cycle in normal, neoplastic and suppressed cells, Biochem. J. 265 (1990) 503–509.
[66] K.A. Brand, U. Hermfisse, Aerobic glycolysis by proliferating cells: a protective strategy against reactive oxygen species, Faseb J. 11 (1997) 388–395.
[67] S. Chakravarthi, C.E. Jessop, N.J. Bulleid, The role of glutathione in disulphide bond formation and endoplasmic-reticulum-generated oxidative stress, EMBO Rep. 7 (2006) 271–275.
[68] D. von Heimburg, K. Hemmrich, S. Zachariah, H. Staiger, N. Pallua, Oxygen consumption in undifferentiated versus differentiated adipogenic mesenchymal precursor cells, Respir. Physiol. Neurobiol. 146 (2005) 107–116.
[69] T. Wallimann, W. Hemmer, Creatine kinase in non-muscle tissues and cells, Mol. Cell. Biochem. 133–134 (1994) 193–220.
[70] D. Chasiotis, K. Sahlin, E. Hultman, Regulation of glycogenolysis in human muscle at rest and during exercise, J. Appl. Physiol. Respir. Environ. Exerc. Physiol. 53 (1982) 708–715.
[71] V.A. Saks, A.V. Kuznetsov, V.V. Kupriyanov, M.V. Miceli, W.E. Jacobus, Creatine kinase of rat heart mitochondria. The demonstration of functional coupling to oxidative phosphorylation in an inner membrane-matrix preparation, J. Biol. Chem. 260 (1985) 7757–7764.
[72] U. Schlattner, N. Mockli, O. Speer, S. Werner, T. Wallimann, Creatine kinase and creatine transporter in normal, wounded, and diseased skin, J. Invest. Dermatol. 118 (2002) 416–423.

Supplementary material

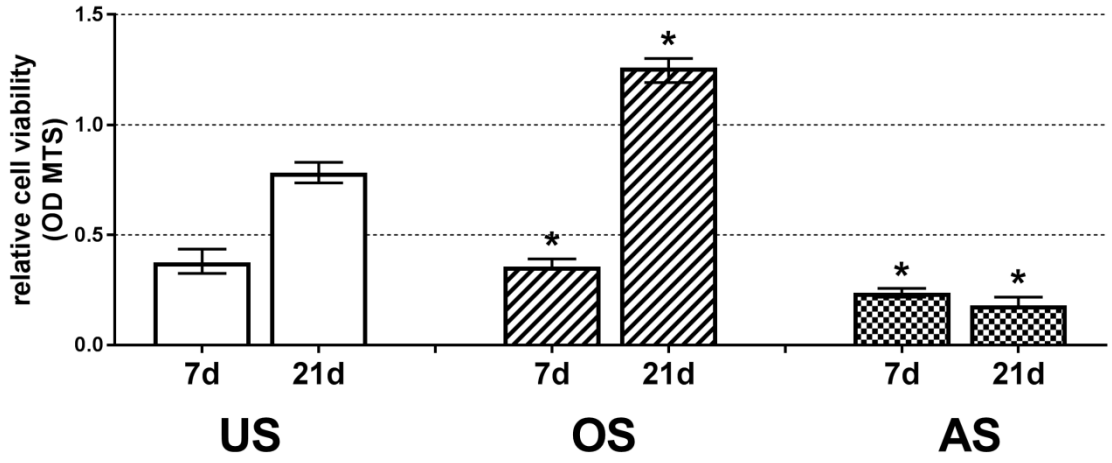

Supplementary Fig. S1. Quantification of adMSC metabolic activity in non-stimulated cultures (US), osteogenically stimulated cultures (OS) and adipogenically stimulated cultures (AS). Cell number after 7 and 21 d (US, OS, AS, n = 4, * significantly different from US 7 d and US 21 d respectively; Mann-Whitney U-Test, $p < 0.05$).

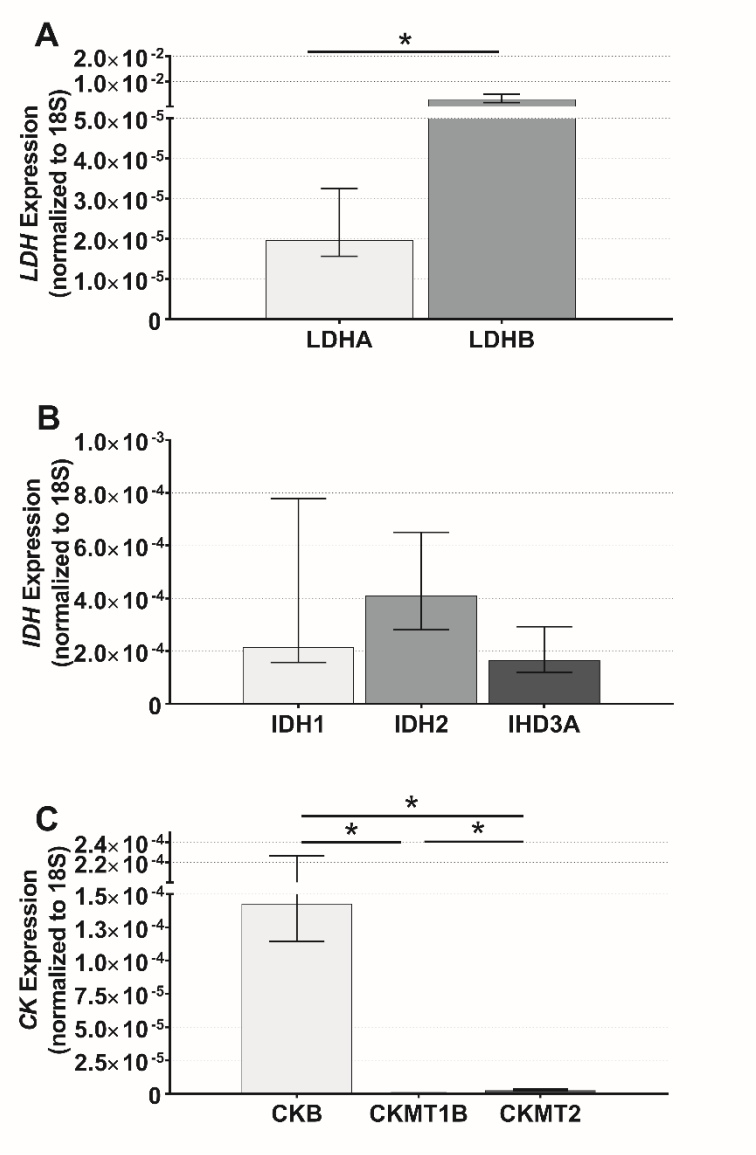

Supplementary Fig. S2.: gene expression levels in non-differentiating at 0 d of the experimentation period. Related to Figure 3 - (A) LDH isoforms *LDHA* and *LDH*B, (B) IDH isoforms *IDH1, IDH2* and *IDH3A,* (C) CK isoforms *CKB, CKMT1B* and *CKMT2* (n = 3, * indicate significant differences, level of significance: $p \leq 0.05$).

Supplementary Table S1: Enzyme activities in mitochondrial homogenates vs. whole cell homogenates. Related to Figure 4 - Activities of GAPDH and HOADH and HOADH/GAPDH ratios in whole cell homogenates (n = 8, U/mg DNA, after 21 d) and mitochondria isolate homogenates (n = 4, U/mg protein 14 d culture) from non-differentiating (US), and osteogenic (OS) or adipogenic (AS) cultures.

	adMSC			**mitochondria**		
	US	**OS**	**AS**	**US**	**OS**	**AS**
HOADH	0.58	2.58	4.09	0.13	0.28	0.40
GAPDH	75.1	100.7	19.9	0.07	0.10	0.09
HOADH/ GAPDH	0.01	0.03	0.23	1.67	2.95	5.29